To the Graduate Council:

I am submitting herewith a thesis written by Jung-He Wu entitled "Computer Simulation of Steady-State Pipe Extrusion." I have examined the final copy of this thesis for form and content and recommend that it be accepted in partial fulfillment of the requirements for the degree of Master of Science, with a major in Chemical Engineering.

Marion G. Hansen, Major Professor

We have read this thesis
and recommend its acceptance:

Accepted for the council

Vice Provost
and Dean of the Graduate School

COMPUTER SIMULATION OF STEADY-STATE PIPE EXTRUSION

A Thesis

Presented for the

Master of Science

Degree

The University of Tennessee, Knoxville

Jung-He Wu

August 1990

ACKNOWLEDGEMENTS

I would like to express my thanks and appreciation to all those who helped in this research. First, I would like to express my sincere thanks to the members of my committee, Dr. Donald C. Bogue, Dr. Frederick E. Weber, Dr. Raymond D. Krieg, and Dr. Marion G. Hansen. I especially thank my major professor, Dr. Marion G. Hansen, for suggesting a challenging topic for my thesis and gratefully acknowledge his patience, guidance, and support throughout my graduate studies. Particular thanks are due to Mr. Rajen M. Patel for providing the valuable experimental data used in numerical computation.

Finally, special appreciation is also extended to my parents whose continual love, support, and encouragement throughout the years at graduate school have extended far beyond the scope of this research.

ABSTRACT

Extruded pipe is made by forcing a molten polymer through an annular die and cooling it; the final properties of the pipe depend on a number of variables, including in particular the cooling step, during which crystallization takes places. An accurate prediction of temperature profile and crystallinity distribution within a semi-crystalline polymer (polypropylene) is of importance in determining the processing conditions. In this study the solidification of the melt during cooling in pipe extrusion has been analyzed by means of a computer simulation. The mathematical model, which involves a steady-state nonlinear energy equation incorporating the crystallization kinetics proposed by Nakamura, simulates the behavior of polymer melt in the cooling chamber during formation of a thick walled pipe. An investigation was carried out into effects of melt inlet temperature, take-off speed, and pipe wall thickness on the temperature profile as well as crystallinity distribution. NACHOS II, a computer program based on finite element method designed for solution of two-dimensional fluid dynamics and heat transfer, is employed for the numerical solution. The numerical model gives therefore a basis for the prediction of the crystallinity distribution and adjustment of the operation conditions.

TABLE OF CONTENTS

LIST OF TABLES

LIST OF FIGURES

LIST OF SYMBOLS

A_c	the area under the crystalline peaks in an X-ray scattering curve.
A_a	the area under the amorphous hump in an X-ray scattering curve.
b_o	thickness of the surface layer.
C_p	specific heat.
D	the transmission of infrared ray.
E_a	transport activation energy.
f	distribution function of nucleus size and shape.
ΔF	transport activation energy.
ΔF^*	free energy of a nucleus having a critical radius.
g	acceleration of gravity.
G, G_o	crystal growth rates.
Gr	Grashof number.
h	Planck's constant.
h	heat transfer coefficient.
H, H_T	enthalpy.
ΔH	latent heat of crystallization.
I	polarized light intensity.
k	thermal conductivity.
K	Boltzmann constant.
κ	cooling (or heating) function.
k_c	crystallization rate constant.
χ_c, χ_{co}	Avrami-like crystallization rate constant.
L	total length of the cooling chamber.
n	Avrami exponent.

N	nucleation rate.
Nu	Nusselt number.
Pe_t, Pe_c	Peclet numbers, thermal and crystalline.
Pr	Prandtl number.
Q	volumetric heat source.
R	gas constant.
R^*	a vector characteristic for the nucleus having critical dimensions.
Re	Reynolds number.
S^*	critical boundary between the regions of unstable and stable nuclei.
t	time.
T	temperature.
T_g	glass transition temperature.
T_m	melting temperature.
T_m^o	equilibrium melting temperature.
T^*	temperature of maximum growth rate.
V	volume.
W	weight.
w	weight factor.
χ_c	degree of crystallinity.
$\chi_{c\infty}$	degree of ultimate crystallinity.
$\chi_c(\infty)$	degree of ultimate crystallinity.
ρ	polymer density.
μ	viscosity.
β	thermal expansion coefficient.
Γ	dimensionless temperature.
η_1, η_2	dimensionless distances.

σ_e end surface free energy.

σ side surface free energy.

θ relative degree of crystallinity.

ξ ratio of pipe thickness to the length of cooling chamber.

ζ ratio of inner radius to the length of cooling chamber.

τ_i induction time.

Φ cooling (or heating) rate.

Φ viscous dissipation heat.

ε constant.

$\Delta\Phi^*$ the work required for formation of a nucleus of critical size.

SUBSCRIPTS:

app denotes apparent value.

a denotes amorphous state.

c denotes crystalline state.

l denotes liquid.

max denotes maximum.

p denotes primary mechanism.

s denotes secondary mechanism.

s denotes solid.

1 denotes first mechanism in equation (1.4-8).

2 denotes second mechanism in equation (1.4-8).

1 denotes axial direction.

2 denotes radial direction.

0.5 denotes half-time.

CHAPTER I

INTRODUCTION

Extrusion is an old fabrication technique. Being a continuous operation with the attendant advantages of speed, volume, and economy, the development of extrusion operation keeps gaining considerable attention in food, metal, and plastics manufacturing. The technique of extrusion was first applied in the ceramic arts by Newley[1] as early as in 1845. The first thermoplastic material was extruded by means of a hydraulic ram dates back to an 1870 process in which cellulose nitrate was given the profile of a rod[2]. Extrusion process is now one of the most important commercial polymer processing operations whereby a granulated thermoplastic is converted continuously to a wide variety of continuous forms such as filament, rod, profile, sheet, film, inner tube, and pipe. More thermoplastics are processed by extrusion than by any other type of processing.

Pipe production is one of the important applications of this widely used process in the polymer industry. The market of plastic pipes, obtained from extrusion process, consists mainly of polyethylene, polypropylene, PVC, and ABS with a total European consumption of about 1.5 million tons in 1979 and more than one billion pounds of plastics are extruded every year to produce plastic pipe[3]. Full description of the pipe production and required machines is given, for example, by Schenkel[1], Simonds[4], Griff[5], and Fisher[6]. The normal process in the production of thermoplastic pipes consists of several steps. The first step is to plasticize the raw material in the extruder. The molten polymer is then extruded horizontally through an annular flow

channel (i.e. a die), where it is shaped to the profile of the pipe. Immediately on leaving the die the soft pipe enters a cooling chamber where the pipe is calibrated and cooled to the required dimensions in a water spray or flood cooling bath. Cutting into convenient lengths follows and the pipes are finally stacked on a suitable rack. The basic components in a pipe line, as shown in Figure 1, include an extruder, a die, a sizing device, a cooling chamber, a pipe takeoff, a transverse cutoff saw, and a dump table.

Limitations of outputs in pipe production are imposed by the capacities of the in-line equipments, especially by the cooling systems. The properties of the extruded pipe is also significantly affected by the cooling operation. For instance, dimensional errors will be found if the cooling time is not enough; and if the cooling is too sudden, residual stress will be produced in the product.

The purpose of the cooling chamber is to cool the extruded pipe as nearly as possible to room temperature. An inner view of the cooling chamber is schematically presented in Figure 2. Two commonly used cooling systems in pipe production are water baths and water spray cooling tank. Water baths which are tanks with running water cool the extruded pipe by means of either mains water or water circulated via a heat exchanger. As compared with water baths, water spray cooling is preferable to submerged cooling for pipe production. Spray cooling has the advantage of avoiding very troublesome buoyancy of the pipe in the water baths and most importantly it can provide a more intensive cooling effect because the heat exchange resistance can be reduced considerably by the impact of the water droplets on the pipe.

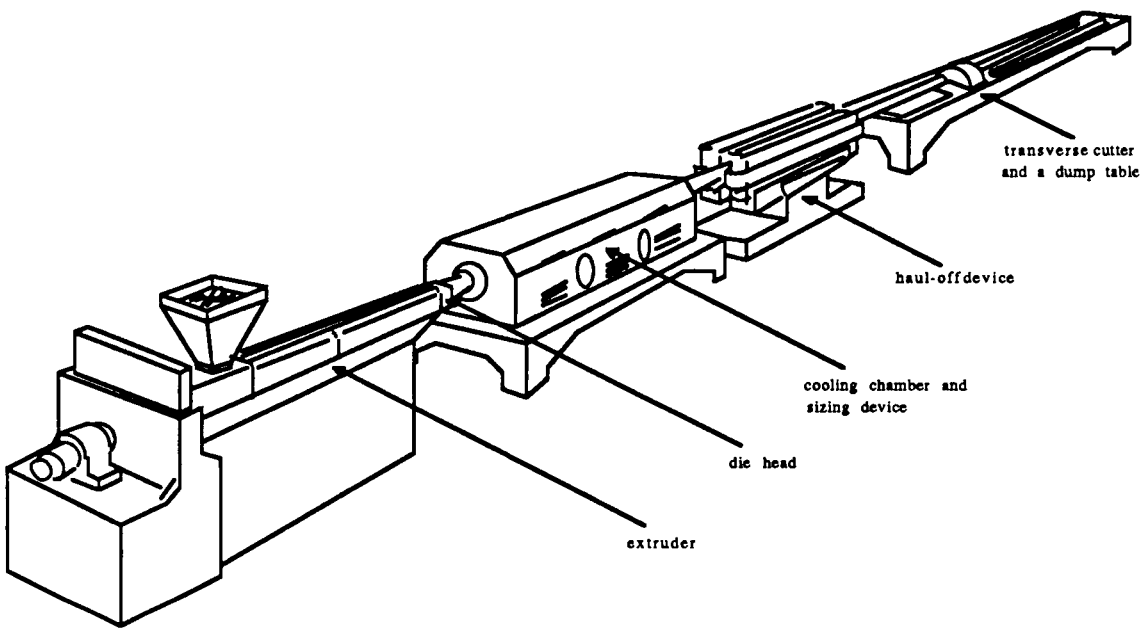

Figure 1. Drawing of a plant for the extrusion of thermoplastic pipes.

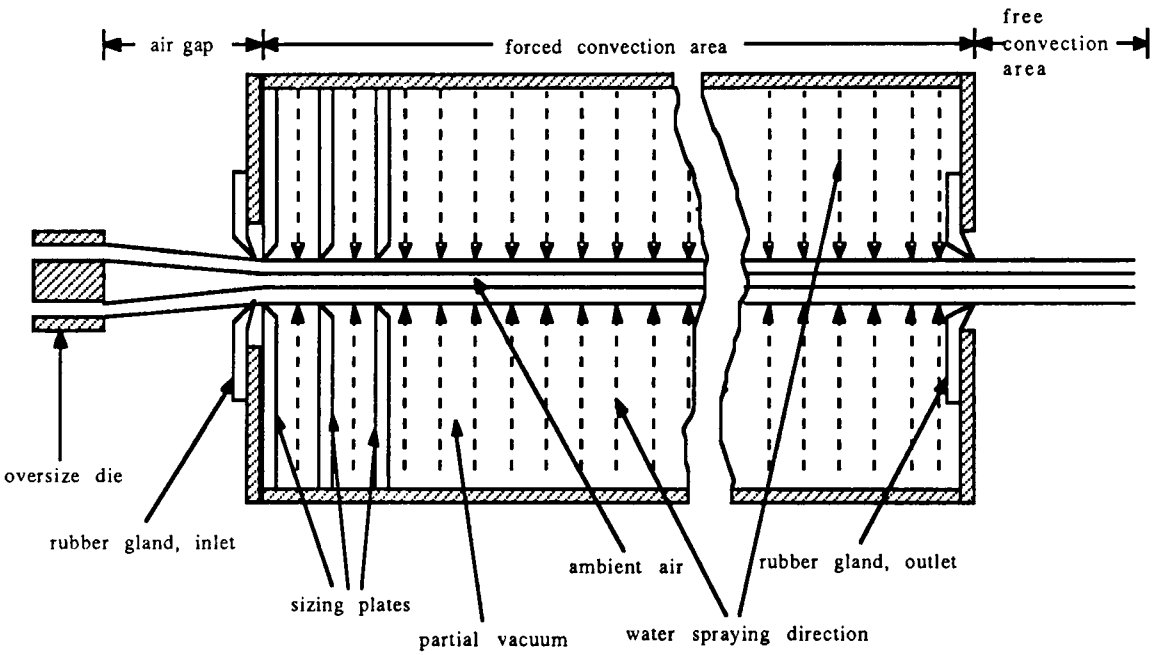

Figure 2. Inner view of the cooling chamber.

Several factors determining the performance of the cooling system include the individual differences between processing and setting temperatures, the thickness of the pipe wall as well as the speed of the haul-off. In the case of the thick-walled polyethylene pipe the use of step-cooling, several cooling chambers connected in series, is recommended since undesirable shrinkage flaws or tension sometimes might be produced in the wall of the pipe by using single cooling chamber[1]. The performance of the cooling tank is also appreciably determined by the polymeric material used for the pipe. For example, the length of the cooling tank needed for PVC or ABS is almost one half that needed for polyolefins[1]. It is because the heat of crystallization of the polyolefins must be removed.

Heat transfer plays a very important role in plastics processing because the rate of heat transfer directly controls the overall rate for the processing and in turns affects the mechanical and physical properties of the extruded polymer. Generally all three modes of heat transfer --- convection, conduction, and radiation --- occur simultaneously in the cooling stage. Due to the low thermal conductivity of the polymer and the heat generated when crystallization occurs, most of the resistance to heat transfer lies within the polymer melt itself. For instance, the time needed for cooling or solidification is usually the longest part of the processing sequence. The time required in cooling for injection molding or blow-molding, as an example, commonly occupies 60%-80% of the cycle time.

Solidification of the crystalline polymer, a cooling step common in polymer processing, starts from the surfaces of the processed articles and proceeds toward the center. As coupled with the indirect effects of

temperature-dependent viscosity, relaxation time and low thermal conductivity, it is reasonable to expect that the degree of crystallinity and the morphology is not uniform throughout the part. This fact is especially illustrated in the experimental observation of a so called skin-core structure[2,7,8,9] found in melt spinning. In such an operation a crystalline polymer is extruded as a filament and quenched quickly in the cooling medium; the outer layer of the product has somewhat different structure than the core, i.e., the outer layer of the product may well be glassy or of lower crystallinity in nature, while the inner region of a bulk specimen, which remains hotter for a longer period, will have crystallized from the melt gradually.

Rapid cooling is, of course, commercially required for the production of polymer pipes. Thus, the skin-core structure may exist in the product. It is worth noting that increasing service temperature reduces thermal barrier and permits more crystallization. The temperature at which the product is used in service will then affect the density of the outer layer of the pipe: the higher the service temperature, the higher the density of the outer layer. However this change will not occur in the core portion of the crystalline polymeric product[2]. The skin-core structure differences which cause pipe in tension because of volumetric shrinkage in high-density region are a source of nuisance when bulk specimens are warmed to high temperatures at any time during service. Such a structure often gives rise to the potential stress cracking or mechanical instability of pipe in service.

The temperature profile in the polymer strongly depends on the rate of heat transfer. However, the heat transfer rate of a polymer will also be

influenced by the crystallization rate which is a strong function of temperature. Crystallization during many polymer processes occurs non-isothermally. As a result, the analysis of heat transfer requires the knowledge of the parallel temperature-dependent crystallization kinetics. The development of an adequate analysis of crystallization for non-isothermal condition has been received much attention for crystalline polymers[10,11].

As elucidated above, the development of microstructure such as morphology, crystallinity, etc. in the manufactured article results from the thermo-mechanical history experienced by the polymer during flow and solidification. The ultimate properties of the article are closely related to the microstructure. Therefore, the control of the cooling process and product quality must be based on understanding of the interactions between polymer properties, equipment design, article geometry, operating conditions, thermo-mechanical history, microstructure, and ultimate product properties.

Cooling is a critical step in the pipe production process because it not only determines the rate of output but also directly relates to the ultimate properties of the extruded pipe. The adjustment in cooling operation for controlling the desired quality of the extruded pipe is based almost entirely on empirical make-and-test and experience. Experimental determination of the temperature and crystallinity would not only be prohibitively expensive and time consuming, but also, frequently, inaccurate. Therefore, there is a compelling reason to eliminate such elaborate and inefficient stages. The main objective of numerical simulation is, then, to improve on the present trial-and-error methods used to reach acceptable properties. The use of

numerical simulation in process analysis gives benefits when entire processes are considered, and when a wide variety of possible numerical values for material properties, machine dimensions, part geometry, and operation conditions are assessed. Consequently, it provides a cheap and rapid alternative to physical experiments on laboratory, pilot-plant or full scale.

The use of numerical simulation gives the advantage of predicting the temperature variation when the extruded polymeric pipe comes in contact with a cooling medium. In addition, details of temperature history in the polymer melt allows inferences or predictions about crystallinity developed in the extruded pipe, thermal stresses and susceptibility to warping and shrinkage.

The analysis of the cooling stage in pipe production, although it looks simple, contains many variables which interact with one another and make it difficult for mathematical treatment. For the case of a crystalline polymer the process of cooling is mainly concerned with the steady-state flow of a viscoelastic crystallizing polymer melt into a cooling chamber wherein heat transfer occurs due to the contact with the cooling medium and the temperature difference in the polymer. The mathematical simulation, therefore, involves simultaneous fluid flow and heat transfer which is associated with crystallization of polymer melt. The comprehensive simulation of the cooling stage to obtain predictions regarding temperature and crystallinity is subject to solving simultaneously a set of equations for continuity, momentum, and energy, along with appropriate crystallization relations and relevant initial and boundary conditions. This thesis is to focus on analyzing the cooling process as nonisothermal, one-dimensional plug flow with incompressible crystalline polymeric material such as

polypropylene. To achieve this, NACHOS II, which is a computer code using finite element methods designed for the solution of two-dimensional, viscous, incompressible fluid dynamics and heat transfer problems, is used for numerical analyses.

CHAPTER II

THEORY AND BACKGROUND

CRYSTALLIZATION OF POLYMERS

Crystallization is the process by which a disordered phase is transformed to an ordered structure, usually from a melt or dilute solution. Crystallization proceeds through the formation of small nuclei of the required ordered atomic arrangement by chain motion of the molecules and subsequent diffusion of additional molecules to align themselves with the nuclei. Generally inorganic and organic molecules with low molecular weight will crystallize completely. It has been observed for many years that polymer materials also possess the ability to crystallize. However, unlike the crystallization of most other crystalline solids, polymers even under the most favorable conditions are normally only partially crystalline, a consequence of their long-chain entanglements, structural imperfections, and insufficient rate of crystallization[12]. For example, typical crystalline polymers are PE, PP, PET acetal, etc. The crystallinity of Polyethylene typically has the range of 60-80%[13]. The level of crystallinity in many other partially crystalline polymers including polypropylene and polyamides is even lower[13].

1.1. Crystallinity in Polymers

Crystalline polymers are properly called semi-crystalline, because they are seen to be only partially crystalline when assessed by a crystallinity-sensitive property such as density. The degree of crystallinity, which is defined as the fraction of the total polymer that is in the crystalline

state, is a characteristic of semi-crystalline polymeric materials. The term crystallinity is often used as a measure of the degree of crystalline order in a semi-crystalline material. On the other hand, there is a maximum value of crystallinity at which polymer can achieve. Such maximum value is usually defined as the ultimate crystallinity, $\chi_{c\infty}$[14].

The existence of crystallinity implies the presence of two distinct phases, i.e., crystalline and amorphous regions. One of these phases, the amorphous phase, is characterized as the state of configurational disorder in which the polymer chain units are random and entangled together. On the contrary, a spontaneous ordering of portions of the molecules is possible for systems which are composed of units of reasonably regular structure under appropriate thermodynamic conditions. This ordering phase is termed the crystalline phase. These two phases are distinguishable because of their vastly different properties.

1.2. Measurements of Crystallinity

The degree of crystallinity is of great technological and practical importance upon the physical properties of a polymer and several methods, which do not always produce precisely the same results, have been devised to measure it. The experimental measurements of crystallinity in polymer systems are of two general types. One type of observation is based on the direct microscopic determination of the isothermal rate of spherulitic formation and growth. The other type is concerned with following the changes of a property very sensitive to crystallinity, such as measurement of the density, and in some favorable cases the changes in an infrared absorption band can be used. The latter type of measurements is performed

on the assumption that a semi-crystalline polymer consists of well defined crystalline and amorphous fractions. Thus if any property for the crystalline and the amorphous state is known, the measurement of this property will yield the relative amounts of the two phases. For example, volume[15] and heat capacity[16] had been used for polyethylene as the properties characterizing the transition from the crystalline to the amorphous state. Different from a sharp break presumably representing the melting of the most perfect crystallites, an extended temperature range over which melting occurs is revealed by both methods. The degree of crystallinity of cellulose was estimated by Hermans and Weidinger[17] according to the ratio of the integrated intensities of X-rays scattered in the sharp diffraction peaks and the amorphous halo. Their approach was greatly improved by Krimm and Tobolsky[18] who estimated the amorphous content of semi-crystalline samples by using the X-ray scattering from a polyethylene melt as a basis of reference. Their results were similar to those obtained by density measurement. In 1960 Ke[19] introduced differential thermal analysis (DTA) to estimate crystallinity in polymers. With more advantages than other traditional methods, it later became the preferred method for the study of phase transitions. Among these methods, density measurement and X-ray diffraction are perhaps the simplest methods to evaluate crystallinity in polymers. The agreement between these two methods is fairly good in most of the cases.

1.2.1. Density Method

The density of a polymer may be used to calculate the degree of crystallinity of a polymer. The determination of crystallinity is based on the observation that there is a relatively large and measurable difference (up to

20%) between the densities of the crystalline and amorphous regions of the polymer. Because the crystalline polymers have a higher density than the non-crystalline polymer, a polymer crystallized from the melt is accompanied by a reduction in specimen volume due to an increase in density. This effect provides the basis of the density method for the determination of the degree of crystallinity. Under the assumption that polymer is composed of two distinct phases, the degree of crystallinity is most commonly derived by the following expression[20]:

$$V = V_a + V_c \tag{1.2-1}$$

$$W = W_a + W_c \tag{1.2-2}$$

$$\rho V = \rho_a V_a + \rho_c V_c \tag{1.2-3}$$

$$f_c = \frac{V_c}{V} = \frac{\rho - \rho_a}{\rho_c - \rho_a} \tag{1.2-4}$$

$$\chi_c = \frac{W_c}{W} = \frac{\rho_c V_c}{\rho V} \tag{1.2-5}$$

where ρ is the measured density of the specimen, ρ_a the density of wholly amorphous fraction, ρ_c the theoretical density of wholly crystalline polymer, f_c and χ_c represents the volume fraction and mass fraction of crystals, respectively. However equations (1.2-4) and (1.2-5) are not valid for the samples containing any hole or void, which is often present in molded samples, or if ρ_a is not constant. Combining equations (1.2-4) and (1.2-5) gives

$$\chi_c = \frac{\rho_c(\rho - \rho_a)}{\rho(\rho_c - \rho_a)} \tag{1.2-6}$$

The term ρ_c can be determined from knowledge of the crystal structure. The

density of the amorphous regions ρ_a can be measured directly from a completely amorphous form obtained by quenching of a polymer melt or it can be calculated by extrapolating either the density of a series of semi-crystalline samples to zero crystallinity or that of the melt to the temperature of interest.

However, the determination of the degree of crystallinity by this method is subject to certain reservations: there are no two completely defined amorphous and crystalline phases.

1.2.2. X-ray Diffraction Method

A powerful method of determining the crystallinity is the X-ray technique which not only permits determination of the quantitative ratio between crystalline and amorphous portions but also gives a deeper insight into the structure of crystalline polymers. Based on the facts that the crystallized portion of polymers gives rise to sharp X-ray diffraction peaks while the amorphous phase produces a very broad X-ray diffraction peak, the degree of crystallinity can therefore be estimated from the relative areas under these two types of peaks. A typical X-ray scattering curve for a semi-crystalline polymer is made up by the broad underlying hump due to scattering from amorphous areas and the relatively sharp peaks due to scattering from the crystalline regions. The determination of the degree of crystallinity is then performed from the ratio of the areas under the crystalline peaks and the amorphous hump. To a first approximation the mass fraction of crystals χ_c is calculated by

$$\chi_c = \frac{A_c}{A_a + A_c} \qquad (1.2\text{-}7)$$

where A_c is the area under the crystalline peaks and A_a is the area remaining under the amorphous hump. The uncertainty of using this method comes when extremely small crystallites give such broad X-ray diffraction peaks that they may be interpreted as amorphous peaks[20].

1.2.3. DSC Method and DTA Method

Differential scanning calorimetry (DSC) and differential thermal analysis (DTA) are similar techniques. They both measure changes in the heat capacity of a sample. The advantages of DSC and DTA over a good adiabatic calorimeter include speed, low cost, and the ability to use small samples. The principles of these methods are described below. A thermogram is known as a plot of ΔT as a function of either time or temperature. Since the specific heat is directly proportional to the temperature difference, the curves resemble inverted heat capacity curves.

If the heat of fusion of the pure polymer crystal is known, the absolute degree of crystallinity may be calculated from calorimetric data according to

$$\chi_c(t) = \frac{\Delta H_m(t)}{\Delta H_f} \qquad (1.2\text{-}8)$$

where $\Delta H_m(t)$ is the heat of crystallization evolved by one gram of the crystallizing melt at time t, ΔH_f refers to the fusion enthalpy of a perfect polymer crystal.

In the case of DSC, experimental data may be used to determine the heat of fusion (or heat of crystallization respectively) per unit weight specimen, permitting an estimate of the fraction of crystalline material. DSC

directly measures the rate of evolution of the enthalpy of crystallization in a sample as a function of temperature. The vertical axis is usually labeled as the heat flow in cal/sec.

For isothermal quiescent crystallization, the crystallinity of the examined sample, $\chi_c(t)$ at time t, at crystallization temperature T_c, is evaluated by integrating the rate curve according to the following equation[21,22]:

$$\frac{\chi_c(t)}{\chi_c(\infty)} = \frac{\int_0^t \left(\frac{dH}{dt}\right) dt}{\int_0^\infty \left(\frac{dH}{dt}\right) dt} \qquad (1.2\text{-}9)$$

where dH/dt is heat evolved during the isothermal crystallization which can be recorded as a function of time, t, and the crystallinity fraction, $\chi_c(\infty)$, of the sample is determined as the ratio of total heat evolved at the end of the crystallization to the fusion enthalpy ΔH_f of a sample with 100% crystallinity according to equation (1.2-8). The upper integral is the crystallization heat evolved at time t, and the lower one is the total heat evolved at the end of the crystallization.

1.2.4. Depolarized Light Intensity Method

The degree of crystallinity of samples can also be determined using a polarizing microscope equipped with a hot-stage, photomultiplier tube, and recorder. Plots of the depolarized light intensity versus crystallization time (or temperature) at various crystallization temperature (or cooling rates) are readily transformed to determine the relative crystallized fraction $\chi_c(t)$ in terms of[23]

$$\chi_c(t) = \frac{I_t - I_o}{I_\infty - I_o} \qquad (1.2\text{-}10)$$

where I_o, I_t and I_∞ represent the polarized light intensities corresponding to the initial, intermediate and final stages of the crystallization process.

1.2.5. Infrared Method

Crystalline polymers often show different infrared absorption bands than amorphous ones. The relative intensity of such absorption bands may be used to calculate the degree of crystallinity. For example, the intensity of the bands 1168, 998, 899, 842 and 809 cm^{-1} of the infrared absorption spectrum of isotactic polypropylene decreases as the crystallinity increases and disappears in the infrared absorption spectrum of the molten polymer. The degree of crystallinity of polypropylene is often calculated from the transmission curves of the 998 cm^{-1} band, assuming a linear relationship between the optical density of the crystalline sensitive bands and the crystallinity of the polymer, using the relationship[24]:

$$\frac{\chi_c(t)}{\chi_c(\infty)} = \frac{\ln \frac{D_o}{D_t}}{\ln \frac{D_o}{D_\infty}} \qquad (1.2\text{-}11)$$

Here D_o denotes the transmission at the moment of beginning of crystallization, D_t is the transmission at the time t, D_∞ is the transmission at the end of crystallization in the test time scale, $\chi_c(t)$ and $\chi_c(\infty)$ are the crystallinity at the time t and at the termination of the crystallization, respectively.

1.3. Effects on Crystallization

It should be noted that the extent to which crystallization occurs in a given polymer is not invariant, but varies with the type of polymer and its molecular microstructure and is also affected by processing variables such as the rate of cooling, the presence of orientation in the melt and the melt temperature[25,26]. Other factors include the stereoregularity and molecular weight of the polymer, the amount of chain branching and the presence of any additives which may act as nucleating agents[27].

Changes in process and material parameters can have a significant effect on the overall rate of crystallization. This leads in turn to determining the ultimate degree of crystallinity achieved in a polymer. Depending on chemical structure, molecular weight and crystallization conditions, the value of crystallinity for homopolymers can range from 25-30% at one extreme to about 90-95% at the other. For copolymers with structurally irregular chains, the degree of crystallinity can be lowered even further[28]. Electron microscopic studies have shown that polymer crystallization is dependent on the molecular weight and crystallization conditions[29].

1.3.1. Effect of Crystallization Temperature

Temperature has a very pronounced effect on the overall rate of crystallization which in turn determines the final crystallinity obtained in the polymer. It is a well established experiment which states that the rate of crystallization with temperature for polymers follows almost an invariant pattern. The rate of crystallization will achieve a maximum at some crystallization temperature as indicated in Figure 3, where reciprocal half-times (i.e. the time required for one-half the final crystallinity as measured

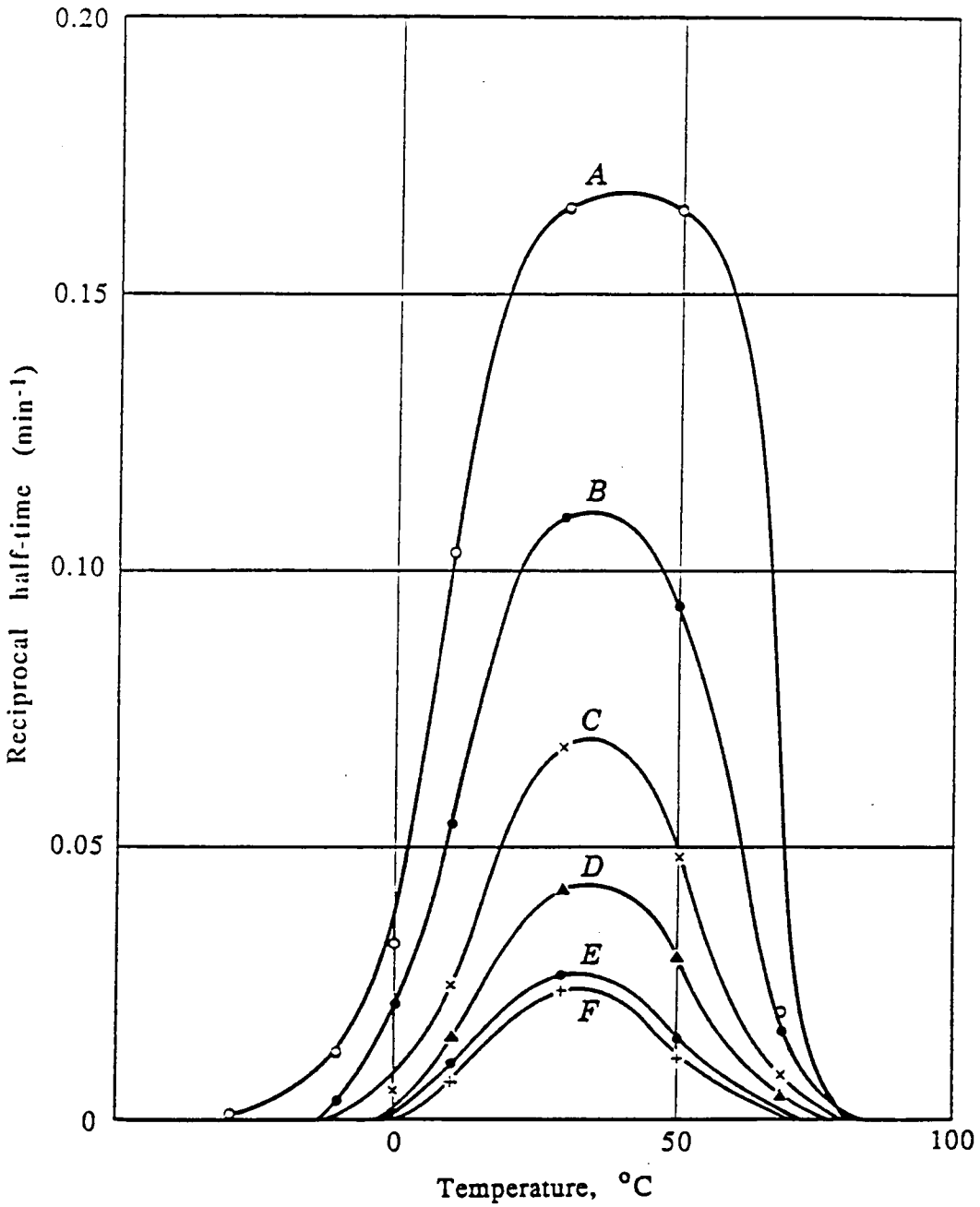

Figure 3. Reciprocal half-times for a family of polyethylene succinates[30]. The molecular weight increases from curve A to curve F.

by dilatometry) of polyethylene succinates are plotted against crystallization temperature[30]. For polymers to crystallize isothermally under quiescent conditions, it is expected then that different extents of crystallinity will develop at different crystallization temperatures.

1.3.2. Effect of Molecular Weight

In many aspects polymer crystallization is similar to low-molecular weight systems. Basically the intermolecular van der Waal's forces tend to align the molecules to obtain a more stable state. However, the huge polymer molecular sizes cause more difficult in their movement. This lack of mobility, therefore, results in a much longer crystallization time and in many cases prohibits complete crystallization.

Molecular weight affects crystallization at both extremes. At a given temperature the chains with low molecular weight have higher mobility and therefore enhance crystals growth. On the contrary, very high molecular weight chains have restricted mobility which in turn depresses the crystallization rate. As a result, it is expected that polymers crystallize with increased rates at lower molecular weights. The dependence of crystallization rate on molecular weight has been demonstrated for several polymers. Figure 3 shows the dependence of crystallization rate on the molecular weight for a family of polyethylene succinates. These variations appear to be quite intimately connected with the influence of molecular weight on the crystallization. Chemical factors tending to produce easily crystallizable polymers are a) simple, relatively branch-free chains so that chain alignment is not hindered; and b) the existence of polar groups on the molecules which increase intermolecular van der Waal's forces[27]. Therefore,

for that reason, branches, particularly of bulky, rigid side groups or grafts, may be expected to reduce the rate of crystallization.

1.3.3. Effect of Cooling Rates

Polymer molecules have sufficient kinetic energy to move at temperatures well above the melting point. As the temperature is lowered, kinetic energy and molecular mobility decrease, and the intermolecular forces tend to align the molecules to produce an ordered structure.

In the case of rapid cooling, the crystallization rate can be depressed to some extent, depending on the crystallization kinetics. In fact, the crystallization can be almost completely suppressed by rapid cooling for some materials with sufficiently slow crystallization kinetics. Poly(ethylene terephthalate) (PET) is observed as a well-known example[28]. PET is almost completely amorphous with a density of about 1.33 gm/cm^3 under the condition of rapid quenching. If it is cooled slowly, it is able to crystallize with a higher density of about 1.40 gm/cm^3. For polymers with rapid crystallization kinetics their percentage of crystallinity is not much affected by the cooling rate; however, the crystallite morphology may be strongly affected. These differences in morphology can cause significant changes in physical properties. As indicated in Figure 4, the final crystallinity achieved at different cooling rate in polypropylene is observed almost the same. It is also observed that the temperature at which polypropylene begins to crystallize shifts to lower temperature at higher cooling rate.

1.3.4. Effect of Nucleating Agents

The overall rate of crystallization in pure polymers depends on the product of the rates of two processes: nucleation and crystal growth. The

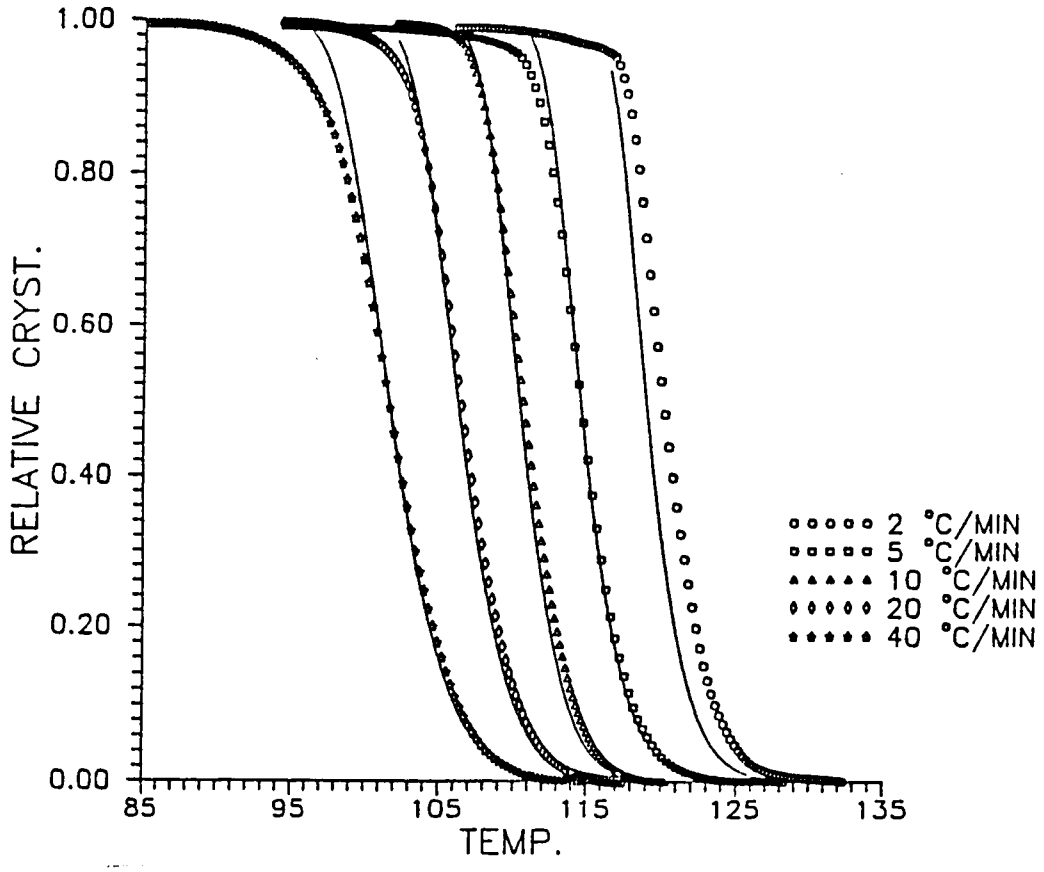

Figure 4. Non-isothermal crystallization data of polypropylene at several cooling rates[31].

existence of nucleating agents favor the nucleation step by increasing the nuclei concentration and thereby accelerates the overall rate of crystallization. Many reports have already shown that heterogeneous nucleators[32], dyes, pigments[33], and other fillers can act as nucleators to increase crystallinity.

The presence of nucleating agents also affects the temperature at which maximum crystallization rate occurs. The maximum crystallization rate temperature for polypropylene, as reported, can be shifted from 100°C without nucleating agents up to 140°C with most effective nucleating agents available[7].

1.3.5. Effect of the Presence of Orientation in Melt

The thermal history of the melt prior to the start of crystallization is also very important in determining the rate of crystallization. Crystallization rates of nylon 6[23] and polypropylene[34] have been observed to be slower when cooled from higher temperatures above their melting points than when cooled from temperatures just above their melting point. The evidence suggests that, after the bulk of the polymer has melted, molecular order tends to persist which aids in the nucleation process upon subsequent cooling. It is now well known that the presence of any pre-orientation order in the melt (sometimes also called 'melt structure') would facilitate the formation of nuclei in the process of crystallization. This melt structure is destroyed by prolonged heating at elevated temperature so that the rate of nuclei formation is reduced. Since the linear rate of growth of a given nucleus is essentially independent of these variations, the overall crystallization rate is significantly reduced. Mechanical stress, by aligning the polymer molecules,

also enhances crystallizability of polymers[35].

1.3.6. Effect of Stereoregularity

Structural regularity is a primary requisite for the crystallization of a polymer. Fulfillment of this requirement is dictated by the long-range order and symmetry that is characteristic of the crystalline state. It follows that, in order to crystallize, a polymer chain must consist of identical units regularly repeated throughout its length. To obtain a high degree of crystallinity, stereochemical regularity in the polymer must be maintained as well. Presence of structural or stereochemical irregularities in macromolecules lowers the melting point and decreases the degree of crystallinity.

Although there is no direct relationship between tacticity and the degree of crystallinity of a particular sample, Natta[36] and Miller[37] have demonstrated the profound effect that tacticity of a sample has on its equilibrium crystallinity. This is evident from an experiment made by Natta that the equilibrium degree of crystallinity decreases as the solubility in heptane decreases (a measure of atactic content)[36].

1.3.7. Effect of Annealing

Annealing is the process of exposing the polymer to an elevated temperature for a certain period of time. This is sometimes performed as a post-extrusion operation to control the polymer morphology as well as physical properties.

Although there is a great deal of uncertainty concerning the details of the effects of annealing crystalline polymers, experimental results suggest that it could increase crystallinity as well as the crystallite size[38]. As one

might expect, annealing a semi-crystalline material should increase its crystallinity also. A polyethylene specimen with a density of 0.952 gm/cm^3 annealed at 149°C for one hour increased its density to 0.953 gm/cm^3. The same material annealed at 212°C increased its density to 0.955 gm/cm^3. It is also observed that increasing the annealing time to 1.5 hours did not change the density at the annealing temperature of 149°C. The same annealing conditions but at 212°C increased the density[39] to 0.954 gm/cm^3. For practical purposes the main advantage of annealing is to relieve internal stresses in semi-crystalline polymers.

Polymers are often cooled rapidly from the melt, particularly when they are being industrially processed. In this situation crystallization is controlled by kinetics and the rate at which the crystals nucleate and grow becomes important. With many crystallizable polymers it is possible to cool the melt so rapidly that crystallization is completely prohibited and an amorphous glassy polymer results. With these systems crystallization can normally be induced by annealing the amorphous polymer at a temperature between the glass transition temperature and the melting-point, T_m, of the material.

1.4. Kinetics of Crystallization

The earliest investigation of polymer crystallization began in 1934 by Bekkedahl with the dilatometric observations of the crystallization of natural rubber[40]. He first observed that the total amount of crystallinity developing in a homopolymer under isothermal condition follows an almost universal pattern. Such typical behavior, the sigmoidal-shaped crystallization curves (when the fractional change in volume, $\Delta V/\Delta V_\infty$, is plotted against log time)

and their superimposability when shifted along the log time axis, are now known as characteristics for the crystallization of all homopolymer studies and again demonstrated as a family of isotherms in Figure 5 for the crystallization from the melt of a linear polypropylene polymer[41]. In this plot V_o represents the initial specific volume, V_∞ the final specific volume and V_t the volume at time t.

A few years later, the intention to describe quantitatively the macroscopic crystallization kinetics in terms of nucleation and linear crystal growth was carried out by Kolmogoroff[42], Johnson and Mehl[43], and Avrami[44,45]. Two processes, initiation and propagation of the new phase within the material, are considered to occur in a phase transformation. Thus the kinetics of an isothermal crystallization can be described by an adequate characterization of the nucleation and growth processes. These assumptions are employed by Kolmogoroff, Johnson and Mehl, and Avrami in the development of crystallization kinetics in monomeric materials[42,43,44,45]. Having the same idea used by Poisson in 1837 in solving the old problem, expanding waves created by raindrops on a pond, Evans[46] also developed similar descriptions for the phase transformation.

In the 1940's Wood and Bekkedahl[47] reported their experimental results in the studies of the crystallization kinetics and melting of natural rubber. They demonstrated the fact that crystalline polymers could be quantitatively studied using methods which were well known for low molecular weight crystalline substances. Flory[48] in 1949 presented thermodynamic theory of the fusion of polymers which has had many major and far reaching consequences. The superimposability of the isotherms and

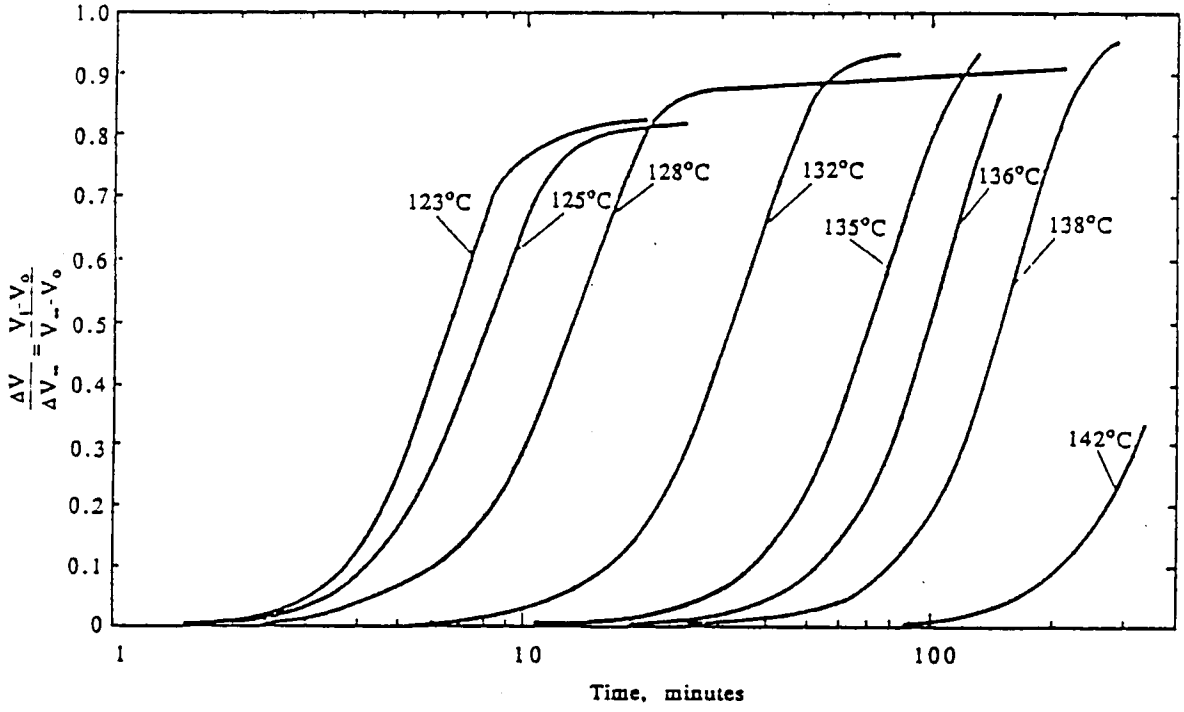

Figure 5. Fractional change in volume during crystallization of polypropylene at various temperatures as a function time[41].

its consequence, the invariance of the temperature coefficient, lend strong support to the assumption that both nucleation and growth rates are concurrent processes which are initiated at zero time.

Two reviews of this work about the process of polymer crystallization have appeared[25,49]. Since then numerous investigations, both experimental and theoretical, have been made of semi-crystalline polymeric materials. Main attention has been concentrated on the kinetics and morphology of crystallization under isothermal conditions. These studies have led to a better understanding of fundamental features of polymer crystallization, but they do not provide adequate information for solidification of the polymer process. The process of polymer crystallization during practical processing occurs non-isothermally, except for some special cases. Examples of typical non-isothermal crystallization process include melt-spinning, blow molding, profile extrusion, and pipe extrusion.

In other words, isothermal crystallizations are rarely used in practice and nonisothermal crystallization is so far not fully understood and only few works can be found until recently. Therefore, the kinetics of nonisothermal crystallization is required to be studied for the analysis of the practical processes in terms of polymer characteristics and cooling conditions.

1.4.1. Induction Time

As in most crystallization processes, in the absence of nucleation, there is an induction period during which disentanglement of chains takes place. This stage is followed by a slow rate of crystal growth. When a polymer is cooled below its melting point, crystallization does not occur immediately since the long chains of the polymer must diffuse through the other long

chains to the growing sites. A time interval is needed for the polymer molecules to align in preparation to crystallize. McKelvey[50] refers to this as the induction time, τ_i. As shown in Figure 5 the induction time for polypropylene at a quench temperature of 123°C is much less than that at 142°C. The results indicate that the induction time is strongly dependent on temperature. It has been known that the relationship between the undercooling ΔT and the induction time can be expressed with a relation of the form

$$\tau_i \propto \Delta T^{-\varepsilon} \qquad (1.4\text{-}1)$$

where ε is a characteristic constant whose value depends on the polymer and ΔT represents the temperature difference between the melting point and the crystallization temperature[51].

1.4.2. Isothermal Crystallization

The studies of isothermal crystallization kinetics of a bulk polymer melts during the crystallization process are usually carried out with the measurement of specific volume by dilatometry, the measurement of changes in the heat capacity by DSC or DTA, or the direct measurement of the rate of growth of spherulites in the supercooled molten polymer, using a microscope. Other methods which have been used include infrared spectrophotometry[24,52,53] and depolarized light intensity technique[54]. The dilatometric technique measures the changes in volume with time[51]. About a gram of sample is examined, and running time is taken in the order of hours. Families of curves may be generated to show the effects of temperature. Polarizing microscopes with hot stage mounted polymer samples have been

used to follow the crystallization process[55,56].

The rate at which crystallization proceeds at constant temperature, once the induction time has passed, has been described by the Avrami[44,45] and presented best in Mandelkern's work[49]. The picture used in their theory has been that nuclei appear randomly in the supercooled melt, and then growth of crystals follows at a constant linear rate in one, two, or three dimensions. The fundamental assumption inherent in their theory is that under isothermal conditions nucleation and growth rates are governed by rate constants that are invariant with time. The degree of phase transformation, $\chi_c(t)$, is related to time and can be stated following the general Avrami equation

$$\chi_c(t) = 1 - \exp(-k_c t^n) \qquad (1.4\text{-}2)$$

where k_c is the kinetic rate constant which is a function of both nucleation and growth rates and n is a parameter, the Avrami exponent, whose value depends on the nature of nucleation and the geometry of the growing crystals. Accordingly,

$$\ln\{-\ln[1- \chi_c(t)]\} = n\cdot\ln(t) + \ln k_c \qquad (1.4\text{-}3)$$

It is observed that the plot of the left-hand side of equation (1.4-3) as a function of ln(t) will give a straight line of slope n. The rate constant, k_c, can then be calculated from the half-time, $t_{0.5}$ (i.e. the time required for half of final crystallinity to develop), and the average value of n, since:

$$k_c = \frac{\ln(2)}{(t_{0.5})^n} \qquad (1.4\text{-}4)$$

The crystallization mechanisms for various values of n are listed in Table 1. Sporadic nucleation mentioned in the table means that the number of nuclei in the supercooled melt continually increases during the solidification process, while predetermined nucleation means that the density of nucleation sites present in the melt does not change during the crystallization process. As stated by Morgan[58], the exponent n in the Avrami equation may even have values ranging from 1 to 8. The Avrami equation, in fact, has not been very successful in distinguishing the different crystallization mechanisms. It should be however kept in mind that the Avrami equation describes only some idealized cases and that for more general conditions, the apparent values of n given by differentiating equation (1.4-3)

$$n_{app} = \frac{d(\ln[-\ln(1-\chi_c(t))])}{d(\ln(t))} \qquad (1.4\text{-}5)$$

do not characterize the crystallization mechanism unequivocally. Often a fractional value for n is found[59,60]. In some cases polymers have been observed with both homogeneous and heterogeneous nucleation, each in different temperature ranges. Also, the experimental data frequently showing deviation from the Avrami equation are obtained over longer crystallization times[22,41] in the crystallization course. This fact is attributed to the onset of secondary crystallization processes. In reality, the Avrami equation is only applicable in the early stages of crystallization, and secondary crystallization becomes dominant in the advanced stages of

Table 1. Relation of Avrami exponent n to special cases of isothermal crystallization[57].

Growth Geometry	Growth Control	Nucleation Type	n
1-Dimensional	Diffusion	Predetermined	$\frac{1}{2}$
1-Dimensional	Interface	Predetermined	1
1-Dimensional	Diffusion	Sporadic	$\frac{3}{2}$
1-Dimensional	Interface	Sporadic	2
2-Dimensional	Diffusion	Predetermined	1
2-Dimensional	Interface	Predetermined	2
2-Dimensional	Diffusion	Sporadic	2
2-Dimensional	Interface	Sporadic	3
3-Dimensional	Diffusion	Predetermined	$\frac{3}{2}$
3-Dimensional	Interface	Predetermined	3
3-Dimensional	Diffusion	Sporadic	$\frac{5}{2}$
3-Dimensional	Interface	Sporadic	4

crystallization[61,62]. For many isothermal cases of polymer crystallization, equation (1.4-2) proved to be adequate within a considerable range of variables[12]. However, without additional information of nucleation, morphology, and the possible mechanism upon which Avrami exponent n depends, the Avrami equation is only a convenient macroscopic way to interpret experimental data of crystallization.

The Avrami equation predicts the hypothetical degree of transformation to be $\chi_c=1$ when time tends to infinity. Unlike crystallization of monomeric substances, polymers do not crystallize completely. The Avrami equation, hence, can be further modified by replacing the absolute degree of transformation, χ_c, by its relative value

$$\frac{\chi_c(t)}{\chi_c(\infty)} = 1 - \exp(-k_c t^n); \qquad \chi_c(\infty) \leq 1 \qquad (1.4\text{-}6)$$

In the case of isothermal crystallization, the experimental data generally is well fitted to the Avrami equation in nucleation processes but many reports have indicated that two distinct crystallization mechanisms occur consecutively or simultaneously: a primary crystallization characterized by the growth of the fibrils of the spherulites, and a secondary crystallization, which is active at larger crystallization times, related to the crystallization of more defective molecules in the intraspherulitic or interfibrillar regions[22,63].

Hillier[64], taking the concurrence of primary and secondary crystallization processes into account, proposed a modified two-stage Avrami equation which is written by:

$$\chi_c(t) = \chi_{c,p}(\infty)\{1-\exp(-k_{c,p}t^n)\} + \chi_{c,s}(\infty)\, k_{c,s} \int_0^t \{1-\exp(-k_{c,p}\tau^n)\}\{\exp(-k_{c,s}(t-\tau))\}d\tau \qquad (1.4\text{-}7)$$

where the subscripts p and s refer to primary and secondary, respectively. This modified two-stage equation, as demonstrated by Chu[65] in his studies of polyethylene, provides a much better fit than the Avrami equation for the experimental data, especially during the latter part of the crystallization process.

Velisaris and Seferis[66] in their studies of isothermal crystallization of PEEK suggested that two separate Avrami type crystallization processes, two nucleation and growth processes, need to be taken into account by dual crystallization mechanisms. Their description of degree of crystallinity as a function of time at isothermal crystallization temperature T may be related to a linear combination of two Avrami equations:

$$\frac{\chi_c}{\chi_{c\infty}} = w_1\{1-\exp(-k_{c,1}(T)t^{n_1})\} + w_2\{1-\exp(-k_{c,2}(T)t^{n_2})\} \qquad (1.4\text{-}8)$$

with $w_1 + w_2 = 1$. Here subscripts 1 and 2 represent the first and second mechanisms, respectively.

This model corresponds to two different nucleation or growth processes occurring in parallel, with the relative importance of each manifested by the value of the weight factor. They also extended the above expression to describe nonisothermal crystallization by utilizing an integral Avrami form[64,65,67] instead of general Avrami expression.

The prior existing theories to predict polymer crystallization were limited in practice to steady, isothermal conditions. The general equation (1.4-2) cannot treat effectively the more complex crystallization conditions, such as solidification in real conditions of polymer processing. Based on direct empirical data and simpler theories which is similar to chemical reaction consideration, Ziabicki[67,68] stated, instead of equation (1.4-2), the first-order kinetic equation[67]

$$\frac{d\chi_c}{dt} = k_c(t)\,[\chi_{c\infty}(t) - \chi_c] \qquad (1.4\text{-}9)$$

which can easily be solved once functions $k_c(t)$ and $\chi_{c\infty}(t)$ are given. In this approach, crystallization rate, $k_c(t)$, and crystallinity, $\chi_c(t)$, can be determined indirectly in appropriately designed experiments when the function, $k_c(t)$, and the equilibrium crystallinity, $\chi_{c\infty}$, can be related to functions of some time-dependent parameter $\phi(t)$ (e.g., temperature, concentration, orientation factor, etc.). Such a transformed model

$$\frac{d\chi_c}{dt} = k_c(\phi(t))\,\{\chi_{c\infty}(\phi(t)) - \chi_c\} \qquad (1.4\text{-}10)$$

can be used to predict the crystallinity development in any slow variations of temperature, composition, etc. If the value, $\chi_{c\infty}$, is a constant, the rate constant, $k_c(\phi)$, can be expressed as a function of crystallization half-time $t_{0.5}$. According to equation (1.4-10), the degree of crystallinity then is given as

$$\ln(1 - \frac{\chi_c}{\chi_{c\infty}}) = -\ln(2)\cdot \int_0^t \frac{d\tau}{t_{0.5}(\phi(\tau))} \qquad (1.4\text{-}11)$$

Cahn[69] and Ozawa[70] also proposed similar approximations. Generally speaking, the first-order kinetic model proposed by Ziabicki corresponds to the Avrami equation only when the Avrami exponent n equals 1.

Nakamura, Katayama, and Amano[71,72] made some simplifying assumptions, namely isokinetic condition, to derive from the Kolmogoroff-Avrami-Evans theory a more tractable equation to describe complex crystallization processes. The assumption is in fact arbitrary. Ziabicki[73] indicated that no theoretical justification has been made for non-isothermal process treatment even if isokinetic conditions can be accepted in isothermal crystallization.

1.4.3. Nonisothermal Crystallization

Experimental information about non-isothermal crystallization of polymers is very scanty. The effect of cooling (or heating) rates on crystallization kinetics remains almost unknown. Ozawa[70] tried to relate the effect of cooling rate to the crystallization of poly(ethylene terephthalate) with a DSC instrument. He assumed that the mathematical derivation of Evans is valid for polymer melt which is heated or cooled at a constant rate and then extended the Avrami equation to nonisothermal conditions in the following expression:

$$\ln\{1 - \frac{\chi_c(T)}{\chi_c(\infty)}\} = \frac{K(T)}{\Phi^n} \qquad (1.4\text{-}12)$$

Here $\chi_c(\infty)$ is the crystallinity at termination of the crystallization process, $\chi_c(T)$ is the crystallinity at temperature T, Φ is cooling (or heating) rate, and $\kappa(T)$ is a cooling (or heating) function. The integer n has a value between 1 and 4 depending on whether nucleation is predetermined or sporadic, and on the number of dimensions in which growth occurs. The agreement between Ozawa's experimental data of DSC measurements and the interpretation with his proposed approximate formulas seems to be consistent, but much higher precision would be needed for critical testing of the approach proposed. The Ozawa equation has been tested[70,74] for the crystallization of poly(ethylene terephthalenc) and nylon 6. Eder and Wlochowicz[75] utilized the Ozawa equation in their studies of effects of cooling rates on nonisothermal crystallization kinetics of polypropylene and high-density polyethylene. They found that the crystallization of polypropylene can be described by the Ozawa equation but is not valid for polyethylene because of secondary crystallization involved. The value of the Ozawa theory therefore remains doubtful in analyzing the crystallization process in polymer processing.

More systematic studies including isothermal and non-isothermal crystallization kinetics of high-density polyethylene have been performed by Nakamura, Katayama, and Amano[71]. The approach of Nakamura et al.[14,71] is concerned about the kinetics of crystallization under nonisothermal conditions with the assumptions of isokinetic condition (i.e. the ratio G/v is an invariant with respect to temperature, where G is the linear growth rate and v is the probability of the formation of a growth nucleus per germ nucleus per unit volume) and independence of the final crystallinity on the cooling process. The generalized form similar to Avrami equation reads as:

$$\frac{\chi_c}{\chi_{c\infty}} = 1 - \exp\left(-\left(\int_0^t \mathcal{K}_c(T)d\tau\right)^n\right) \qquad (1.4\text{-}13)$$

where $\mathcal{K}_c(T)$ is a sort of crystallization rate which is dependent on temperature and related to $k_c(T)$ in the Avrami equation through the following relation:

$$\mathcal{K}_c(T) = \{k_c(T)\}^{(1/n)} \qquad (1.4\text{-}14)$$

According to their approach, nonisothermal crystallization can be analyzed in terms of data from isothermal crystallization experiments. In many cases, a differential form of equation (1.4-13) is convenient. The differential form is[31]:

$$\frac{d\theta}{dt} = n\cdot\mathcal{K}_c(T)\cdot(1-\theta)[\ \ln(\frac{1}{1-\theta})\ ]^{(n-1)/n} \qquad (1.4\text{-}15)$$

where $\theta = \chi_c(t)/\chi_c(\infty)$ is defined as the relative degree of crystallinity.

Ziabicki[67] considered the nonisothermal crystallization as a sequence of isothermal crystallization steps and neglected the effects of secondary crystallization, a modified Avrami equation leads to:

$$\chi_c(t) = \chi_c(\infty)\{1-\ \exp(-\int_0^t k_c(T(t))n\tau^{n-1}d\tau)\ \} \qquad (1.4\text{-}16)$$

where $k_c(T(t))$ is a function of temperature T, but not explicitly of time t. The temperature dependence of the crystallization rate constant required by the model could be obtained from the results of isothermal crystallization studies.

An empirical approach proposed by Dietz[76] describes the nonisothermal crystallization taking into account the effects of secondary crystallization in the differential form:

$$\frac{d\theta}{dt} = n \cdot k_c(T) \cdot t^{n-1}(1-\theta)\exp(\frac{-a\theta}{1-\theta}) \qquad a \geq 0 \qquad (1.4\text{-}17)$$

In addition to temperature, molecular orientation has the effect of accelerating the rate of crystallization at a constant temperature. So far, there is no quantitative formula expressing the relation between the rate of crystallization and molecular orientation, and experimental studies seeking this relation are very difficult because of the extremely high crystallization rates[77,78,79,80]. As being observed that direct use of the Avrami equation to describe crystallization kinetics with increasing molecular orientation, the rate constant k_c increases rapidly and the Avrami exponent n decreases[81] to 1 or even below[82].

1.4.4. Crystallization Rate

Since the time required to complete crystallization in polymers is sometimes indefinite, it is convenient to define the rate of crystallization at a given temperature as the inverse of the time taken for half of the final crystallinity to develop. The rate so defined is a characteristic function of temperature. In polymeric systems the overall rate of crystallization has already been known in general to be highly temperature dependent. The overall temperature range, wherein crystallization is possible, is constrained between the melting temperature and the glass transient temperature. The variation of the crystallization rate with temperature is first typified by the data of Wood and Bekkedahl[83] for natural rubber. Using a dilatometric

technique, they found that the rate of crystallization passes through a maximum at -25°C, being negligible at -50°C and 0°C. They also found that the melting range moves to higher temperatures as the crystallization temperature is raised. Similar behavior has been observed for a wide variety of polymer types including poly(ethylene terephthalate), poly(ethylene adipate), and poly(ethylene succinate)[49].

The variation of crystallization rate with temperature can be explained as a competition of the driving forces for crystallization, such as the formation of nuclei, and molecular mobility. At temperatures just below the melting temperature T_m, the crystallization rate becomes measurable but is very slow. When the temperature is lowered further, the rate accelerates because of the effects of increasing concentration of nuclei. The rate eventually passes through a maximum. At crystallization temperatures below the maximum the overall rate of crystallization decreases again as a result of the mobility of the molecules decreasing and crystallization becoming diffusion controlled. As the glass transition temperature is approached the rate becomes very slow, the polymer may be supercooled and maintained in the amorphous state. If the polymer is quenched rapidly from a temperature above T_m to a temperature below T_g, the solid polymer will be amorphous due to insufficient time for crystallization to occur.

Furthermore, for many polymers the crystallization rate becomes so rapid at temperatures further below T_m that it is extremely difficult to investigate isothermal crystallization experimentally and the determination of the temperature at which maximum rate occurs is almost impossible. In this case, a useful but approximate empirical rule states that the temperature

at which the polymer melt crystallizes at its maximum rate equals to about nine-tenths of its melting point on the absolute temperature scale[84]. For example, crystallizable isotactic polystyrene melts at 235°C and its temperature of maximum crystallization rate has been suggested to occur near 184°C. This is known to be about the correct value[85].

The presence of nuclei of sufficient size is required for crystals to grow from a polymer melt or solution. The formation of such nuclei is a function of temperature. Above the melting temperature thermal energy is large enough to disperse small nuclei that form and prevent their growth. As the material cools from the melting point, the kinetic effects decrease and the chances for formation of larger nuclei become greater. At each temperature below the melting point, there is a critical nucleus size above which the required energy for adding new molecules becomes greater than that for dispersing them. Just below the melting point this critical size reaches a maximum and decreases with temperature. Thus, as the temperature is lowered the average nucleus size increases, and the required critical size for crystal growth decreases. At some temperature in a rapidly cooling condition, many small nuclei suddenly reach critical size, and at the same time crystallization proceeds rapidly with many small crystallites forming simultaneously. On the contrary, fewer nuclei form and take longer time to reach critical size when the polymer is held at higher temperature; crystallization is slower but produces larger crystallites.

It is expected that the concentration of nuclei is high at low crystallization temperatures, where molecular chains are characterized by low energy levels. On the other hand, high crystallization temperatures

favor rapid crystal growth rates since the molecular chains have larger energy to move from the melt to the crystallizing surface. High temperatures decrease the barrier to chain movement, thus increase chain mobility and the rate of crystal growth. It is then expected that the rate of crystallization will have a maximum at some crystallization temperature.

This temperature dependence of the rate of crystallization is typical of phase transformations that require a nucleation step. An analysis of such a process is performed by Becker[86] for the decomposition of a solid solution and he pointed out that the activation energy should be the sum of two contributions, one representing the activation energy for the formation of a nucleus with the critical size, the other, the activation energy for diffusion across the phase boundary. As mentioned above the size of the critical nucleus decreases with an increasing increment of the temperature below the melting point, it was predicted that the nucleation rate would pass through a maximum. Mandelkern et al.[87] developed a specific theory for the rate of crystallization of chain molecules and concluded that not only the rate of nucleation but also the rate of crystal growth should pass through a maximum with the temperature variation. They predicted that the maximum rate of crystallization should be observed between 0.8 and 0.9 T_m, which agrees with the observation[52] that poly(ethylene terephthalate) crystallized most rapidly at 0.85 T_m. It should be noted that these theories applied to crystallization with homogeneous nucleation. Gent[88] showed for rubber that small additions of nucleating agents leads to large increases in the rate of crystallization and Price[89] pointed out that heterogeneous nucleation means a constant number of spherulites during polymer crystallization.

Flory and McIntyre[90] first made efforts to separately determine the rates of nuclei formation and spherulite growth as functions of temperature. They studied a polymer close to its melting point, where the temperature dependence of these rates is particularly pronounced. As expected, decreasing temperature accelerated both nucleation and spherulite growth: a drop of 5°C increased the nucleation rate by a factor of 10^4, and also increased the rate of spherulite growth by a factor of 10^3.

In the view of the theory of Johnson and Mehl[43], Avrami[44,45], and Mandelkern[12], the overall rate constant, k_c, depends on both nucleation rate and crystal growth rate and is proportional to NG^n, where N is the nucleation rate per unit volume, G the linear growth rate, and n the Avrami exponent. As stated by Ziabicki[91], the nucleation rate, N, consists of two different contributions

$$N = N_{th} + N_{ath} \tag{1.4-18}$$

in which N_{th} and N_{ath} represent the thermal and athermal nucleation rates, respectively, and have the following forms[91,92]

$$N_{th} = \text{Const.}\left(\frac{cKT}{h}\right)\exp\{\frac{-E_a}{KT}\}\exp\{\frac{-\Delta F^*}{KT}\} \tag{1.4-19}$$

$$N_{ath} = -\left(\frac{\partial R^*}{\partial T}\right)\left(\frac{dT}{dt}\right)\iint_{s^*} f\,dS \tag{1.4-20}$$

where h and K are Planck's and Boltzmann constants, respectively, R* a vector characteristic for the nucleus having critical dimensions, f the

distribution function of nucleus size and shape, S* the critical boundary between the regions of unstable and stable nuclei, E_a is the activation energy required for transport a segment across the nuclei-liquid interface, and ΔF^* is the free energy of a nucleus having a critical radius whose expression depends on the nature of the geometry of the crystal. The thermal nucleation rate is concerned with thermal fluctuations which result in the formation of nuclei and the athermal nucleation rate appears only when the thermodynamic state of the system, such as variable temperature, pressure, etc., is changed.

An impressive body of microscopic examination of crystallizing polymers in a wide range of temperatures has shown that the radial growth of isothermal spherulite is linear with time[43,44,45,46]. As an extension of the Turnbull-Fisher[93] general scheme for nucleation theory, growth processes, which are nucleation control, are usually described in terms of two-dimensional nucleation on the crystal surface. Therefore the isothermal, steady-state, linear growth rates, G, are also considered in the same form as equation

$$G = G_o \exp\{-\frac{\Delta F}{KT}\} \exp\{-\frac{\Delta \Phi^*}{KT}\} \qquad (1.4\text{-}21)$$

Here, G_o is a pre-exponential factor which is generally assumed to be temperature independent. The transport term, $\exp\{-\Delta F/KT\}$, is the probability of a chain segment of critical length to reach the surface of the crystal in the local transport process. The nucleation term, $\exp\{-\Delta \Phi^*/KT\}$, stands for the probability that the surface nucleus will reach a critical size. Accordingly, ΔF is the free activation energy necessary to transport a

polymer segment across the liquid-solid interface and $\Delta\Phi^*$ is the work required for formation of a nucleus of critical size, T is the crystallization temperature, K being the Boltzmann constant.

Suzuki and Kovacs[94] analyzed a variety of approximations for ΔF and $\Delta\Phi^*$ for polymers and showed that a particular relation proposed by Hoffman[95] for the growth rate is a good approximation:

$$G = G_o \exp\{-\frac{\Delta F_{WLF}}{RT}\} \exp\{-\frac{\Delta\Phi^*}{KT}\} \qquad (1.4\text{-}22)$$

In this equation $G_o = b_o KT^*/h$, h is Planck's constant, and T^* is the temperature of maximum growth rate. The WLF equation[96] gives an accurate prediction of the temperature dependence of the viscoelastic parameters between T_g and $T_g + 100^oK$, it seems reasonable to adopt a similar expression for calculating the transport term in equation (1.4-22). This was first pointed out by Hoffman et al.[97,98] and applied successfully by several authors[99,100,101] for representing the temperature dependence of spherulitic growth rate. The transport term ΔF_{WLF} is usually expressed as the activation energy for viscous flow according to the relation of Williams-Landel-Ferry:

$$\Delta F_{WLF} = \frac{C_1 T}{C_2 + T - T_g} \qquad (1.4\text{-}23)$$

where C_1 and C_2 are "universal" constants equal to 17.2 kJ/mol and 51.6 ^oK, respectively[102], and T_g is the glass transition temperature.

The nucleation term $\Delta\Phi^*$, according to the theoretical treatment of coherent surface nucleation in chain folded polymers given by Lauritzen

and Hoffman[97,103], may be expressed to a good approximation by:

$$\Delta\Phi^* = \frac{Yb_o\sigma\sigma_e T_m^o}{\Delta H_f \Delta T} \qquad (1.4\text{-}24)$$

where b_o is the thickness of the surface layer, defined by the crystalline lattice parameters, σ_e and σ are, respectively, the interfacial free energies per unit area in the directions parallel and perpendicular to the chain direction, T_m^o the equilibrium melting temperature, ΔH_f is the heat of fusion, ΔT ($=T_m^o - T$) is the extent of supercooling of the sample, and Y usually equals 4.

Equation (1.4-22) describes the growth rate of the lamellar spherulites. Using this equation, for predetermined nucleation with N_o nuclei the crystallization rate constant $k_c(T)$ in the Avrami equation can be expressed by the general form,

$$\{k_c(T)\}^{(1/n)} = \chi_{co} \exp\{-\frac{\Delta F_{WLF}}{RT}\}\exp\{-\frac{\Delta\Phi^*}{KT}\} \qquad (1.4\text{-}25)$$

where χ_{co} is a constant. After substituting the expressions for ΔF_{WLF} and $\Delta\Phi^*$, one obtains

$$\{k_c(T)\}^{(1/n)} = \chi_{co} \exp\{-\frac{C_1}{R(C_2+T-T_g)}\}\exp\{-\frac{Yb_o\sigma\sigma_e T_m^o}{K\Delta H_f T\Delta T}\} \qquad (1.4\text{-}26)$$

By introducing the following variables $U^* = C_1$, $T_\infty = T_g - C_2$, $C_3 = Yb_o\sigma\sigma_e T_m^o/K\Delta H_f$, and combining with equation (1.4-4) the above equation becomes

$$\frac{1}{t_{0.5}} = \left(\frac{1}{t_{0.5}}\right)_o \exp\{-\frac{U^*}{R(T-T_\infty)}\}\exp\{-\frac{C_3}{T\Delta T}\} \qquad (1.4\text{-}27)$$

where $(1/t_{0.5})_o = \mathcal{K}_{co}/(\ln(2))^{1/n}$ is a material characteristic constant. This expression provides a straightforward method to extrapolate the values of the rate constant to lower temperatures by obtaining the value of C_3 from the slope of a plot of $\{\ln(1/t_{0.5}) + U^*/R(T-T_\infty)\}$ against $\{1/T\Delta T\}$[104,105].

Nucleation and crystal growth rates and also, in consequence, the resulting crystallization rate are all very sensitive to temperature. At higher temperatures, the transport term, $\exp\{-U^*/R(T-T_\infty)\}$, being small compared to the nucleation term, the temperature dependence is determined in practice by the $\exp\{-C_3/T\Delta T\}$ term. At lower temperatures the transport term becomes important, and nucleation (or growth) rates pass through a maximum at some temperature T_{max}. This temperature could in principle be predicted using equations (1.4-26) or (1.4-27) if the parameters in these equations were known.

On the other hand, several empirical relations have been presented to predict the temperature dependence of half-times or overall rate constants. Ziabicki proposed that experimentally-observed crystallization half-times, $t_{0.5}$, can be reproduced well by the empirical relation[68]

$$\frac{1}{t_{0.5}} = \left(\frac{1}{t_{0.5}}\right)_{max} \exp\{-4\cdot\ln(2)\ \frac{(T-T_{max})^2}{\mathcal{D}^2}\} \qquad (1.4\text{-}28)$$

where $(1/t_{0.5})_{max}$ is the maximum rate at the temperature T_{max} and $\mathcal{D}$ is the half-width of the rate curve. It is well known that crystallization rates are limited to that range well below melting temperature, T_m, and above the glass transition temperature, T_g, below which macromolecular motions are frozen. In general, the values of $(1/t_{0.5})_{max}$, T_{max}, and $\mathcal{D}$ can be obtained from the data

of isothermal crystallization experiments.

Another relation for temperature dependence of half times has been proposed by Takayanagi and Kusumoto[106]

$$\frac{1}{t_{0.5}} = A \exp\{-\frac{BT}{(T-T_g+51.6)^2} - \frac{CT_m}{T(T_m-T)}\} \qquad (1.4\text{-}29)$$

where A, B, and C are three adjustable constants, T_m and T_g are two characteristic temperatures. However, equation (1.4-29) is derived from the nucleation rate theory on the conditions of small supercoolings and can cause major errors in the range of maximum crystallization rate temperature T_{max}, which is usually of the order of $0.8T_m$.

Assuming that nucleation is controlled by both the activation energy of the short distance diffusion of a crystallizing element across the phase boundary and the activation energy of formation of a nucleus with critical size, Wunderlich[107] proposed the overall crystallization rate constant takes on the same form as the nucleation rate constant[96], via:

$$k_c(T) = C_1 T \exp\{-\frac{C_2}{T-T_g+51.6} - \frac{C_3}{T(T_m-T)^2}\} \qquad (1.4\text{-}30)$$

where C_1 is a constant whose value depends on the temperature, C_2 an empirical parameter associated with the temperature dependence of viscosity, and C_3 denotes a parameter related to the free enthalpy of nucleation.

The effects of temperature on crystallization rate also has been

described[108] in the following equation:

$$k_c(T) = B - \left(\frac{4E_a}{k_c(T)}\right)\left(\frac{DT_m^2}{T^2(T_m-T)^2}\right) \qquad (1.4\text{-}31)$$

where k_c is the crystallization rate constant, B and D are characteristic constants for a given polymer, E_a is the activation energy for molecular diffusion, and T_m and T are the melting and crystallization temperatures, respectively.

Empirical correlations may predict polymer behaviors quite well; however, they are derived from experimental data fitting and are limited to some group of polymers. Based on theoretical considerations, equations (1.4-27), (1.4-29), and (1.4-30) are able to interpret the variation of crystallization rate with temperatures for a variety of polymers. As compared with the equation (1.4-27) proposed by Hoffman et al., equations (1.4-29) and (1.4-30) suffer from either inappropriate assumption or difficulty in finding three appropriate constants. Especially, equation (1.4-27), with fewer assumptions, can predict the variation of crystallization rate with temperatures in a wide range of temperatures and can accurately obtain the values of $(1/t_{0.5})_o$ and C_3 from isothermal experimental data.

HEAT TRANSFER IN POLYMERS

A key element in many polymer processing operations is the heat transfer from the surface of a solid or molten polymer to a surrounding medium, usually water or air. Transfer of heat from polymer melt to ambient media takes place by three mechanisms: radiation, free or natural convection, and forced convection. In most polymer processes the

contribution of radiative heat transfer is negligible when compared with convective heat transfer.

2.1. Convective Heat Transfer Coefficient

Heat transfer between polymer and ambient fluid is dependent upon the temperature, velocity, and physical properties of the fluid, shape and size of the fluid-solid interface, and the nature of fluid flow. There is no easy way to determine the value of convective heat transfer coefficient. However, convection heat transfer coefficient h usually can be expressed in dimensionless form by the Nusselt number

$$Nu = \frac{hL}{k} \tag{2.1-1}$$

where L is some characteristic length of the solid and k is the thermal conductivity of the fluid. The Nusselt number, characterizing the heat transfer coefficient, is basically a dimensionless temperature gradient averaged over the heat transfer surface. Physically it stands for the ratio of the actual heat transfer resistance, h, to the heat transfer resistance estimated by the characteristic dimension of the body (k/L) and is expressed as a function of two other dimensionless groups, $Nu = Nu(Gr,Pr)$, i.e. the Grashof and Prandtl numbers, respectively. These dimensionless numbers are defined as the expressions

$$Pr = \frac{C_p \mu}{k} \tag{2.1-2}$$

$$Gr = \frac{g\beta\rho^2 L^3 \Delta T}{\mu^2} \tag{2.1-3}$$

Here, C_p, μ, β, ρ denote, respectively, specific heat, viscosity, thermal expansion coefficient and density of the cooling medium; ΔT represents the temperature difference between the surface and the medium and g is the acceleration due to gravity. The Prandtl number physically represents the importance of the rate of molecular diffusion relative to the rate of thermal diffusion. The Grashof number, found in most correlations of natural convection heat transfer, serves in much the same role as Reynolds number in forced convection heat transfer. Note that the Prandtl number relates only to the fluid properties, while the Grashof number, in addition, upon temperature difference ΔT and characteristic dimension of the object. Furthermore, it is customary to use the fluid properties evaluated at the mean temperature between the surface and the bulk of the cooling fluid in convection equations.

The method of estimating values of the convection heat transfer coefficient for the special case of interest, heat loss by natural convection from a single stationary horizontal cylinder, is considered. The Nusselt number for heat transfer due to natural convection from a stationary horizontal cylinder can be computed with the following empirical equation:

$$Nu = 0.52\,[Gr \cdot Pr]^{1/4} \qquad (2.1\text{-}4)$$

This equation is applicable only when the product of the Grashof and Prandtl numbers is greater than about 10^4. In addition, the diameter of the cylinder as the characteristic length L is frequently used to evaluate the Nusselt and Grashof numbers.

When the polymer melt moves at a velocity or a transverse or parallel cooling medium is applied, heat transfer due to forced convection prevails and the Nusselt number which depends on the Prandtl number, the Reynolds number, and the exposed length of the cylinder, L, can be represented by a function of the form.

$$Nu = Nu(Pr,Re,L/D) \qquad (2.1\text{-}5)$$

In the case of melt spinning, a number of investigators have done extensive work, both theoretical and experimental, to predict the heat transfer coefficients for various systems with free and forced convections in the atmosphere of air. For the air cooling of a large-diameter rod, a first approximation, assuming an average heat transfer coefficient, is carried out. If, for instance, air were stagnant, the Reynolds number for air would be based on the speed of the moving cylinder. The Nusselt number, according to Rohsenow and Hartnett[109], can be calculated from

$$Nu = 0.648 \cdot Re^{1/2} \cdot Pr^{1/3} \qquad (2.1\text{-}6)$$

where $Re = \rho D V/\mu$ and $Pr = C_p\mu/k$. Here ρ, μ, C_p, and k are the physical properties of the cooling air, D the diameter, and V is the velocity of the moving cylinder.

2.2. Thermal Conductivity

Another inherent element of understanding the heat transfer concerns the properties of the polymer. Conduction heat transfer is always a

predominant mechanism within the molten polymer, especially when the viscosity of the polymer melt is relatively high.

Several correlations have been proposed in the review papers of Anderson[110] and Van Krevelen et al.[111]. However, in most cases data required for these correlations are not always available for a given polymer. For example, a correlation of semi-crystallized solid behavior with the ratios k_c/k_a, ρ_c/ρ_a, and degree of crystallinity was proposed by Eiermann[112]. This correlation needs the degree of crystallinity and three of the four quantities, thermal conductivities (k_c and k_a) and densities (ρ_c and ρ_a) of completely crystalline and amorphous polymers.

Luba and his coworkers[113] found for amorphous polymers at temperatures above $1.1T_g$, the following relation holds

$$k = \frac{6.3 \cdot 10^{-3}[1-0.00015(T-T_g)]}{T_g^{0.0216} M^{0.3}} \qquad (2.2\text{-}1)$$

where k is the thermal conductivity at polymer temperature T, T_g is the glass transition temperature, and M is the polymer molecular weight. For polystyrene and poly(methyl methacrylate) deviation of calculated values from experimental data is found generally to be about 1-2%. Also they found for semi-crystalline polymers at temperatures greater than their melting point thermal conductivity can be predicted by an expression similar to equation (2.2-1),

$$k = \frac{1.2 \cdot 10^{-2}(C_p)(\rho)^{1.33}}{T_m^{0.216} M^{0.3}} \qquad (2.2\text{-}2)$$

where k is the thermal conductivity, T_m the melting point, M is the polymer molecular weight, C_p the specific heat of the melt at the temperature desired, and ρ is the density of the examined polymer at 25°C. Values of k calculated from this equation were generally within 1% of deviation from experimental values for various polyethylene and nylon. Unfortunately, for temperatures below the melting point, this correlation can not correctly predict the behavior of semi-crystalline polymers[113].

2.3. Modelling of Heat Transfer

Heat transfer phenomena which are accompanied by a simultaneous phase change, such as solidification (or crystallization), are frequently encountered in polymer processing. In order for a phase change to take place in a one-component system, two conditions must be satisfied: a) the thermodynamic criteria which dictate the phase change, for example, the transformation temperature must be met; b) the appropriate latent heat of fusion must be liberated. In order to predict the behavior of phase change in the examined materials, a variety of work has been devoted to solution of the equation analyzing the transient cooling problem with a phase change.

In a classical analysis, it is assumed for most low molecular weight materials, that solidification takes place at a sharp solid-melt interface at some specified temperature, with a jump (discontinuity) in heat flux across the phase change interface, so that an alternative interfacial condition of heat flux is required. The phase transformation problem in this way is formulated by establishing a heat balance across two infinitesimal volume elements in melt and solid portions, respectively. For simplification, a stationary system, shown in Figure 6, with unsteady state unidirectional heat

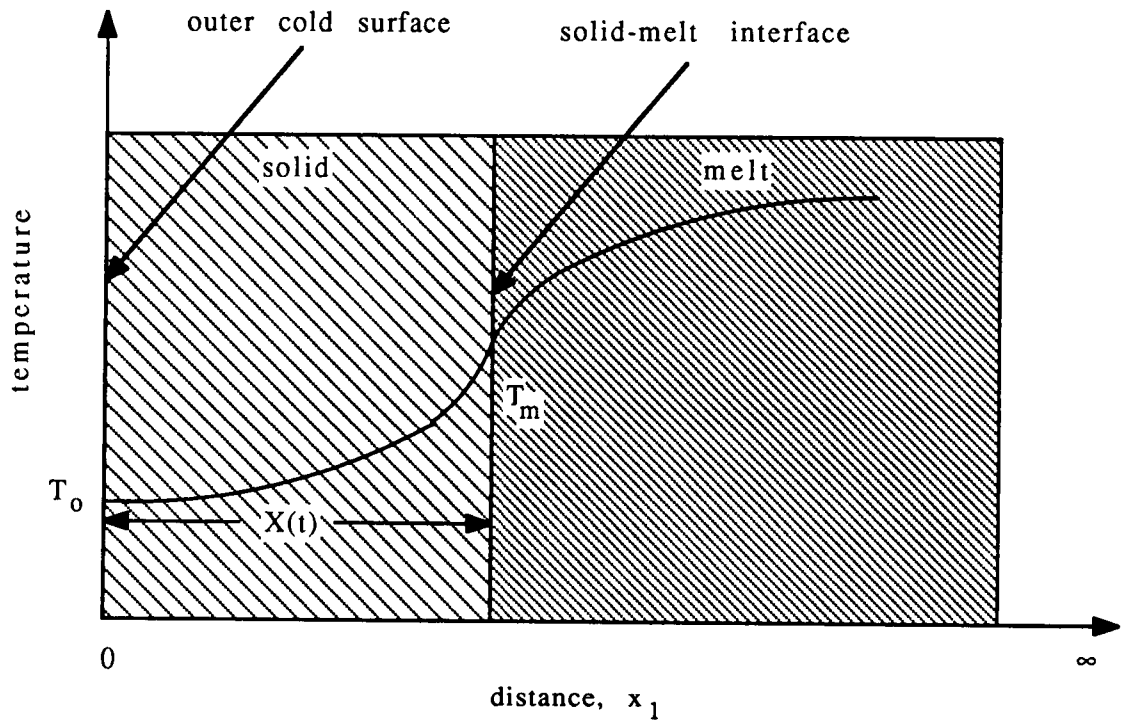

Figure 6. Solidification in a semi-infinite melt.

flow through the solid element (subscript s) is considered and the heat conduction in solid phase is then governed by

$$\rho_s C_{p,s} \frac{\partial T_s}{\partial t} = \frac{\partial}{\partial x_1}\left(k_s \frac{\partial T_s}{\partial x_1}\right) \qquad \text{for } 0 \le x_1 \le X(t) \qquad (2.3\text{-}1)$$

where k_s is the thermal conductivity of the solid. Similarly, for the melt volume element (subscript l)

$$\rho_l C_{p,l} \frac{\partial T_l}{\partial t} = \frac{\partial}{\partial x_1}\left(k_l \frac{\partial T_l}{\partial x_1}\right) \qquad \text{for } X(t) \le x_1 \le \infty \qquad (2.3\text{-}2)$$

where k_l is the thermal conductivity of the melt.

For a one-component system, the interface of the solid and molten phase at $x_1 = X(t)$ is time dependent, and the temperatures of solid and melt phases must obey

$$T_l = T_s = T_m \qquad \text{at } x_1 = X(t) \qquad (2.3\text{-}3)$$

in which T_m is the melting temperature. If the natural convection in the melt is assumed to be negligible in comparison with the rate of heat transfer by conduction, the advance of the solidification plane X(t), which relates to themelt and solid temperatures as well as to time, is obtained through energy conservation at the X(t) plane and can be expressed as the following form[114]:

$$k_l \frac{\partial T_l}{\partial x_1} - k_s \frac{\partial T_s}{\partial x_1} = \rho_s \Delta H \frac{dX(t)}{dt} \qquad (2.3\text{-}4)$$

where $\rho_s \Delta H$ stands for the latent heat release on solidification per unit volume of the melt.

Any analytical or numerical treatment of the problem in the form corresponding to that just described involves the difficulty of tracking the solid-melt interface X(t) and including the appropriate latent heat release. For numerical use, the heat conduction equation is derived based on a heat balance over an infinitesimal volume element:

$$\begin{matrix}\text{heat input by} \\ \text{conduction}\end{matrix} - \begin{matrix}\text{heat output by} \\ \text{conduction}\end{matrix} = \begin{matrix}\text{rate of acc.} \\ \text{of heat}\end{matrix} \qquad (2.3\text{-}5)$$

Taking the sum of the sensible and latent heat content of the material as H_T, the above equation can be expressed by an alternative formulation in terms of enthalpy, H_T,

$$\rho \frac{\partial H_T}{\partial t} = \frac{\partial}{\partial x_1}\left(k \frac{\partial T}{\partial x_1}\right) \qquad \text{for } 0 \le x_1 \le \infty \qquad (2.3\text{-}6)$$

where

$$H_T = \int_0^T C_{p.s}\, d\tau \qquad \text{for } T < T_m$$

$$H_T = \int_0^{T_m} C_{p.s}\, d\tau + \Delta H + \int_{T_m}^{T} C_{p.l}\, d\tau \qquad \text{for } T > T_m \qquad (2.3\text{-}7)$$

in which ΔH denotes the latent heat of fusion.

The advantages of this approach are that equation (2.3-6) applies for both the solid and melt phases (i.e. the interface no longer has to be tracked

explicitly and it is not necessary to consider solid and liquid regions separately) and allows for the variation of k and H_T with temperature (and, therefore, with distance) within each phase. It is also easier to generalize to more than one space-dimension. The mathematical basis of this weak solution method is examined by Atthey[115]. However, since discontinuities of this nature cannot be handled easily in the numerical solution of differential equations, it is usually eased by replacing the step changes by continuous curves[116,117]. This approach is acceptable for most materials since they, like foodstuffs or the metal alloys, contain a certain amount of impurities and consequently exhibit a melting range rather than a melting point. This feature suggests that the phase change can be approximated to occur over a small temperature interval $T_m \pm \varepsilon$ and formulated as follows:

$$H_T = \int_0^T C_{p.s}\, d\tau \qquad \text{for } T < T_m - \varepsilon$$

$$H_T = \int_0^{T_m-\varepsilon} C_{p.s}\, d\tau + \Delta H^* + \int_{T_m+\varepsilon}^{T} C_{p.l}\, d\tau \qquad \text{for } T > T_m + \varepsilon \qquad (2.3\text{-}8)$$

Here ΔH^*, different from ΔH in equation (2.3-7), is not a true latent heat since it includes sensible heats of the melt and solid over the phase transient range. Similarly changes in thermal conductivity k can be regarded as a smoothed variation subjected to the conditions

$$k = k_s(T) \qquad \text{for } T < T_m - \varepsilon$$

$$k = k_l(T) \qquad \text{for } T > T_m + \varepsilon \qquad (2.3\text{-}9)$$

The last formulation frequently associates to the physics of the

problem of interest in polymer processing, namely the crystallization of a partially crystalline material over a finite temperature interval which is usually wide enough to avoid the discontinuities of cooling curves with respect to H_T and k. In this application the required information on ΔH^* for polymer solidification can strictly be obtained only by taking into account the kinetics and degree of crystallization in the polymer. However, the problem can be approximately formulated in terms of temperature and an apparent specific heat to solve the conduction equation with variable properties over the whole region containing both solid and melt.

H_T is a unique function of temperature. Using the chain rule of differentiation, the expression becomes

$$\rho\left(\frac{\partial H_T}{\partial T}\right)\frac{\partial T}{\partial t} = \rho C_{p,app}\frac{\partial T}{\partial t} = \frac{\partial}{\partial x_1}\left(k\frac{\partial T}{\partial x_1}\right) \qquad (2.3\text{-}10)$$

where $C_{p,app}=(\partial H_T/\partial T)$ is referred to apparent specific heat. Corresponding to latent heat effects, the apparent specific heat will contain a peak over the solidification range, and its appearance is likely to depend on cooling rate and pressure through their influence on the crystallization kinetics.

The approach of apparent specific heat has been widely used for a variety of materials in the analysis of phase transformation. In the simplest consideration, the assumption which states the independence of apparent specific heat on temperature and pressure is taken. With this assumption Bonacina et al.[118] employed a three-time level implicit scheme for the numerical solution of one-dimensional phase-transition problems. The numerical calculation for a water-ice system gave satisfactory results

compared with the available analytical solutions. Gutfinger et al.[119] combined a Crank-Nicolson implicit finite difference scheme and the concept of flow analysis network (FAN), a finite element method developed for solving polymer flow problems, to model the solidification of polymers. In the case of high density polyethylene, the results illustrate the applicability of his approach. Two groups, Kamal et al.[120] and Ryan and Dutta[121], have obtained finite difference solutions in one space dimension for polymer processing problems, using central differences in space and first order explicit time-stepping. Dietz[122] modelled the cooling of a crystallizing polymer considering expansion cooling effect, the effect of pressure drop, and pressure dependence of properties. Good agreement between his results and experimental measurements was obtained.

Due to the complexity, only a very limited amount of research applied to polymers has related multi-dimensional analyses of heat transfer with phase transition. Discussing the problem of heat conduction in a perfect material with constant thermal properties in which a phase change occurs, Atthey[115] has described a two-dimensional finite difference scheme based on enthalpy formulation, including an internal heat generation term, and applied it to the problem of resistance spot welding of thin steel sheets. These ideas were carried further by Tacke[123]. The finite element methods have the advantages of handling complicated geometry and interpolating variable physical properties within the elements, many practical problems are being solved by this method. Comini et al.[124] used the finite element method, incorporating phase change based on the apparent specific heat formulation with temperature dependence of thermo-physical properties and nonlinear radiation-convection boundaries, but in cases where phase change occurs

over a small temperature interval, they preferred to interpolate enthalpy rather than specific heat within elements. Various treatments of differentiating enthalpy to get integration point values of specific heat have been discussed[124,125].

2.4. Analyses Including Crystallization Kinetics

A limitation of the foregoing analysis using apparent specific heat is that it takes no account of the temperature history of the polymer, upon which its degree of crystallinity develops. The correct approach, of course, needs to incorporate crystallization kinetics in parallel with the thermal problem. However, such an approach seems difficult to implement because of the difficulty of obtaining the required rate parameters and the complexity of the physics. Early work has already been performed by Sifleet et al.[10] With the assumption that all of the physical properties of the polymer are constants, the one-dimensional heat conduction equation was written with a heat source term Q representing latent heat release upon crystallization

$$\rho C_p \frac{\partial T}{\partial t} = k \frac{\partial^2 T}{\partial x_1^2} + Q \qquad (2.4\text{-}1)$$

Here Q was related to crystallization rate at the given temperature through the Avrami equation for relative crystallinity, θ,

$$\theta = 1 - \exp\{-k_c t^n\} \qquad (2.4\text{-}2)$$

in which k_c is a kinetic rate constant and n is an integer which is a function of the type of crystallization and nucleation taking place. Values were

obtained as a function of temperature based on isothermal crystallization studies of the examined polymers. The crystallization model coupled with the conduction problem was numerically solved using the Crank-Nicolson implicit finite difference method. However, no experimental comparisons were made. A similar treatment can be found in the work of Muzzy, Bright, and Hoyos[11]. They used the same concept to incorporate polymer crystallization in a one dimensional conduction equation but used a generalized, phenomenological model for the crystallization kinetics of polymers. Their differential equation under quiescent conditions was given as

$$\rho C_p \frac{\partial T}{\partial t} = k \frac{\partial^2 T}{\partial x_1^2} + \rho_c \Delta H \frac{d\chi_c}{dt} \qquad (2.4\text{-}3)$$

where the density, ρ, heat capacity, C_p, and thermal conductivity, k, are assumed to be functions of the instantaneous degree of crystallinity, χ_c, the latent heat of crystallization, ΔH, and the density of crystalline phase, ρ_c.

More recently Kamal and Chu[126] have studied the isothermal crystallization kinetics of a high density polyethylene and then used the data to model non-isothermal crystallization. In a similar way to Sifleet et al., they used an extension of the Avrami equation based on the idea that crystallization over a transient temperature interval can be regarded as a sequence of isothermal steps. Results of the non-isothermal crystallization model were compared with experimental values for relative crystallinity as a function of time obtained from DSC at various scanning speeds. Deviation was within 15%.

In a continuation of the work, Kamal and Lafleur[127] coupled the crystallization model with a one-dimensional finite difference heat conduction analysis and compared predictions with results obtained from solidification experiments on a disk of HDPE. Degree of crystallinity varied experimentally from about 45% at the wall to 55% in the core and predicted values agreed within about 3% relative crystallinity. The crystallization model was also coupled with an analysis of transient flow and heat transfer in mold filling. Results for degree of crystallinity in a molded sample were similar to those obtained in the static cooling experiments, which was to be expected in view of the short injection time in the experiment.

FINITE ELEMENT METHOD

When some problems of interest have complicated expressions without closed form solution, it is often necessary to look for approximate solution methods of which the computer numerical techniques are the most powerful and versatile. The numerical techniques used to solve such problems are subject to several different approaches. Two of these, finite difference and finite element methods, are almost invariably used for field equations. The basic concept behind both methods is to transform the continuous problem defined in terms of a set of non-linear partial-differential equations to discrete or piecewise approximations in space and time, resulting in a system of linear or nonlinear algebraic equations. Although these methods appear similar on the surface as well as in name, the formulation and solution algorithms are quite different.

The use of finite element methods has gained widespread acceptance in structural analysis applications, but not in coupled heat transfer and fluid

flow problems. The development of finite element approaches is much newer than finite differences for solving viscous flow problems. The first paper published in 1970 on finite elements for solving Navier-Stokes equations is attributed to Oden[128], and a continuous stream of scientific papers has revealed that the intensive search for the best finite element formulation is still far from being ended. Several observations are indicated by many investigators when finite differences are compared to finite elements: a) finite difference methods are easier than the equivalent finite element techniques in realization and implementation; b) a finite element, once constructed, has a tremendous advantage over finite differences for solving flows in complex geometries, although there is some evidence to suggest that finite differences can also be applied for this purpose[129].

The fundamental concepts of finite difference technique are quite simple. The solution domain of interest is first broken into a net with a finite number of grid points which are referred to as nodes. The nodes usually lie in rows parallel to the coordinate axes and are frequently, though not necessarily, equispaced along these rows. The continuous ordinary or partial derivative expressions at each node are then replaced by appropriate algebraic differences between values in adjacent nodal points. As a result, these equations can be solved by any of the common techniques for solution of systems of algebraic equations.

In the finite element approach, the continuum region of interest, Ω, is divided into a number of small subdomains commonly called finite elements. The local approximation of the continuous function over each element is then uniquely related to the discrete values of the continuous function at the

finite number of predetermined points in its domain. A variety of polygonal shape elements, with either linear or curved sides, are used. Different types of elements may be used in the same solution domain. For example, as shown in Figure 7, a two-dimensional region may be divided into a mesh of triangles or quadrilaterals. The corners of the elements (and sometimes additional points on the element boundaries) are referred to as the nodal points of a finite element mesh. On each element, the number of nodal point values for the solution variables (i.e. u_i, T, P) may differ from one node to another. As can be seen, the pressure is only defined at the corner nodes, while u_i is defined at all nodes.

3.1. Weighted Residual Formulations

The development of weighted residual techniques has only a short history and this scheme has been found widely used in the solution of differential equations and other non-structural applications. Instead of tediously searching for a mathematically equivalent variational statement, the weighted residual method starts with the governing differential equations. In general, an approximate solution is assumed first and then substituted into the differential equation. This operation will introduce a residual error term in the differential equation due to the approximation assumption. The residual error term cannot be made to vanish; however, it is possible to force a weighted integral, over the solution domain, of the residual to vanish.

For example, using the weighted residual method, a desired function $f(\cdot)$ in an element can be approximated by,

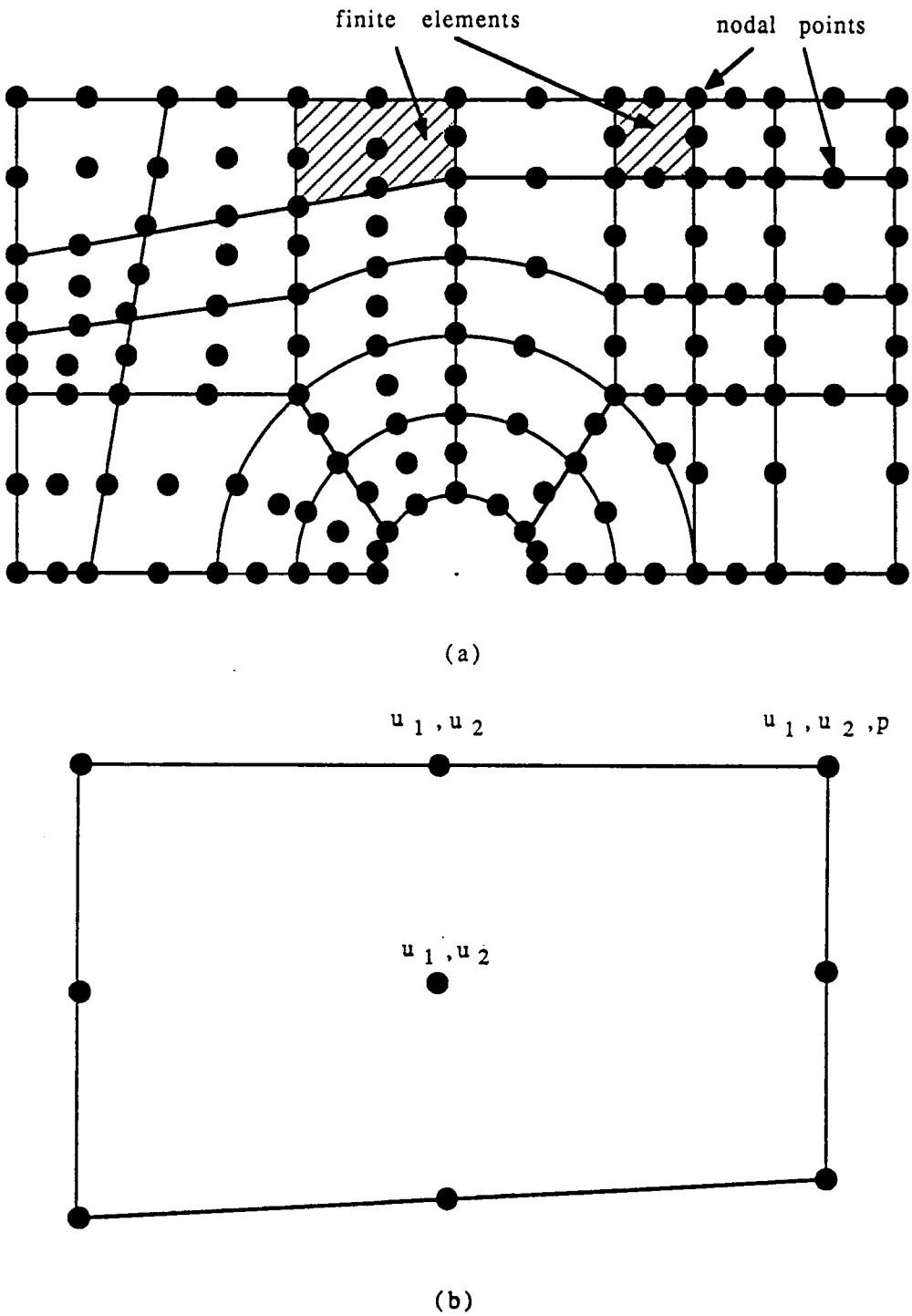

Figure 7. (a) Typical finite element discretization. (b) Nine-node quadrilateral element and the solution vectors at each node.

$$f(\cdot) \approx \sum_{i=1}^{N} f_i \phi_i(\cdot) \qquad (3.1\text{-}1)$$

where $\phi_i(\cdot)$, i = 1,2,...,N, are a set of interpolation functions and can be defined over both the time and space domain, $[(\cdot) \equiv (t,x_1,x_2)]$, f_i, i = 1,2,...,N, are unknown coefficients at element nodal points, and N the number of nodal points in an element. Generally, though not invariably, the $\phi_i(\cdot)$ are selected to be a set of polynomials which satisfy all the boundary conditions imposed on the problem. Substitution of $f(\cdot)$ into the partial differential equation describing the problem, for instant, $a \cdot f - g = 0$, yields a residual, R,

$$a \cdot \sum_{i=1}^{N} f_i \phi_i(\cdot) - g = R(\cdot) \qquad (3.1\text{-}2)$$

The following task is then to make this residual small in some sense by choosing appropriate unknown coefficients f_i at element nodal points. To reduce the error to zero over each element domain, a straightforward scheme is to set the integral of $R(\cdot)$ to vanish:

$$\int_t \int_V R(\cdot) dV dt = 0 \qquad (3.1\text{-}3)$$

The above equation can be modified further. In a weighted sense, weighting functions, $w_j(\cdot)$, j = 1,2,...,N, are introduced. By making the residuals orthogonal to the weighting functions over each element, it then leads to a set of N independent equations

$$\int_t \int_V R(\cdot) w_j(\cdot) dV dt = 0, \qquad j = 1,2,...,N. \qquad (3.1\text{-}4)$$

When the same procedure is performed element by element, a system of algebraic equations is produced by which the unknown vectors over the whole solution domain can be solved.

CHAPTER III

MATERIAL AND METHOD

MATERIAL

Among the principal polymers used as pipe, polyethylene and PVC are the leading pipe materials. Polypropylene is being increasingly introduced in the plastic pipe market as a versatile piping material due to great advantages in its application including high resistance to temperature and deformation under stress, great resistance to chemical and electrolytic attack, ease and economy of handling and installation, etc. For being an important piping material, polypropylene was chosen as the material throughout this study. The required material properties of polypropylene, a product of Exxon Chemical company, are listed in Table 2. On the basis of calculation according to equation (1.4-27) with parameters in Table 2, the crystallization rate of polypropylene as indicated by the reciprocal half-time is illustrated in the curve (a) of Figure 8. It indicates that this polymer has a maximum crystallization rate in the range of 60° to $65^{\circ}C$ and could crystallize at an appreciable rate at room temperature.

MATHEMATICAL MODEL FOR PIPE EXTRUSION

The transport of energy between the moving polymer melt and the melt surroundings can be due to convection, conduction, and radiation. Within the polymer melt conduction predominates, in particular when the melt is a highly viscous fluid. For the case of a crystallizing polymer the kinetic equation for temperature distribution may be obtained from the energy balance equation

Table 2. Material properties of a polypropylene[31,130].

Density, ρ (gm/cm^3)	0.77
Heat capacity, C_p ($erg/gm-^oC$)	3.10E+07
Thermal conductivity, k ($erg/cm-s-^oK$)	2.25E+04
Ultimate degree of crystallinity, $\chi_c(\infty)$	0.65
Latent heat of crystallization, ΔH (cal/g-mole)	2.37E+03
Equilibrium melting temperature, T_m^o (^oK)	460.5
Glass transition temperature, T_g (^oK)	253.0
Avrami exponent, n	2.5
Maximum Avrami-like rate constant, χ_{co} (1/sec)	7.696E+07
Characteristic temperature, T_∞ (^oK)	223.0
Characteristic activation energy, U* (cal/g-mole)	1.5E+03
Characteristic constant, C_3 ($^oK^2$)	5.0E+05
Molecular weight, M_w (gm/g-mole)	42.0

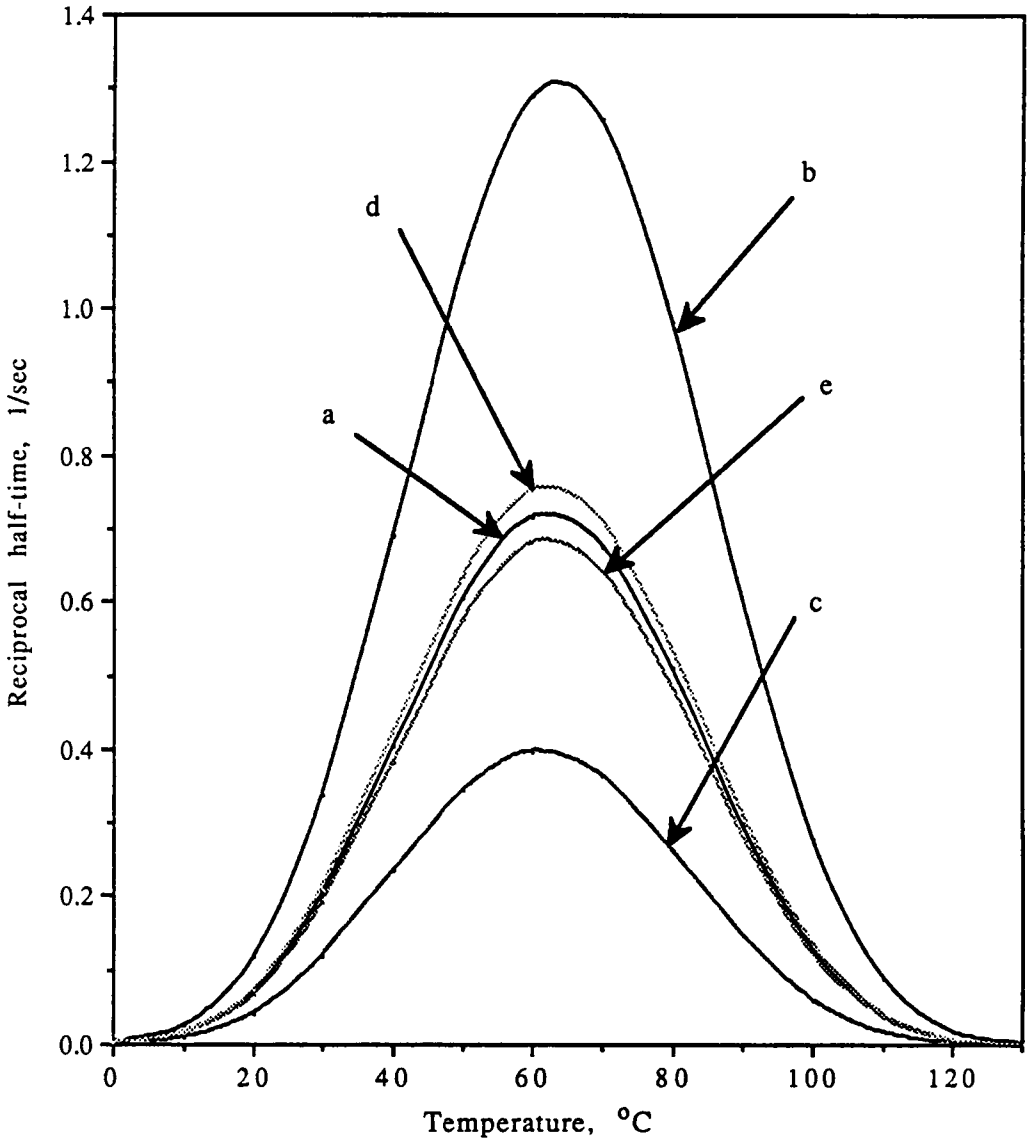

Figure 8. Reciprocal half-times of polypropylene, $1/t_{0.5}$, as a function of the crystallization temperature calculated using equation (1.4-27) with (a) χ_{co} = 7.696E+07(sec^{-1}), C_3 = 5.0E+05($^oK^2$) in Table 2; (b) χ_{co} = 7.696E+07(sec^{-1}), C_3 = 4.75E+05($^oK^2$)(-5% deviation of C_3 from 5.0E+05($^oK^2$)); (c) χ_{co} = 7.696E+07(sec^{-1}), C_3 = 5.25E+05($^oK^2$)(+5% deviation of C_3 from 5.0E+05($^oK^2$)); (d) χ_{co} = 8.0808E+07(sec^{-1})(+5% deviation of χ_{co} from 7.696E+07(sec^{-1})), C_3 = 5.0E+05($^oK^2$); (e) χ_{co} = 7.3112E+07(sec^{-1})(-5% deviation of χ_{co} from 7.696E+07(sec^{-1})), C_3 = 5.0E+05($^oK^2$).

$$\rho C_p\left(\frac{\partial T}{\partial t} + \mathbf{U}\cdot\nabla T\right) = \nabla\cdot(k\,\nabla T) + \Phi + Q \qquad (3.2\text{-}1)$$

where Φ denotes the viscous dissipation heat, and Q represents the rate of internal heat generation which takes into account the heat generated due to crystallization in the polymer.

Let us consider the system shown in Figure 9. For assumed plug melt flow in pipe production, the generation of viscous dissipation heat due to fluid friction is zero. With the reasonable assumption, the resulting expression for the axial symmetry of the system in cylindrical coordinates x_1(or z-axis), x_2(or r-axis) is then obtained

$$\rho C_p\left(\frac{\partial T}{\partial t} + u_1\frac{\partial T}{\partial x_1} + u_2\frac{\partial T}{\partial x_2}\right) = \frac{\partial}{\partial x_1}\left(k\frac{\partial T}{\partial x_1}\right) + \frac{1}{x_2}\frac{\partial}{\partial x_2}\left(k x_2\frac{\partial T}{\partial x_2}\right) + Q \qquad (3.2\text{-}2)$$

Assuming further that when a phase change from melt to solid occurs, any accompanying changes of ρ, C_p, and k will be neglected and the variation with time is determined in practice by the axial velocity of the melt, u_1. The heat transfer equation becomes,

$$\rho C_p u_1\frac{\partial T}{\partial x_1} = k\left(\frac{\partial^2 T}{\partial {x_1}^2} + \frac{1}{x_2}\frac{\partial}{\partial x_2}\left(x_2\frac{\partial T}{\partial x_2}\right)\right) + Q \qquad (3.2\text{-}3)$$

Consequently the extruded polymer melt, as illustrated in Figure 9, is considered as an incompressible annular plug flow along the x_1 direction with negligible u_2 velocity component. The quantity Q represents the volumetric heat source for phase change of a semi-crystalline polymer and is given by

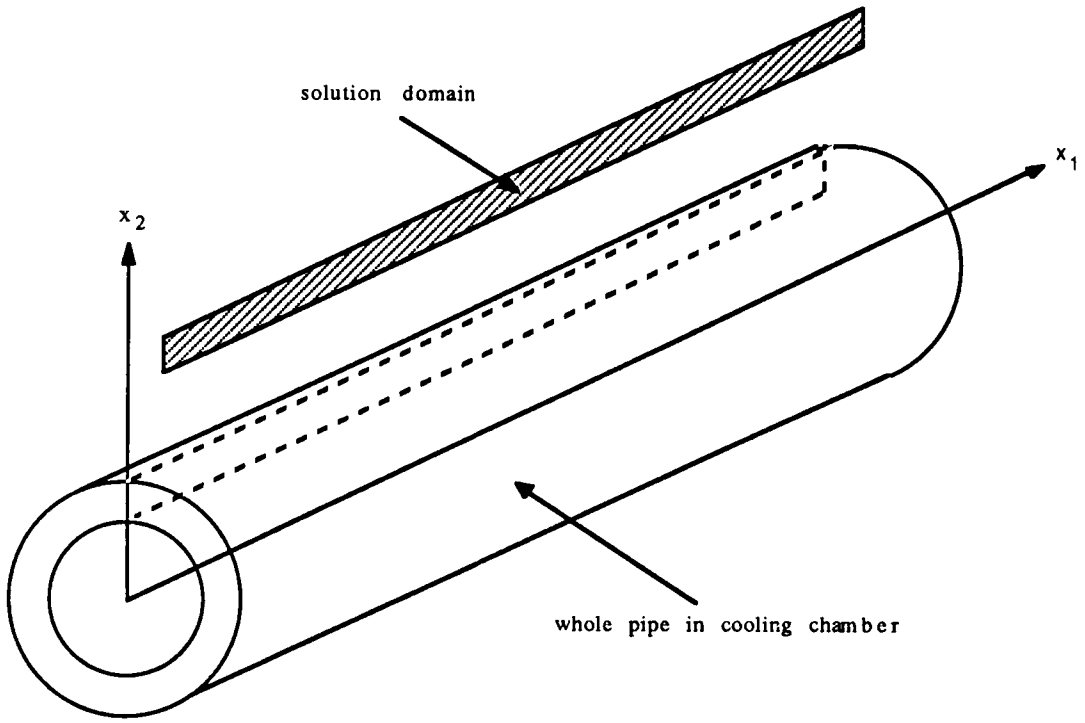

(a)

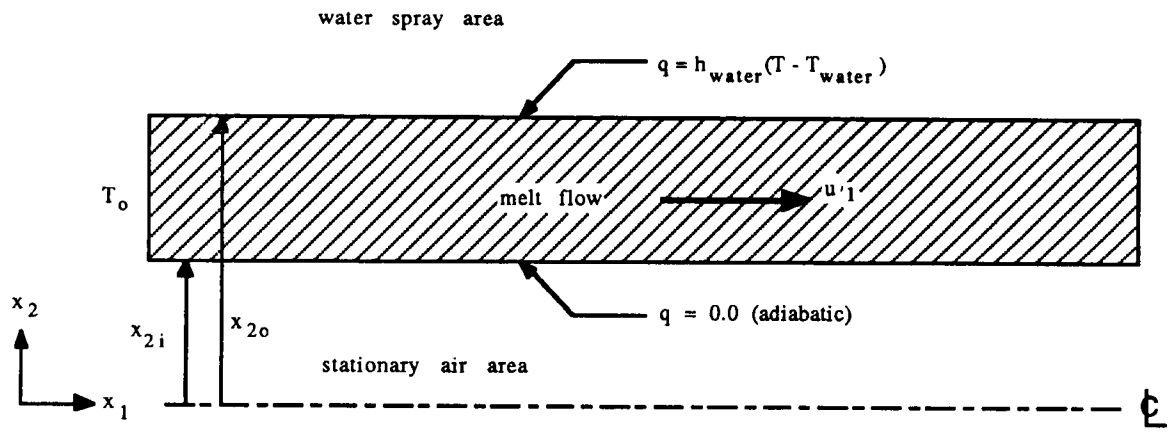

(b)

Figure 9. Schematic illustration of (a) the solution domain chosen, and (b) the boundary conditions considered in the solution domain.

$$Q = \rho \cdot \Delta H \cdot u_1 \frac{\partial \chi_c}{\partial x_1} \qquad (3.2\text{-}4)$$

where $\chi_c = \chi_c(x_1, x_2)$ is the absolute degree of crystallinity with a value less than one. Let $\chi_c(\infty)$ be the maximum degree of crystallinity, a constant, that the semi-crystalline polymer attains after a long time of crystallization. Thus equation (3.2-4) can be expressed with the relative degree of crystallinity $\theta = \chi_c/\chi_c(\infty)$ as

$$Q = \rho \cdot \Delta H \cdot u_1 \cdot \chi_c(\infty) \cdot \frac{\partial \theta}{\partial x_1} \qquad (3.2\text{-}5)$$

where $0 \leq \theta \leq 1$. Incorporating the differential form of the crystallization model proposed by Nakamura in equation (1.4-15) with the negligible velocity component in the x_2 direction and the temperature dependence of half-times in equation (1.4-27), the derivative term in equation (3.2-5) becomes

$$\frac{\partial \theta}{\partial x_1} = \left(\frac{1}{u_1}\right) \cdot n \cdot \mathcal{K}_c(T) \cdot (1-\theta) \cdot \left\{ \ln\left(\frac{1}{1-\theta}\right) \right\}^{(n-1)/n} \qquad (3.2\text{-}6)$$

with

$$\mathcal{K}_c(T) = \mathcal{K}_{c0} \exp\left\{ - \frac{U^*}{R(T-T_\infty)} \right\} \exp\left\{ - \frac{C_3}{T\Delta T} \right\} \qquad (3.2\text{-}7)$$

where $\mathcal{K}_{c0} = \{(\ln 2)^{1/n}/(t_{0.5})_0\}$ is a constant unique to a given material. Combining equations (3.2-5) and (3.2-6), the last term on the right side of equation (3.2-3) reads as

$$Q = \rho \cdot \Delta H \cdot \chi_c(\infty) \cdot n \cdot \chi_c(T) \cdot (1-\theta) \cdot \left[\ln\left(\frac{1}{1-\theta}\right) \right]^{(n-1)/n} \qquad (3.2\text{-}8)$$

The boundary conditions again in Figure 9 relevant for the running melt are treated as follow: the melt inlet temperature is assumed to be uniform over the cross-section area because of the short air gap and low thermal conductivity of polymer; the water spray cooling is assumed to be applied symmetrically around the pipe line; and no heat flux occurs on the inner surface of the pipe.

$$T(0,x_2) = T_o \quad \text{(uniform melt inlet temperature)} \qquad (3.2\text{-}9)$$

$$k\left(\frac{\partial T}{\partial x_2}\right)_{x_2=x_{2o}} = -h\left(T(x_1,x_{2o}) - T_{water}\right) \qquad (3.2\text{-}10)$$

$$k\left(\frac{\partial T}{\partial x_2}\right)_{x_2=x_{2i}} = 0.0 \quad \text{(adiabatic condition)} \qquad (3.2\text{-}11)$$

where h is the surface heat transfer coefficient, and T_{water} is the temperature of the surrounding cooling water.

In mathematical treatment it is quite common to describe some phenomena by relating dimensionless combinations of physical variables. These combinations are referred to as dimensionless groups or dimensionless numbers. If the dimensionless numbers describing the problem remain the same, then the solution to the problem will remain unchanged, even if individual variables are varied. This latter characteristic is very useful in scale-up problems.

For the sake of generality, the following dimensionless variables will be introduced,

$$\Gamma = \frac{T-T_{water}}{T_m-T_{water}} = \frac{T-T_{water}}{\Delta T_{mw}} \qquad ; Pe_t = \frac{\rho C_p u_1 L}{k}$$

$$\eta_1 = \frac{x_1}{L} \qquad ; \eta_2 = \frac{x_2-x_{2i}}{x_{2o}-x_{2i}} = \frac{x_2-x_{2i}}{\Delta x_2} \qquad (3.2\text{-}12)$$

where T_{water} is the water temperature, T_m the polymer melting temperature, x_1 the axial distance from the inlet, x_2 the radial distance from the axis of the pipe, L the total length of the chamber, and u_1 is the velocity in the axial (x_1) direction. The dimensionless number, Pe_t, is defined as the thermal Peclet number which provides a measure of the importance of thermal convection relative to thermal conduction. Incorporation of these variables into equation (3.2-3) leads to

$$Pe_t \cdot \left(\frac{\partial \Gamma}{\partial \eta_1} - (JH) \frac{\partial \theta}{\partial \eta_1} \right) = \frac{1}{(\xi \eta_2 + \zeta)\xi} \frac{\partial \Gamma}{\partial \eta_2} + \frac{1}{\xi^2} \frac{\partial^2 \Gamma}{\partial \eta_2^2} + \frac{\partial^2 \Gamma}{\partial \eta_1^2} \qquad (3.2\text{-}13)$$

with $\frac{\partial \theta}{\partial \eta_1} = (\frac{n}{Pe_c}) \cdot f(\Gamma) \cdot g(\theta)$ and constants

$$JH = \frac{\Delta H \cdot \chi_c(\infty)}{C_p \Delta T_{mw}} \qquad ; \xi = \frac{\Delta x_2}{L} \qquad ; \zeta = \frac{x_{2i}}{L} \qquad (3.2\text{-}14)$$

Here n is the Avrami exponent; $Pe_c = u_1/L\chi_{co}$, a Peclet number for crystallization, indicates the ratio of crystallization time for a specified material to element transport time; JH is a material characteristic constant which can be considered to be the ratio of the maximum released crystallization heat to the total transportable thermal energy of the system. Detailed derivation of dimensionless energy kinetics equations and the expressions of $f(\Gamma)$ and $g(\theta)$ are derived in appendix A.

FINITE ELEMENT PROGRAM-NACHOS II

In this thesis a computer program, NACHOS II which is based on the Galerkin form of the finite element method, is modified for the analysis of the desired pipe extrusion problem. The NACHOS II program, developed by D. K. Gartling at Sandia National Laboratories, is designed for the two-dimensional analysis of viscous incompressible fluid dynamics problems[131]. The fluid flow analyzed may be isothermal, nonisothermal or may incorporate the effects of heat transfer and other transport processes under steady or transient state. The computer code also provides the facilities for users to simulate changes in material properties, volumetric heat generation, and boundary conditions. In addition, users may choose different types of elements in the NACHOS II element library, which consists of isoparametric and subparametric triangles and quadrilaterals. Within each of these elements, biquadratic interpolation functions are used to approximate the values for velocity components and temperature; the pressure is approximated by either a continuous, bilinear function or a discontinuous, linear function.

Several assumptions inherent in the theoretical formulation include a) all materials are considered to be homogeneous and isotropic, b) all fluids are assumed to be Newtonian or inelastic, non-Newtonian, and c) the motion of a viscous fluid is constrained to incompressible and laminar flows. In spite of these restrictions, NACHOS II is limited to those problems described by the two-dimensional (plane or axially symmetric), incompressible form of the linear momentum equation coupled with an energy equation when heat transfer effects are important. The program is applicable for analysis of the following flow problems:

a) Isothermal flow problems

b) Forced, free, or mixed convection problems

c) Conjugate heat transfer problems

d) Flow in saturated porous media with or without heat transfer

e) Inelastic, non-Newtonian flows with or without heat transfer

The essential part of NACHOS II is the solution algorithms for the finite element equations. Steady-state problems are analyzed using either of two iteration schemes - a Picard iteration procedure or a full Newton procedure. The frontal solution method, a special form of Gauss elimination, is used as a solution technique for each iteration process. The overall operation of the code for steady-state problems is shown in the flow chart of Figure 10. Detailed description of the theoretical basis and many of the numerical schemes used in the program is illustrated in Gartling's work[131].

Before being used to analyze the problem of interest, the modified NACHOS II program was first tested using two examples provided by Gartling[132]. The first example involves the solution of a steady-state Newtonian, isothermal flow problem. A fluid is forced to flow through an axisymmetrical tube containing a smooth, internal constriction. The second example involves the solution of a buoyancy driven flow problem. This system consists of an isothermal rectangular enclosure in which a circular cylinder is mounted horizontally with a temperature higher than the enclosure. The space between the enclosure and the cylinder is filled with air at atmospheric pressure. The geometries for both systems are given in Figure 11 along with the material properties and boundary conditions used in the analyses. The resulting contour plots, stream function and/or

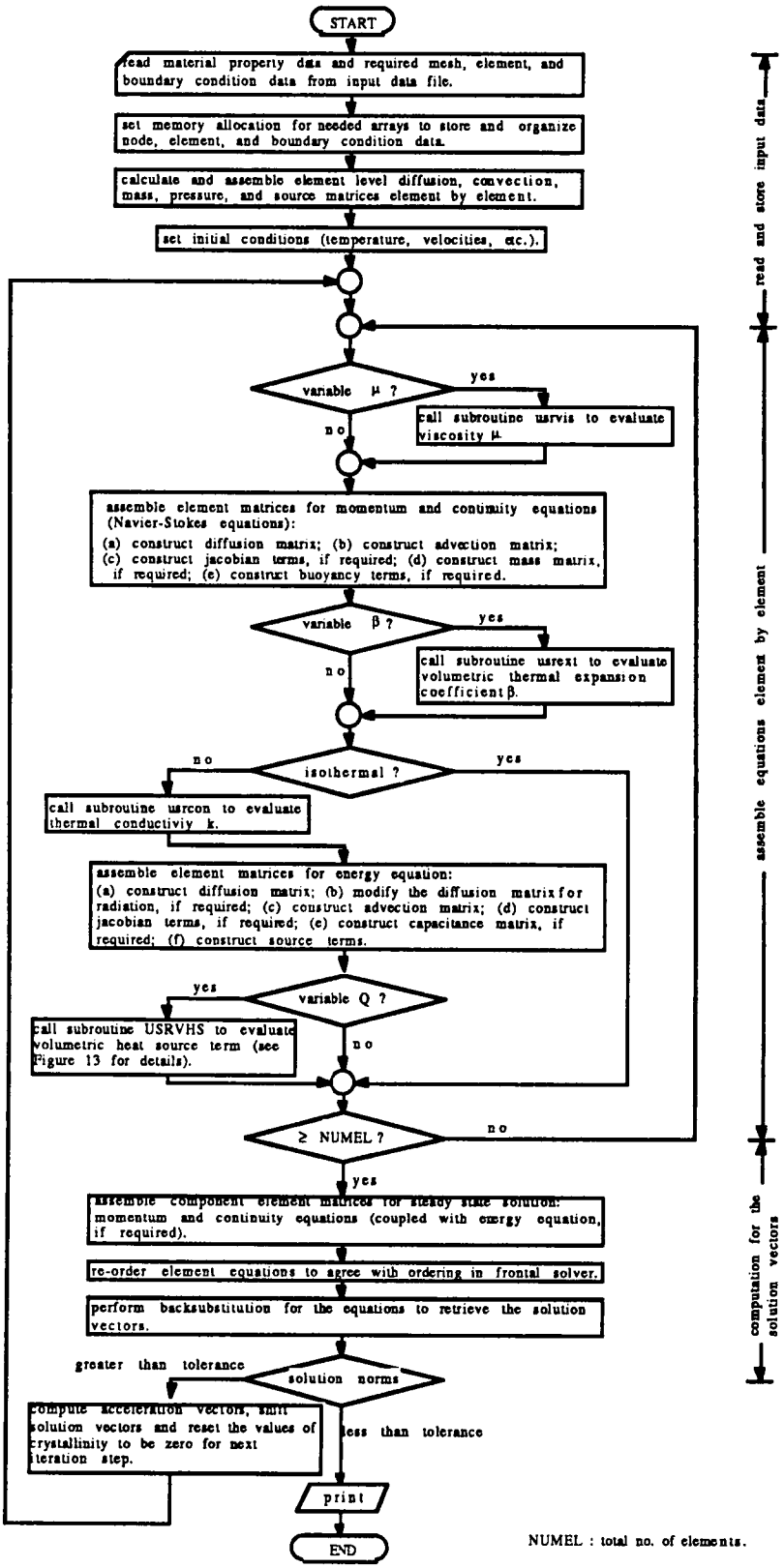

Figure 10. Flow chart for steady-state solution procedure.

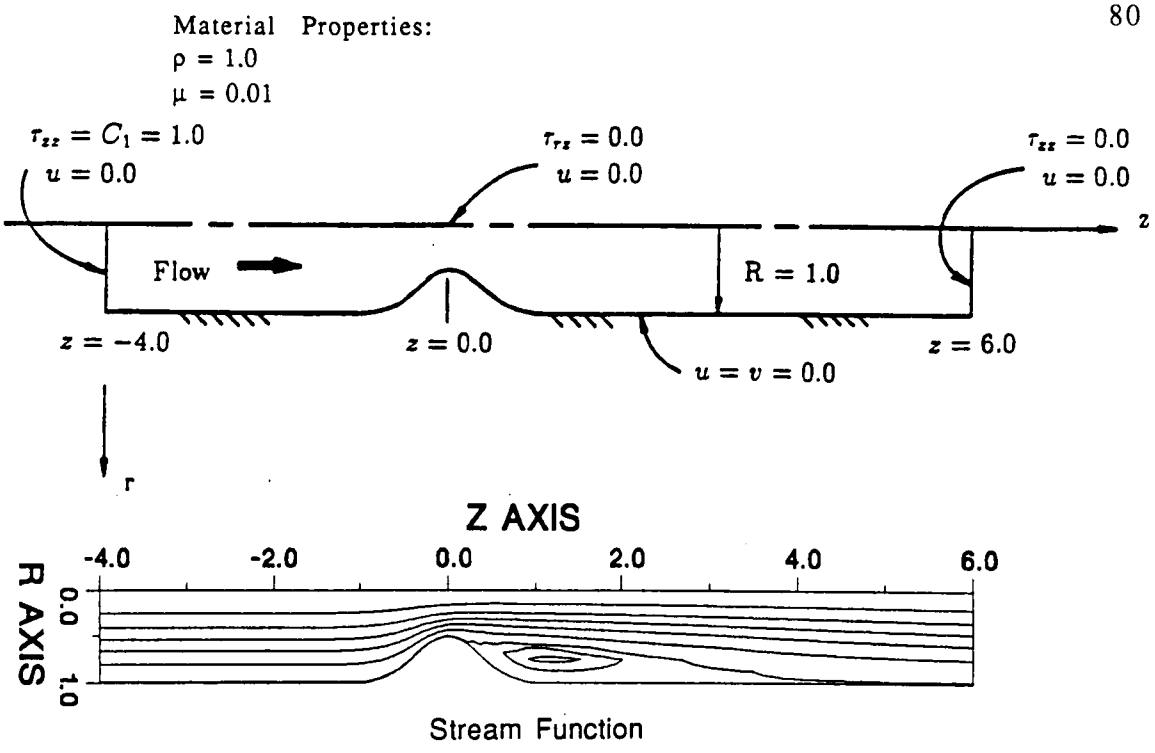

(a)

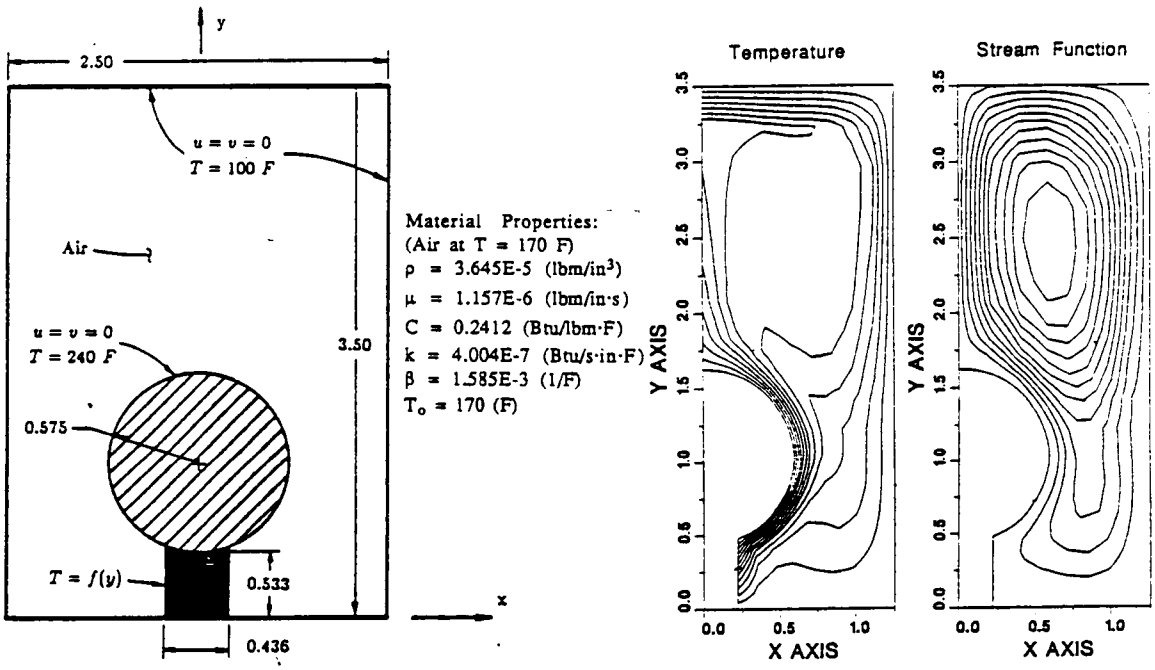

(b)

Figure 11. Assumed geometries for testing the modified NACHOS II program: (a) schematic for example 1 and its corresponding contour plot; (b) schematic for example 2 and its corresponding contour plots.

temperature, obtained for each problem using the modified program are also shown in Figure 11. The fact that these results are the same as those obtained using original NACHOS II program demonstrates the applicability of the modified program.

The system considered in this thesis, shown in Figure 9, is analyzed using steady-state solution algorithms. Because of the axial symmetry of the system, the analysis invokes the two-dimensional axisymmetric formulation. A mesh of nine-node isoparametric quadrilaterals, as shown in Figure 12, is used to represent the polymer strip in the cooling chamber. The melt entrance of the cooling chamber is at $\eta_1 = x_1/L = 0.0$ and polymer melt flows from left to right along the x_1 direction. In order to obtain accuracy in regions of large temperature gradient, smaller elements are used for the regions near chamber inlet and outer pipe surface. Calculation of the heat generation due to polymer crystallization according to equation (3.2-5) is carried out through the subroutine "USRVHS". One-element information is given each time when this subroutine is called by NACHOS II main program. The arrangement of the nodal points in a nine-node isoparametric element is shown in Figure 13. With the rectangular element geometry and seeking for the solutions of first-order differential equations, Runge-Kutta-Fehlberg method is applied to calculate crystallinity and its derivative with respect to distance at each node along x_1 direction element by element. Subroutine "RKF45", a program which uses Runge-Kutta-Fehlberg method to solve a set of first-order differential equations written by Watts and Shampine[133], is then served as the numerical solver for such purpose. The subroutine "USRVHS", basically, has the profile given in Figure 14 and is reproduced in Appendix B.

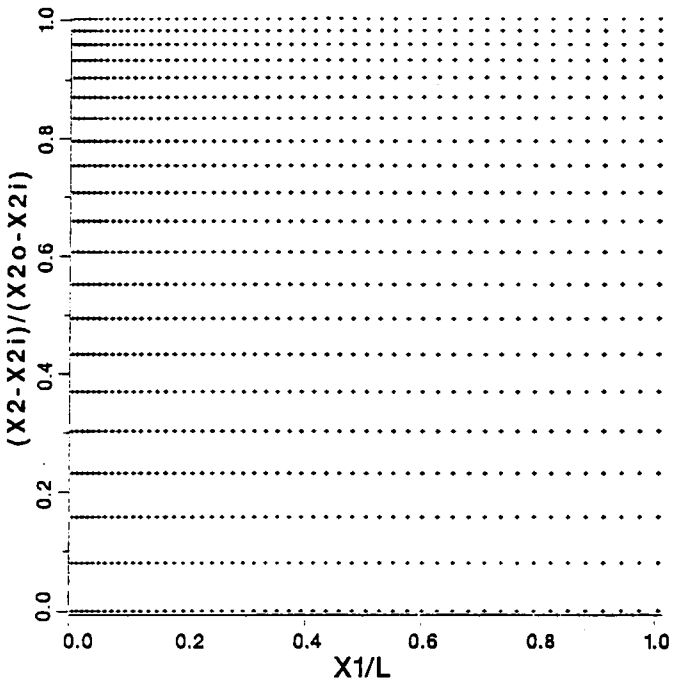

(a)

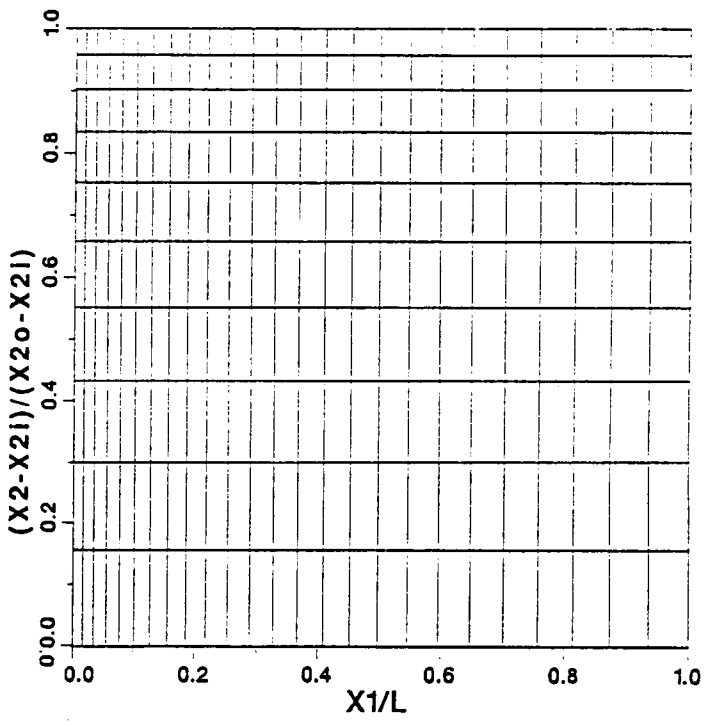

(b)

Figure 12. (a) Point plot for the polymer strip in the cooling chamber;
(b) element plot for the polymer strip in the cooling chamber.

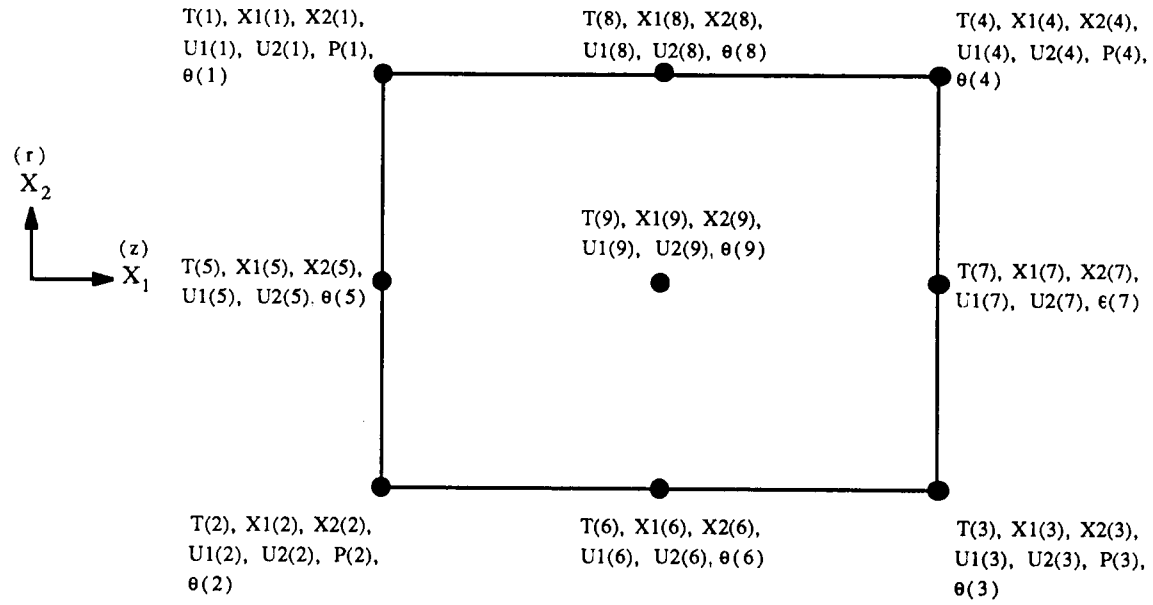

Figure 13. The arrangement of the nodes in one of the nine-node isoparametric elements used to represent the polymer strip in the cooling chamber. Number of degrees of freedom (T, P, u_1, u_2, θ) in an element is 40.

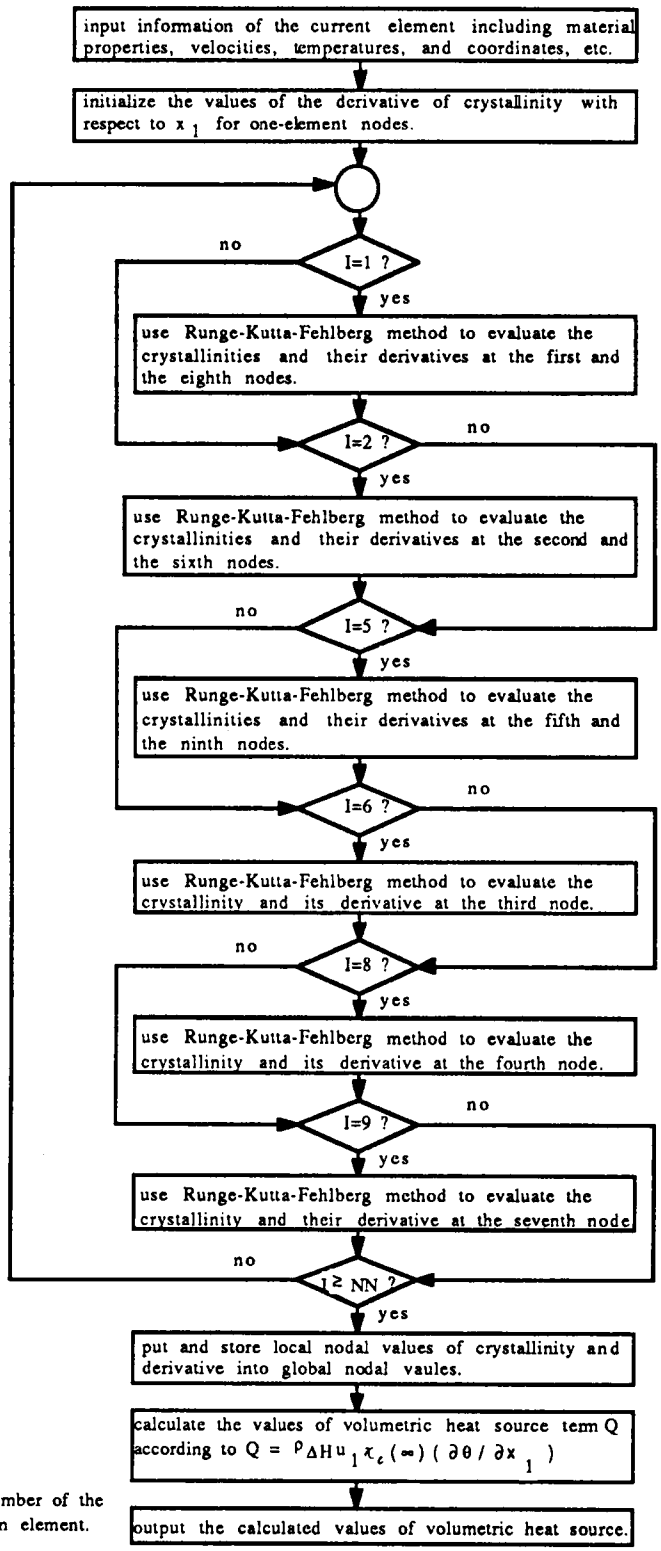

Figure 14. Flow chart for the calculation of volumetric heat source of crystallization by subroutine USRVHS.

CHAPTER IV

RESULTS AND DISCUSSION

The results of the numerical simulation of different cooling operation, different melt velocity, and melt inlet temperature, for the system shown in Figure 9 are summarized from Figure 15 to Figure 29. Also, the effect of pipe thickness is considered and the results are illustrated from Figure 30 to Figure 39. Three plots are present for each case. The first plot, (a), represents the temperature isotherms for amorphous material, i.e. without consideration of polymer crystallization. The middle plot, (b), shows the temperature profile for semi-crystalline material which takes into account the evolution of crystallization heat. The last plot, (c), gives the iso-crystallinity contours corresponding to the semi-crystalline material.

As defined in chapter III, a thermal Peclet number for the system is given in equation (3.2-12)

$$Pe_t = \frac{\rho C_p u_1 L}{k} \qquad (3.2\text{-}12)$$

which indicates the importance of energy transport by convection relative to that by conduction. Thus, a high value of the Peclet number means that heat transfer due to convection is large in comparison with heat transfer due to conduction. For the present system, the lowest value of the Peclet number is 53,044, indicating rapid cooling by conduction over a short melt flow distance, as evident in Figure 15, 20, and 25 for different melt inlet temperatures. For constant material properties and fixed length of cooling

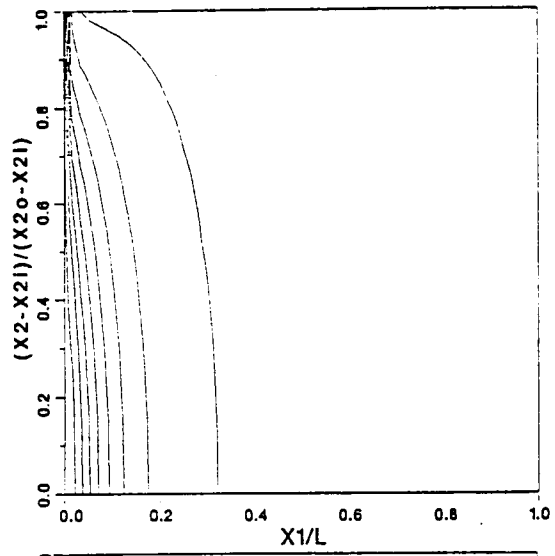

(a) amorphous material

temperature isotherms from left to right:
170°C
150°C
130°C
110°C
90°C
70°C
50°C
30°C

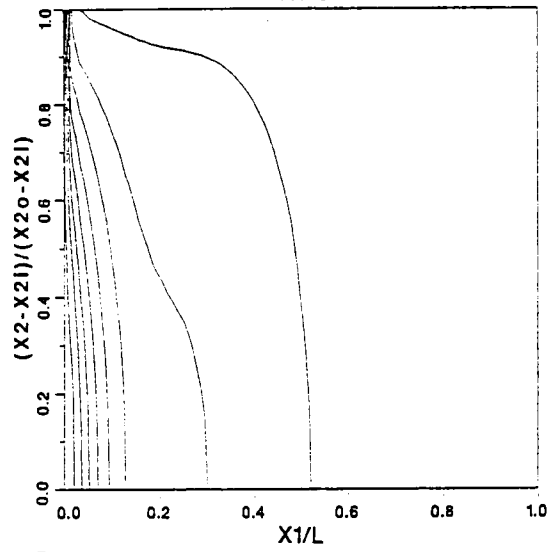

(b) semi-crystalline material

temperature isotherms from left to right:
170°C
150°C
130°C
110°C
90°C
70°C
50°C
30°C

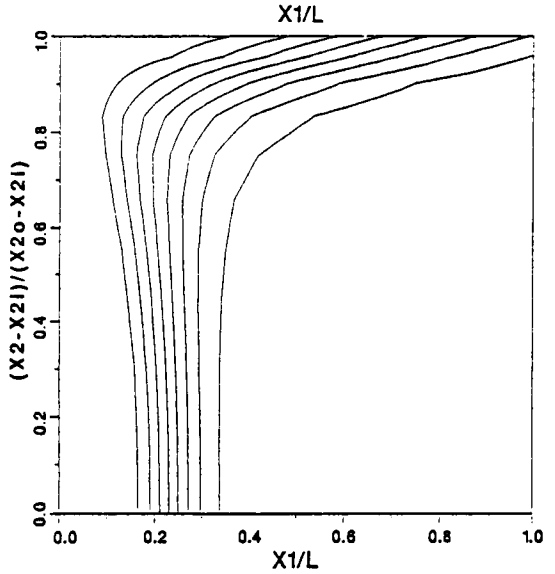

(c) semi-crystalline material

iso-crystallinity curves from left to right (relative values):
0.1111
0.2222
0.3333
0.4444
0.5555
0.6666
0.7777
0.8888

Figure 15. Temperature contours and crystallinity distribution for melt inlet temperature 180°C, Pe_t = 5.3044E+04, Pe_c = 2.60E-12, ξ = 2.0E-03, and ζ = 1.8E-02.

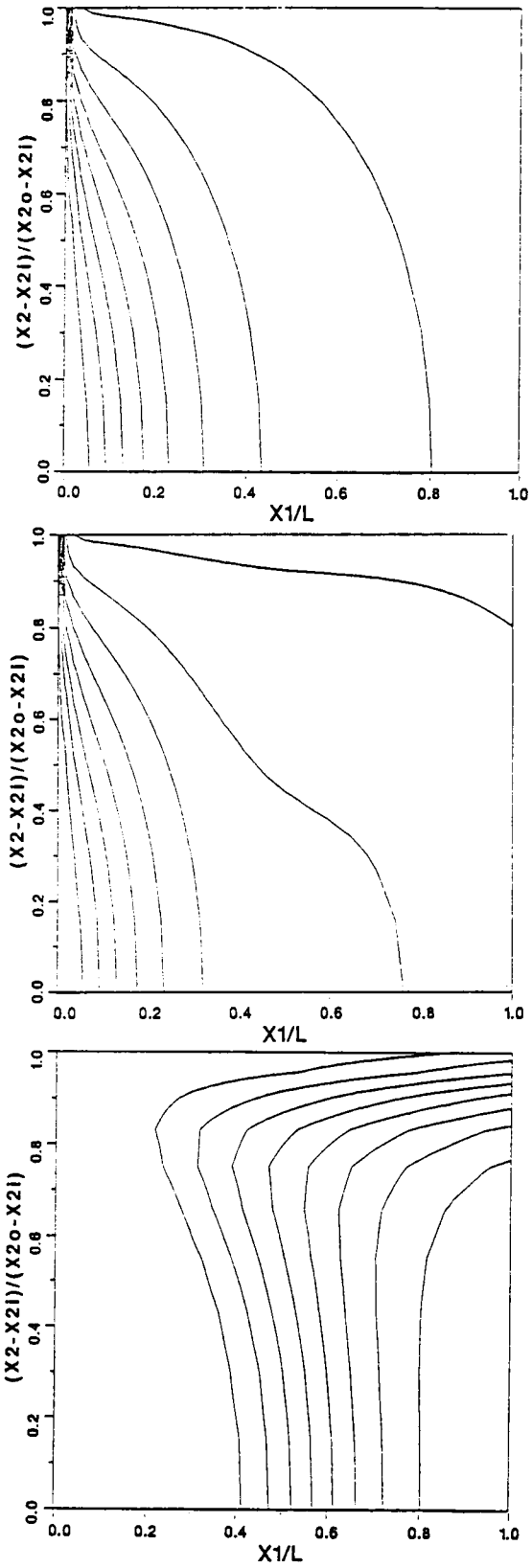

(a) amorphous material

temperature isotherms from left to right:
170°C
150°C
130°C
110°C
90°C
70°C
50°C
30°C

(b) semi-crystalline material

temperature isotherms from left to right:
170°C
150°C
130°C
110°C
90°C
70°C
50°C
30°C

(c) semi-crystalline material

iso-crystallinity curves from left to right (relative values):
0.1072
0.2145
0.3217
0.4289
0.5362
0.6434
0.7507
0.8579

Figure 16. Temperature contours and crystallinity distribution for melt inlet temperature 180°C, Pe_t = 1.32611E+05, Pe_c = 6.50E-12, ξ = 2.0E-03, and ζ = 1.8E-02.

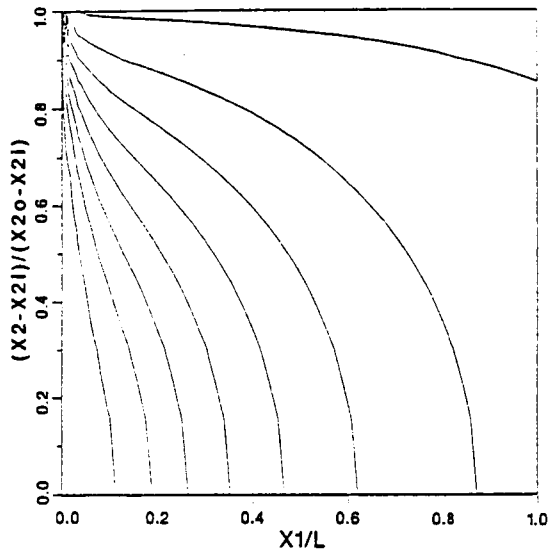

(a) amorphous material

temperature isotherms from left to right:
170°C
150°C
130°C
110°C
90°C
70°C
50°C
30°C

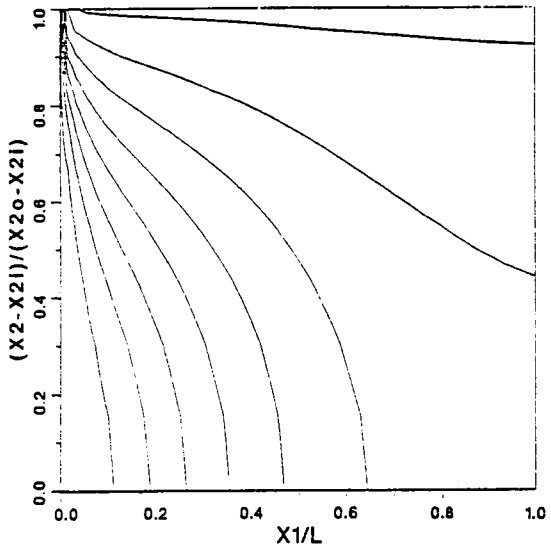

(b) semi-crystalline material

temperature isotherms from left to right:
170°C
150°C
130°C
110°C
90°C
70°C
50°C
30°C

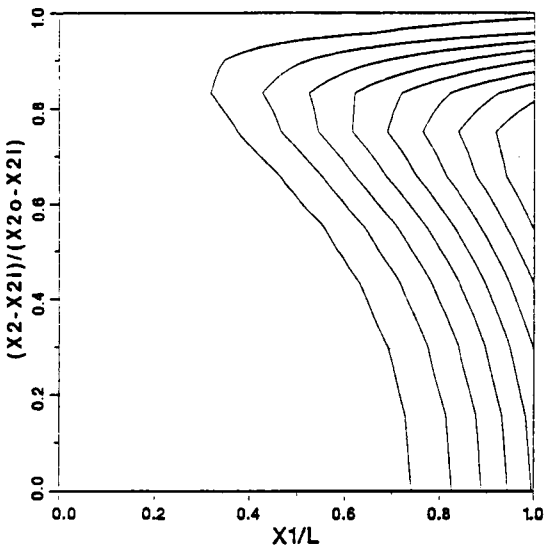

(c) semi-crystalline material

iso-crystallinity curves from left to right (relative values):
0.0519
0.1038
0.1557
0.2076
0.2595
0.3114
0.3633
0.4152

Figure 17. Temperature contours and crystallinity distribution for melt inlet temperature 180°C, Pe_t = 2.65222E+05, Pe_c = 1.30E-11, ξ = 2.0E-03, and ζ = 1.8E-02.

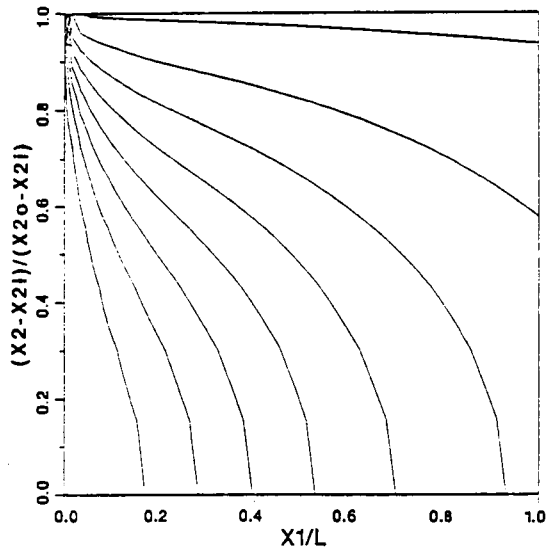

(a) amorphous material

temperature isotherms from left to right:
170°C
150°C
130°C
110°C
90°C
70°C
50°C
30°C

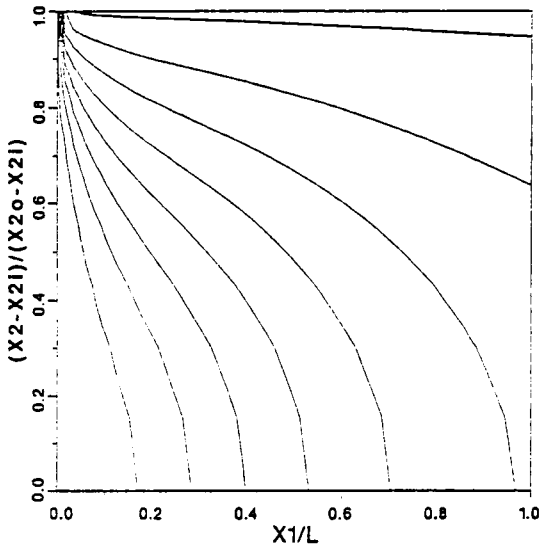

(b) semi-crystalline material

temperature isotherms from left to right:
170°C
150°C
130°C
110°C
90°C
70°C
50°C
30°C

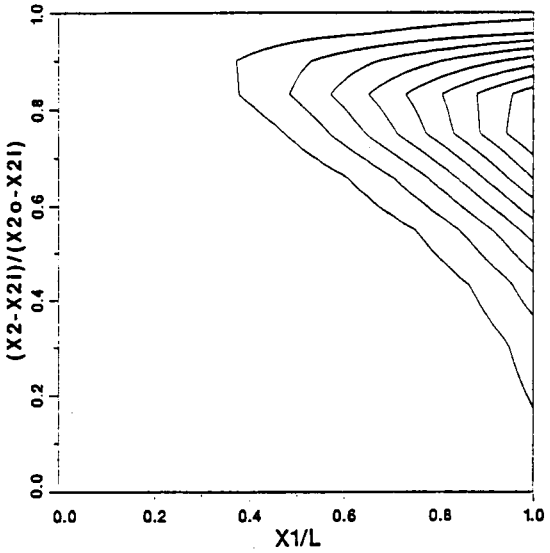

(c) semi-crystalline material

iso-crystallinity curves from left to right (relative values):
0.0270
0.0539
0.0809
0.1079
0.1348
0.1618
0.1887
0.2157

Figure 18. Temperature contours and crystallinity distribution for melt inlet temperature 180°C, Pe_t = 3.97833E+05, Pe_c = 1.95E-11, ξ = 2.0E-03, and ζ = 1.8E-02.

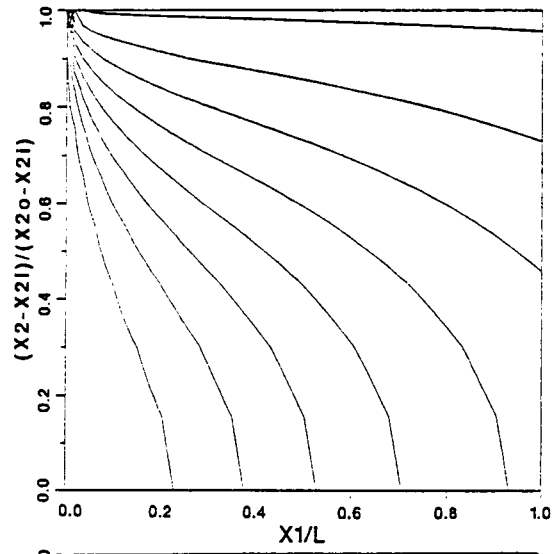

(a) amorphous material

temperature isotherms from left to right:
170°C
150°C
130°C
110°C
90°C
70°C
50°C
30°C

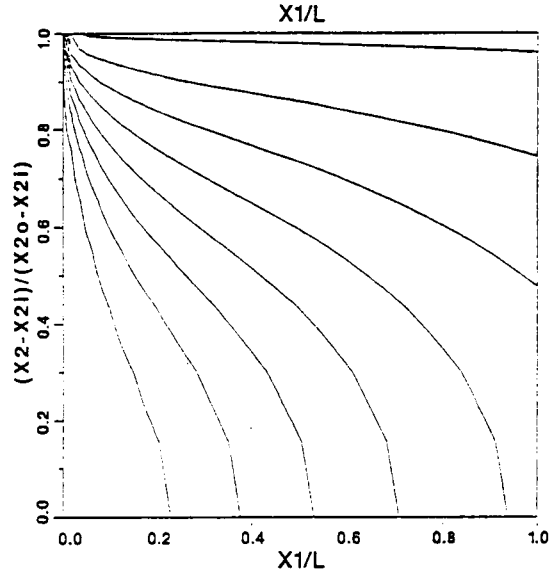

(b) semi-crystalline material

temperature isotherms from left to right:
170°C
150°C
130°C
110°C
90°C
70°C
50°C
30°C

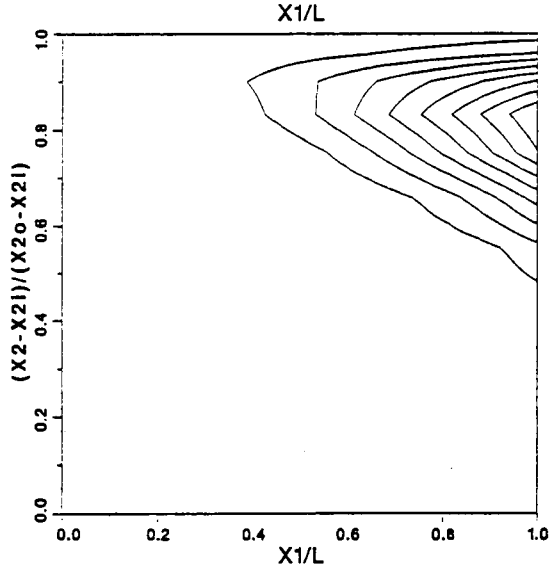

(c) semi-crystalline material

iso-crystallinity curves from left to right (relative values):
0.0158
0.0315
0.0473
0.0631
0.0789
0.0946
0.1104
0.1262

Figure 19. Temperature contours and crystallinity distribution for melt inlet temperature 180°C, Pe_t = 5.3044E+05, Pe_c = 2.60E-11, ξ = 2.0E-03, and ζ = 1.8E-02.

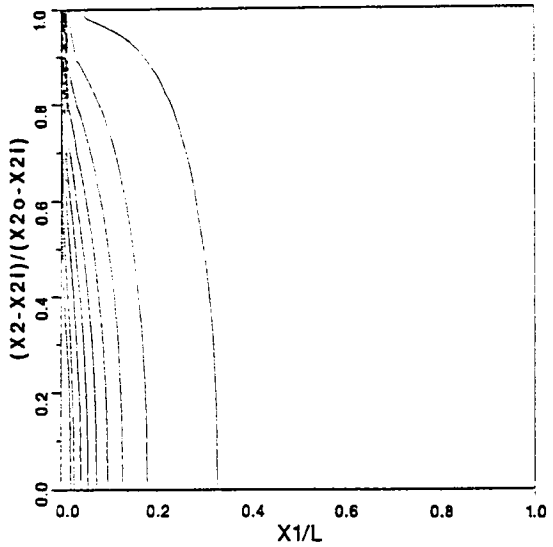

(a) amorphous material

temperature isotherms from left to right:
180°C
170°C
150°C
130°C
110°C
90°C
70°C
50°C
30°C

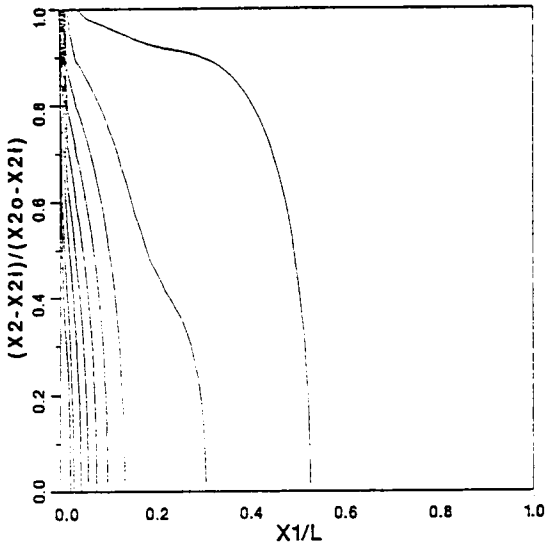

(b) semi-crystalline material

temperature isotherms from left to right:
180°C
170°C
150°C
130°C
110°C
90°C
70°C
50°C
30°C

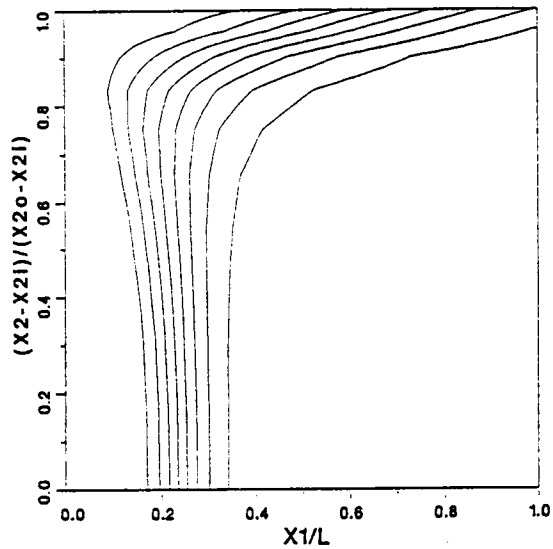

(c) semi-crystalline material

iso-crystallinity curves from left to right (relative values):
0.1111
0.2222
0.3333
0.4444
0.5555
0.6666
0.7777
0.8888

Figure 20. Temperature contours and crystallinity distribution for melt inlet temperature 190°C, Pe_t = 5.3044E+04, Pe_c = 2.60E-12, ξ = 2.0E-03, and ζ = 1.8E-02.

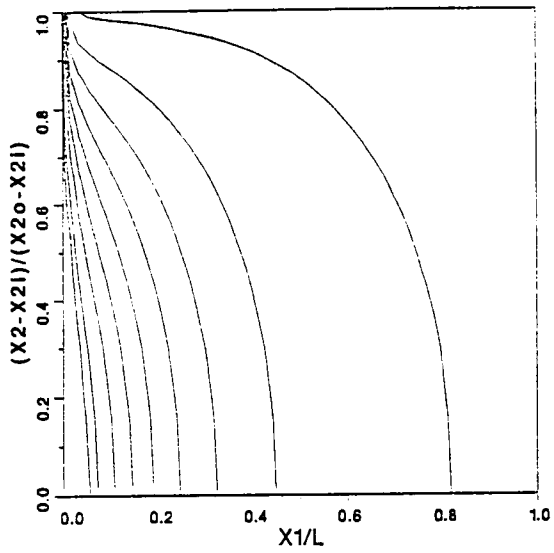

(a) amorphous material

temperature isotherms from left to right:
180°C
170°C
150°C
130°C
110°C
90°C
70°C
50°C
30°C

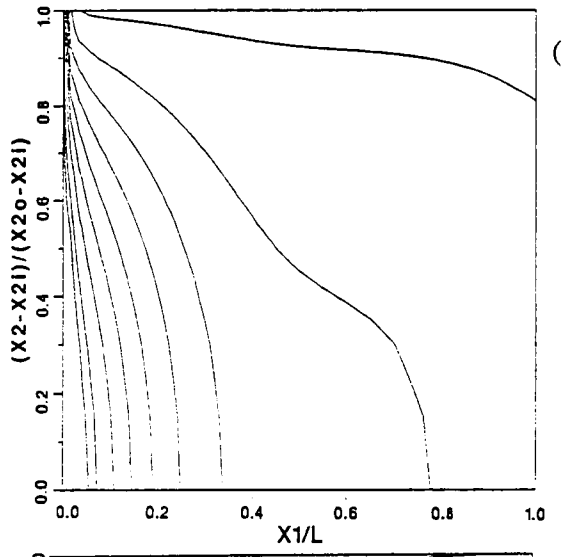

(b) semi-crystalline material

temperature isotherms from left to right:
180°C
170°C
150°C
130°C
110°C
90°C
70°C
50°C
30°C

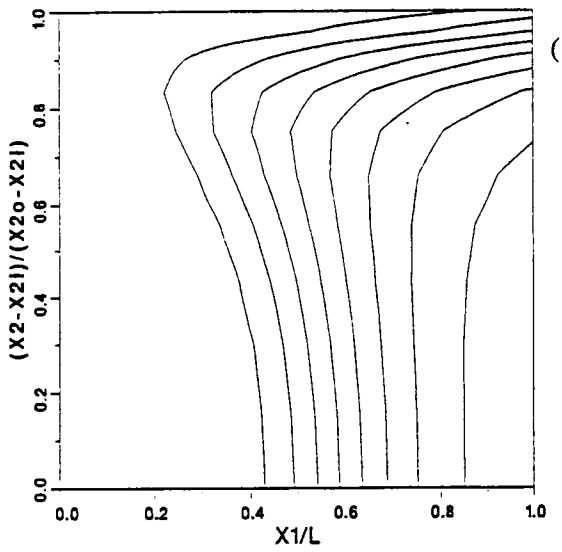

(c) semi-crystalline material

iso-crystallinity curves from left to right (relative values):
0.1072
0.2145
0.3217
0.4289
0.5362
0.6434
0.7507
0.8579

Figure 21. Temperature contours and crystallinity distribution for melt inlet temperature 190°C, Pe_t = 1.32611E+05, Pe_c = 6.50E-12, ξ = 2.0E-03, and ζ = 1.8E-02.

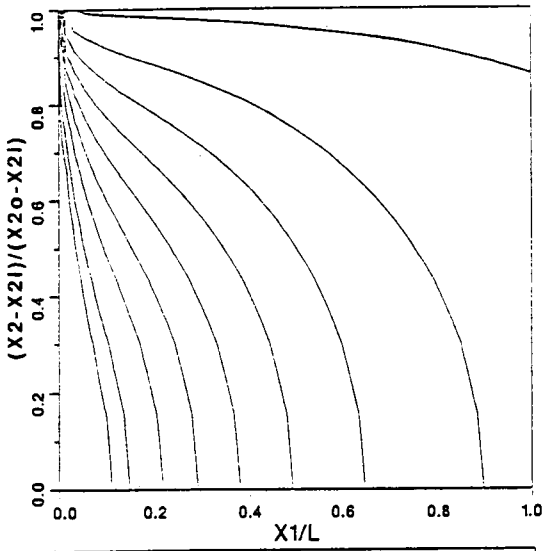

(a) amorphous material

temperature isotherms from left to right:
180°C
170°C
150°C
130°C
110°C
90°C
70°C
50°C
30°C

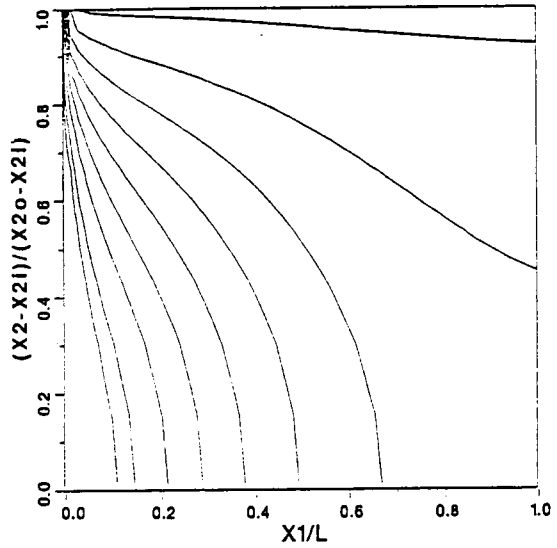

(b) semi-crystalline material

temperature isotherms from left to right:
180°C
170°C
150°C
130°C
110°C
90°C
70°C
50°C
30°C

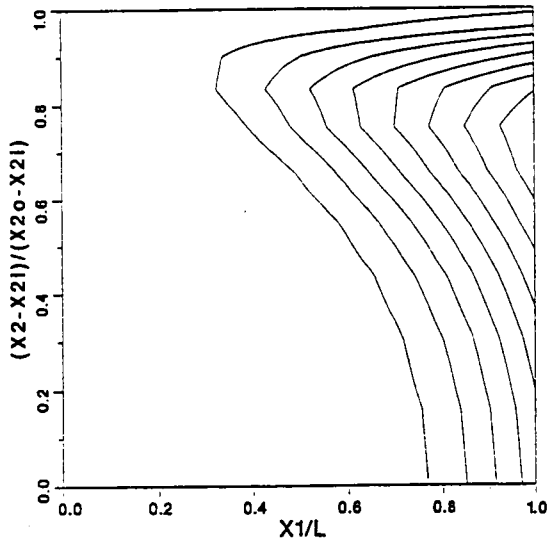

(c) semi-crystalline material

iso-crystallinity curves from left to right (relative values):
0.0519
0.1038
0.1557
0.2076
0.2595
0.3114
0.3633
0.4152

Figure 22. Temperature contours and crystallinity distribution for melt inlet temperature 190°C, Pe_t = 2.65222E+05, Pe_c = 1.30E-11, ξ = 2.0E-03, and ζ = 1.8E-02.

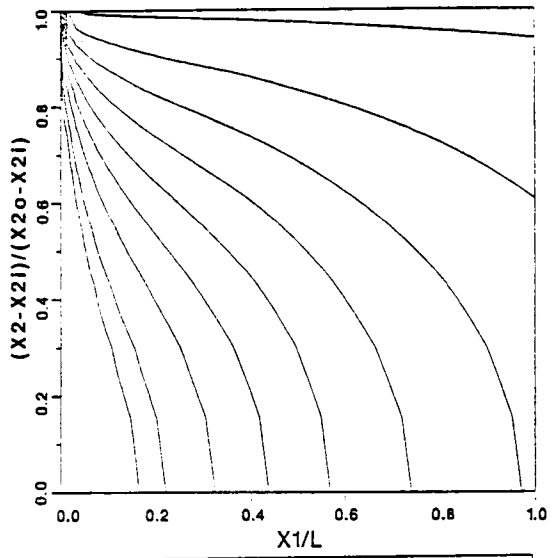

(a) amorphous material

temperature isotherms from left to right:
180°C
170°C
150°C
130°C
110°C
90°C
70°C
50°C
30°C

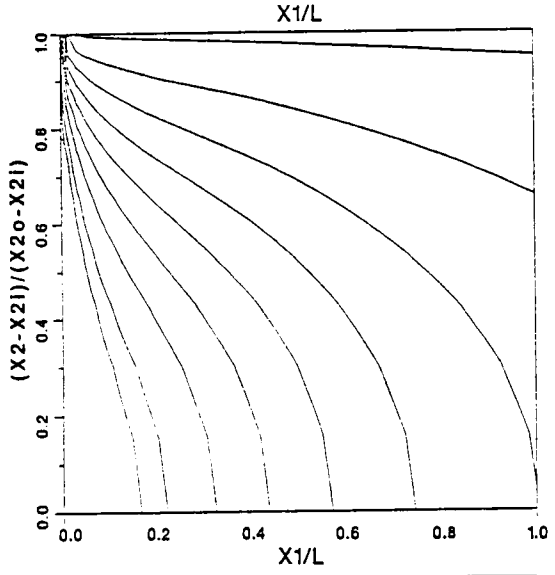

(b) semi-crystalline material

temperature isotherms from left to right:
180°C
170°C
150°C
130°C
110°C
90°C
70°C
50°C
30°C

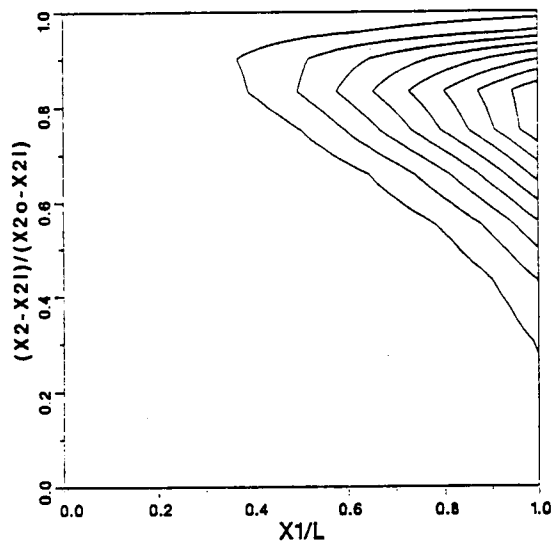

(c) semi-crystalline material

iso-crystallinity curves from left to right (relative values):
0.0270
0.0539
0.0809
0.1079
0.1348
0.1618
0.1887
0.2157

Figure 23. Temperature contours and crystallinity distribution for melt inlet temperature 190°C, Pe_t = 3.97833E+05, Pe_c = 1.95E-11, ξ = 2.0E-03, and ζ = 1.8E-02.

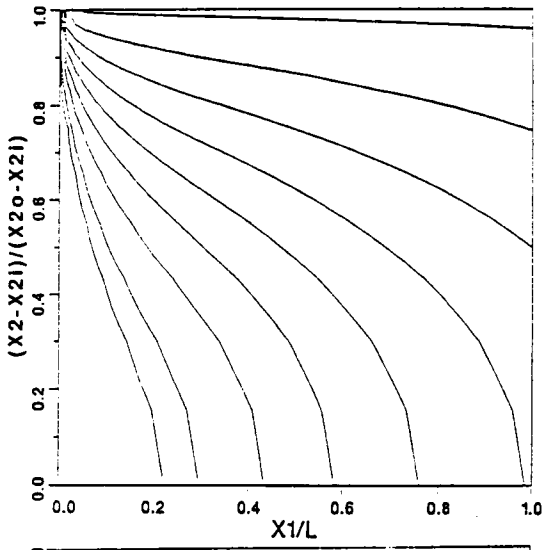

(a) amorphous material

temperature isotherms from left to right:
180°C
170°C
150°C
130°C
110°C
90°C
70°C
50°C
30°C

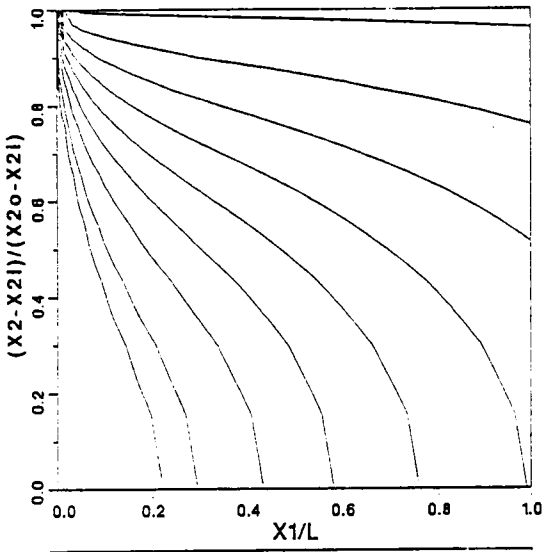

(b) semi-crystalline material

temperature isotherms from left to right:
180°C
170°C
150°C
130°C
110°C
90°C
70°C
50°C
30°C

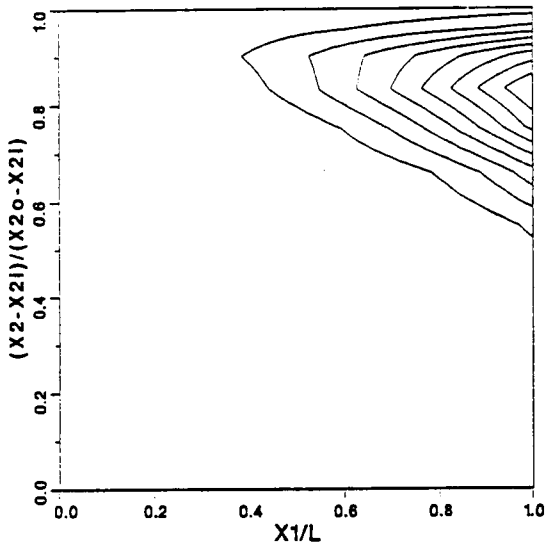

(c) semi-crystalline material

iso-crystallinity curves from left to right (relative values):
0.0158
0.0315
0.0473
0.0631
0.0789
0.0946
0.1104
0.1262

Figure 24. Temperature contours and crystallinity distribution for melt inlet temperature 190°C, Pe_t = 5.3044E+05, Pe_c = 2.60E-11, ξ = 2.0E-03, and ζ = 1.8E-02.

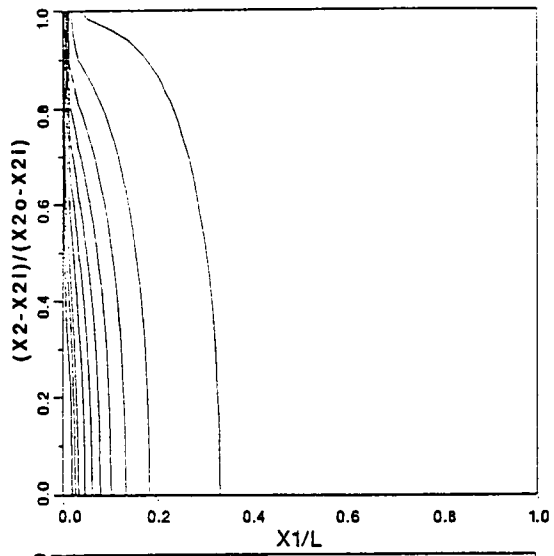

(a) amorphous material

temperature isotherms from left to right:
190°C
180°C
170°C
150°C
130°C
110°C
90°C
70°C
50°C
30°C

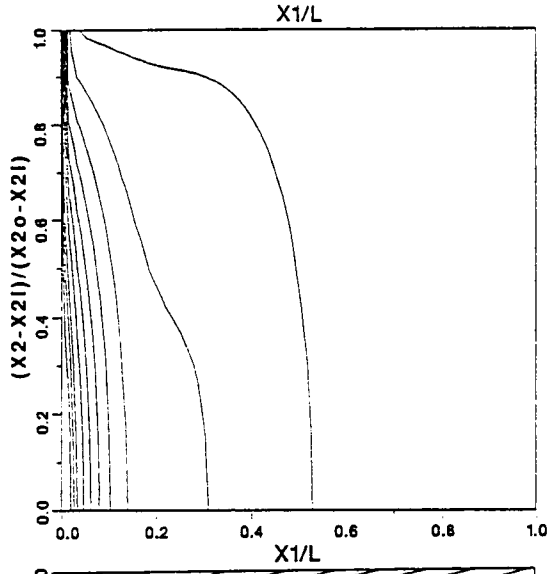

(b) semi-crystalline material

temperature isotherms from left to right:
190°C
180°C
170°C
150°C
130°C
110°C
90°C
70°C
50°C
30°C

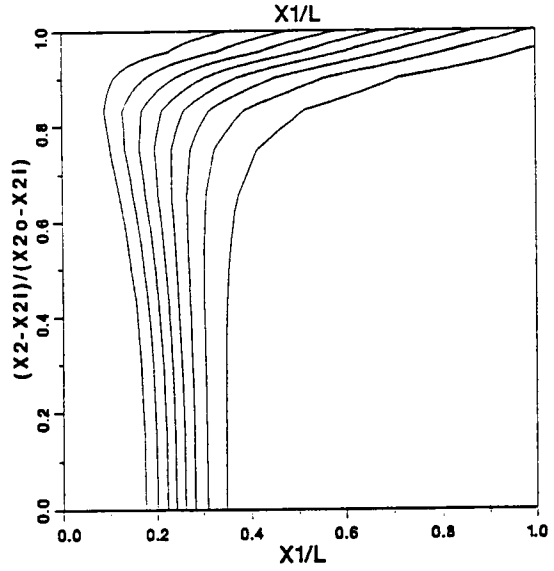

(c) semi-crystalline material

iso-crystallinity curves from left to right (relative values):
0.1111
0.2222
0.3333
0.4444
0.5555
0.6666
0.7777
0.8888

Figure 25. Temperature contours and crystallinity distribution for melt inlet temperature 200°C, Pe_t = 5.3044E+04, Pe_c = 2.60E-12, ξ = 2.0E-03, and ζ = 1.8E-02.

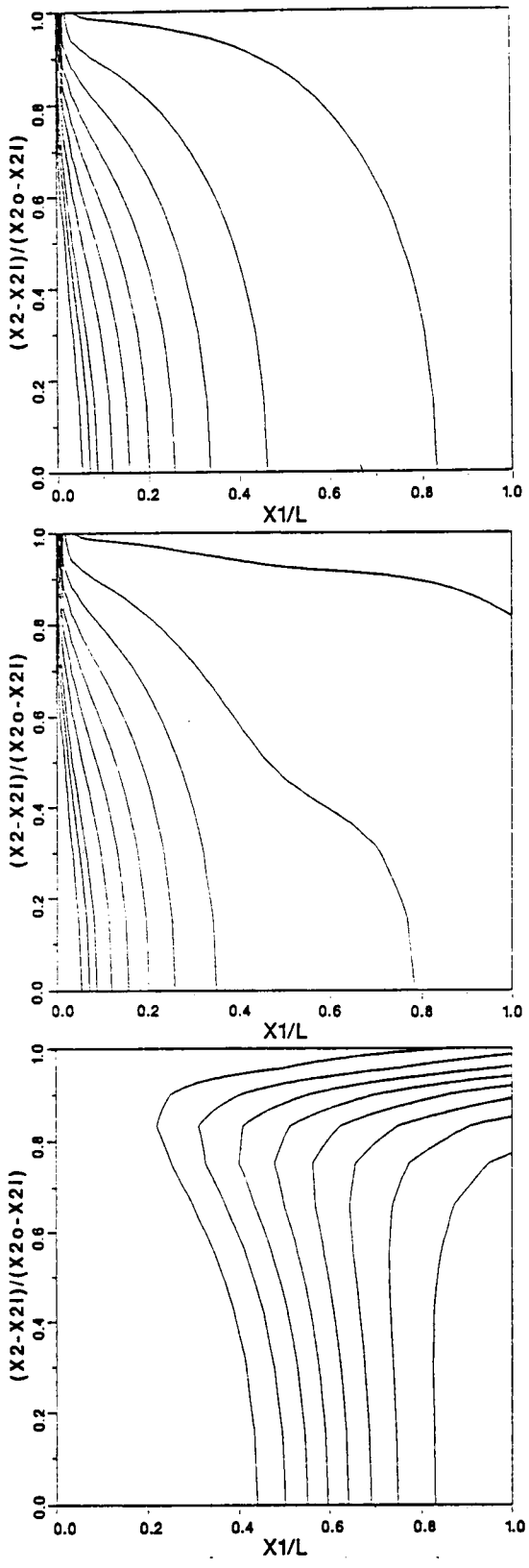

(a) amorphous material

temperature isotherms from left to right:
190°C
180°C
170°C
150°C
130°C
110°C
90°C
70°C
50°C
30°C

(b) semi-crystalline material

temperature isotherms from left to right:
190°C
180°C
170°C
150°C
130°C
110°C
90°C
70°C
50°C
30°C

(c) semi-crystalline material

iso-crystallinity curves from left to right (relative values):
0.1072
0.2145
0.3217
0.4289
0.5362
0.6434
0.7507
0.8579

Figure 26. Temperature contours and crystallinity distribution for melt inlet temperature 200°C, Pe_t = 1.32611E+05, Pe_c = 6.50E-12, ξ = 2.0E-03, and ζ = 1.8E-02.

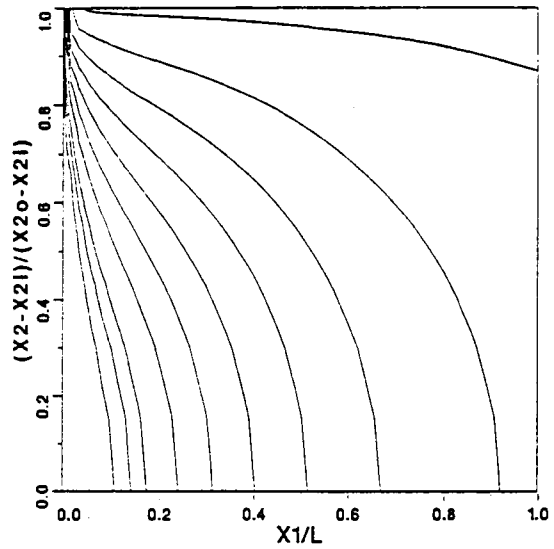

(a) amorphous material

temperature isotherms from left to right:
190°C
180°C
170°C
150°C
130°C
110°C
90°C
70°C
50°C
30°C

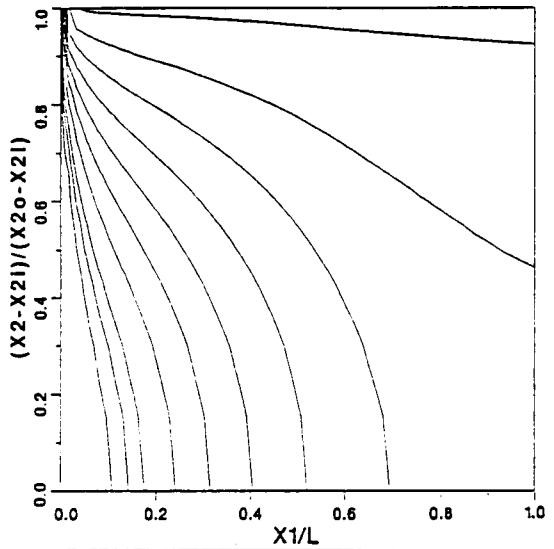

(b) semi-crystalline material

temperature isotherms from left to right:
190°C
180°C
170°C
150°C
130°C
110°C
90°C
70°C
50°C
30°C

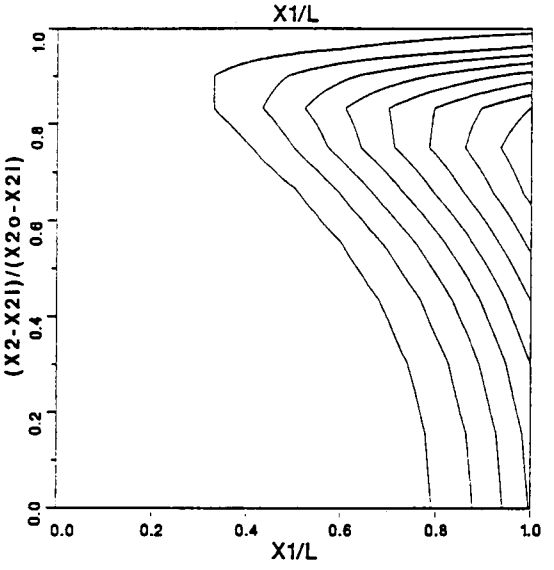

(c) semi-crystalline material

iso-crystallinity curves from left to right (relative values):
0.0519
0.1038
0.1557
0.2076
0.2595
0.3114
0.3633
0.4152

Figure 27. Temperature contours and crystallinity distribution for melt inlet temperature 200°C, Pe_t = 2.65222E+05, Pe_c = 1.30E-11, ξ = 2.0E-03, and ζ = 1.8E-02.

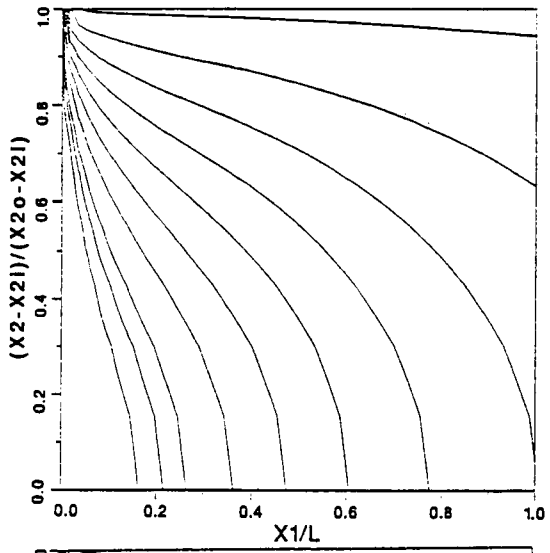

(a) amorphous material

temperature isotherms from left to right:
190°C
180°C
170°C
150°C
130°C
110°C
90°C
70°C
50°C
30°C

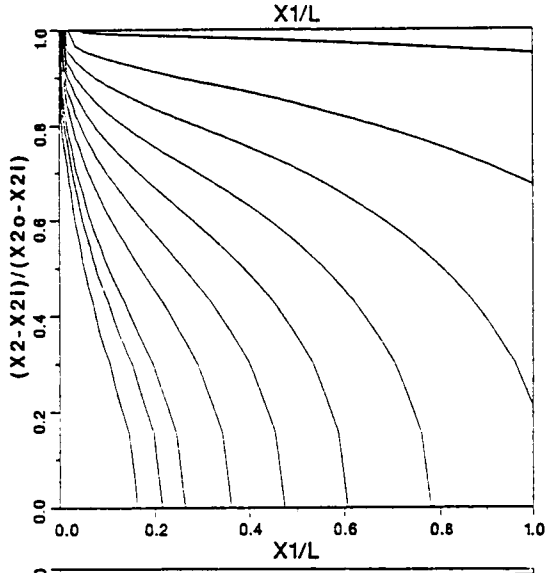

(b) semi-crystalline material

temperature isotherms from left to right:
190°C
180°C
170°C
150°C
130°C
110°C
90°C
70°C
50°C
30°C

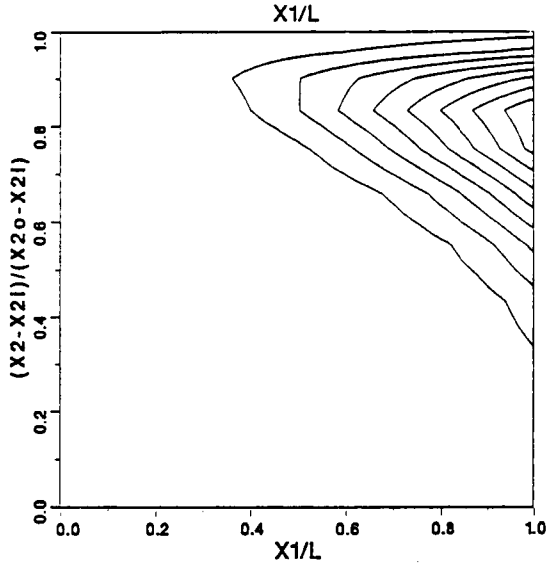

(c) semi-crystalline material

iso-crystallinity curves from left to right (relative values):
0.0270
0.0539
0.0809
0.1079
0.1348
0.1618
0.1887
0.2157

Figure 28. Temperature contours and crystallinity distribution for melt inlet temperature 200°C, Pe_t = 3.97833E+05, Pe_c = 1.95E-11, ξ = 2.0E-03, and ζ = 1.8E-02.

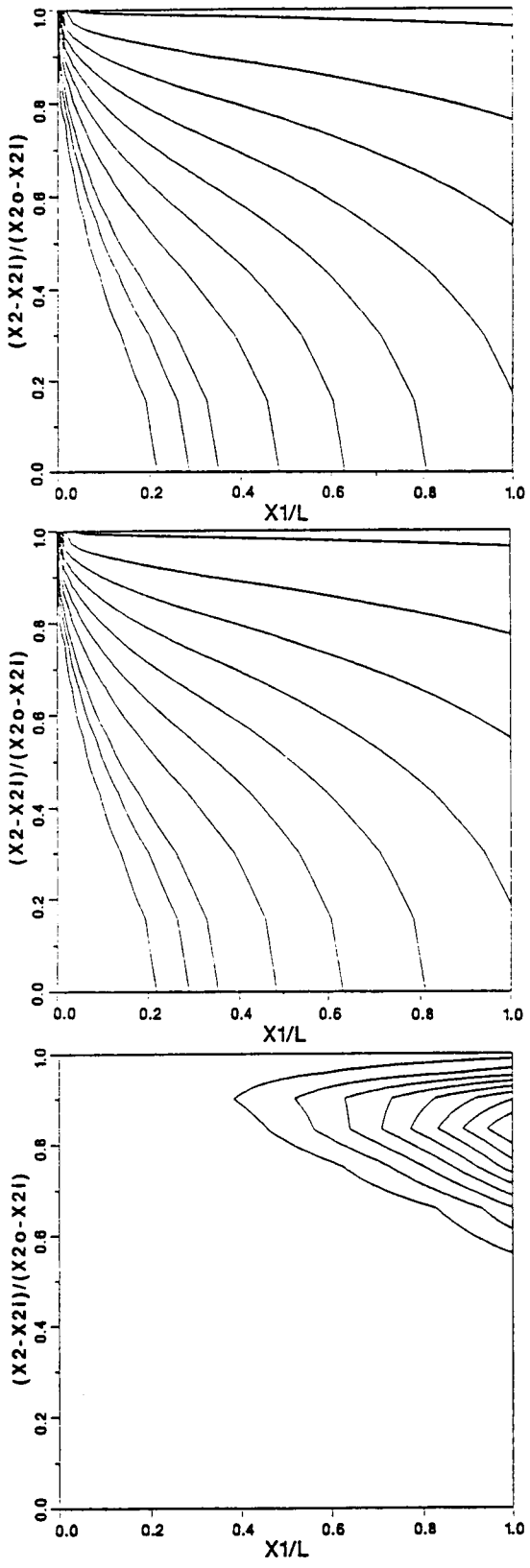

(a) amorphous material

temperature isotherms from left to right:
190°C
180°C
170°C
150°C
130°C
110°C
90°C
70°C
50°C
30°C

(b) semi-crystalline material

temperature isotherms from left to right:
190°C
180°C
170°C
150°C
130°C
110°C
90°C
70°C
50°C
30°C

(c) semi-crystalline material

iso-crystallinity curves from left to right (relative values):
0.0158
0.0315
0.0473
0.0631
0.0789
0.0946
0.1104
0.1262

Figure 29. Temperature contours and crystallinity distribution for melt inlet temperature 200°C, Pe_t = 5.3044E+05, Pe_c = 2.60E-11, ξ = 2.0E-03, and ζ = 1.8E-02.

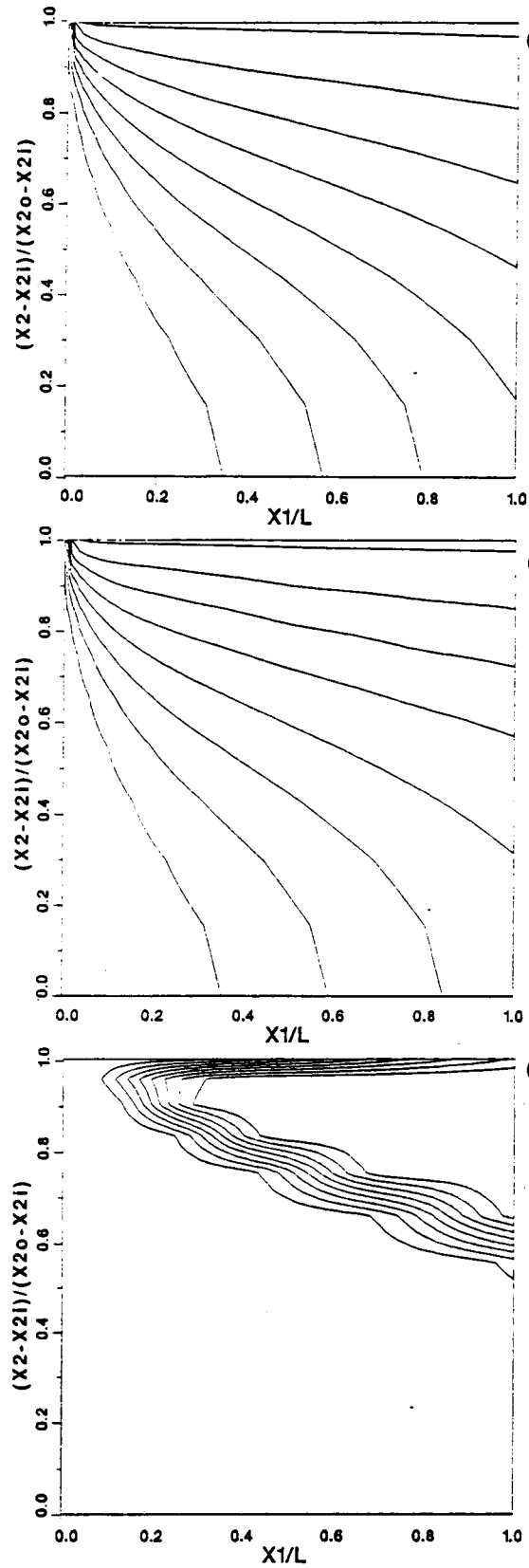

(a) amorphous material

temperature isotherms from left to right:
170°C
150°C
130°C
110°C
90°C
70°C
50°C
30°C

(b) semi-crystalline material

temperature isotherms from left to right:
170°C
150°C
130°C
110°C
90°C
70°C
50°C
30°C

(c) semi-crystalline material

iso-crystallinity curves from left to right (relative values):
0.1111
0.2222
0.3333
0.4444
0.5555
0.6666
0.7777
0.8888

Figure 30. Temperature contours and crystallinity distribution for melt inlet temperature 180°C, Pe_t = 5.3044E+04, Pe_c = 2.60E-12, ξ = 8.0E-03, and ζ = 1.8E-02.

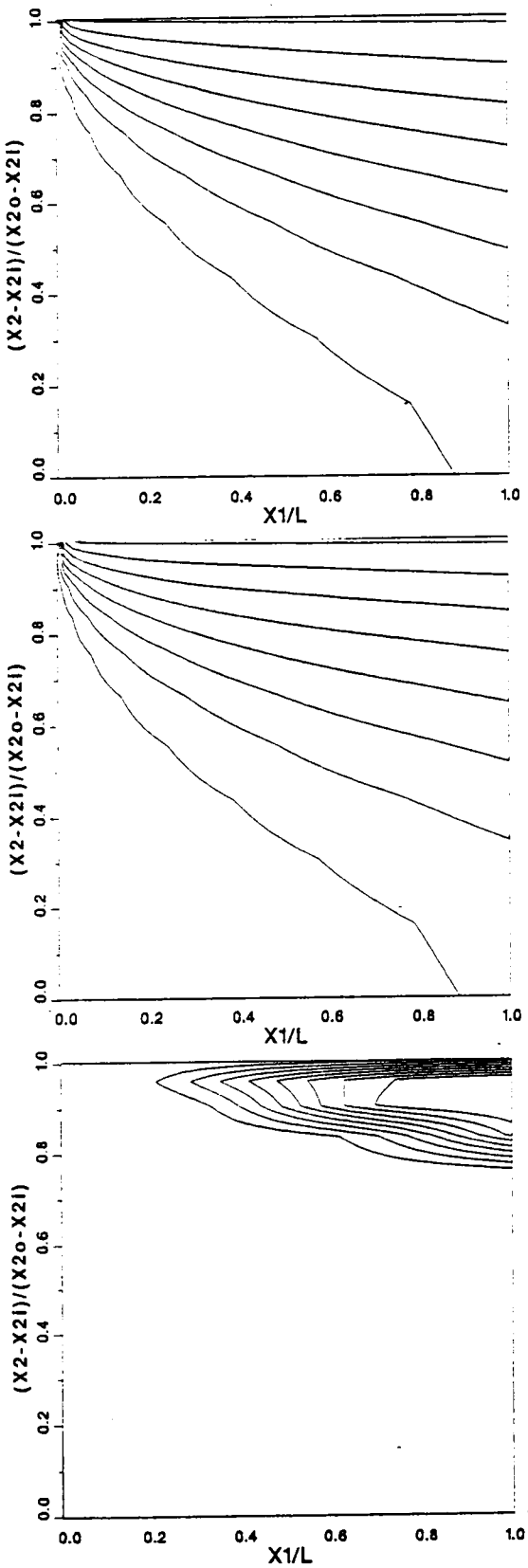

(a) amorphous material

temperature isotherms from left to right:
170°C
150°C
130°C
110°C
90°C
70°C
50°C
30°C

(b) semi-crystalline material

temperature isotherms from left to right:
170°C
150°C
130°C
110°C
90°C
70°C
50°C
30°C

(c) semi-crystalline material

iso-crystallinity curves from left to right (relative values):
0.1072
0.2145
0.3217
0.4289
0.5362
0.6434
0.7507
0.8579

Figure 31. Temperature contours and crystallinity distribution for melt inlet temperature 180°C, Pe_t = 1.32611E+05, Pe_c = 6.50E-12, ξ = 8.0E-03, and ζ = 1.8E-02.

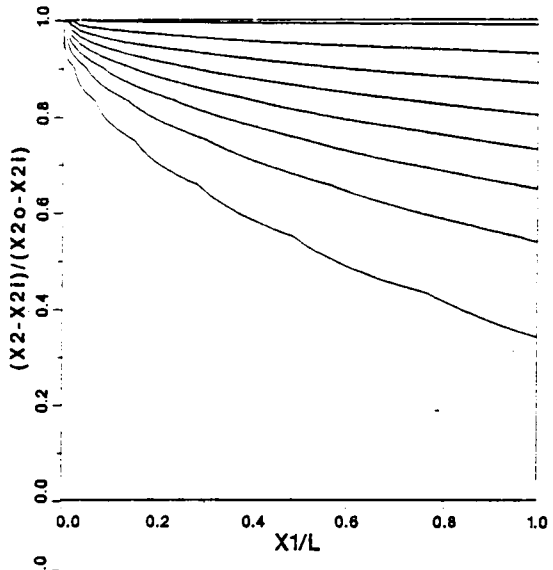

(a) amorphous material

temperature isotherms from left to right:
170°C
150°C
130°C
110°C
90°C
70°C
50°C
30°C

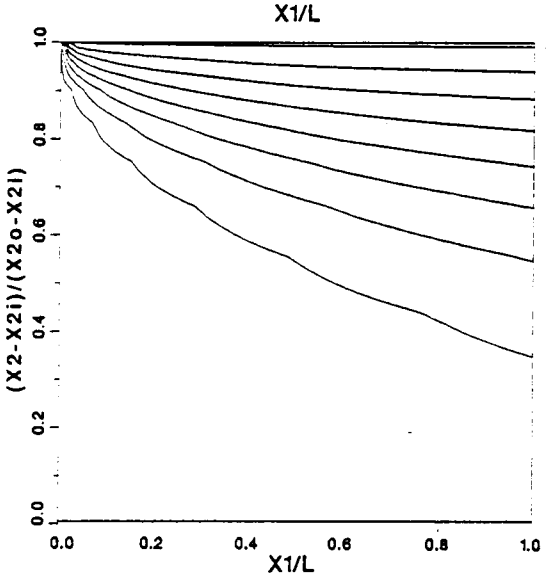

(b) semi-crystalline material

temperature isotherms from left to right:
170°C
150°C
130°C
110°C
90°C
70°C
50°C
30°C

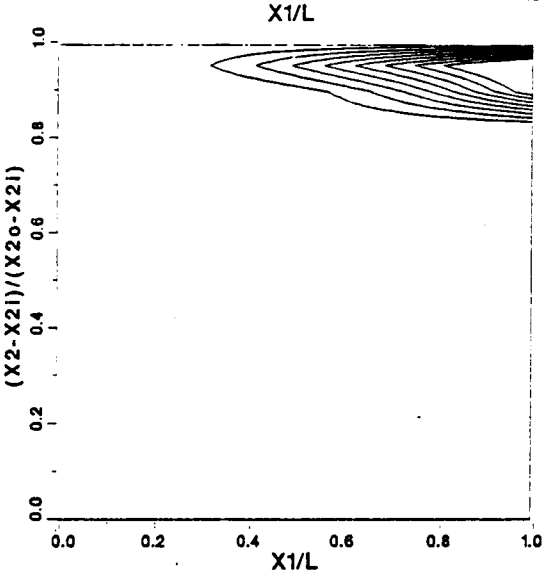

(c) semi-crystalline material

iso-crystallinity curves from left to right (relative values):
0.0519
0.1038
0.1557
0.2076
0.2595
0.3114
0.3633
0.4152

Figure 32. Temperature contours and crystallinity distribution for melt inlet temperature 180°C, Pe_t = 2.65222E+05, Pe_c = 1.30E-11, ξ = 8.0E-03, and ζ = 1.8E-02.

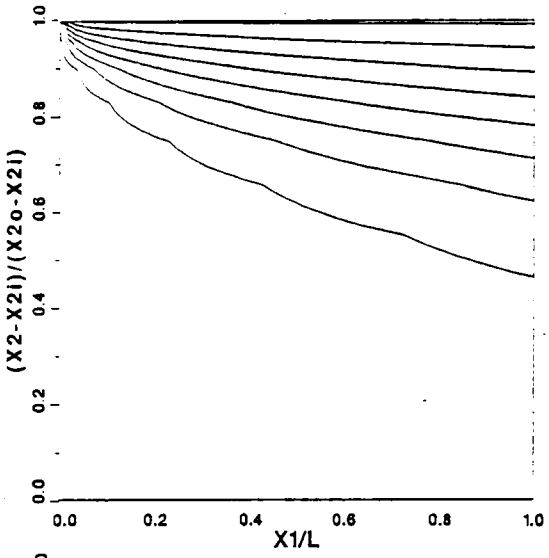

(a) amorphous material

temperature isotherms from left to right:
170°C
150°C
130°C
110°C
90°C
70°C
50°C
30°C

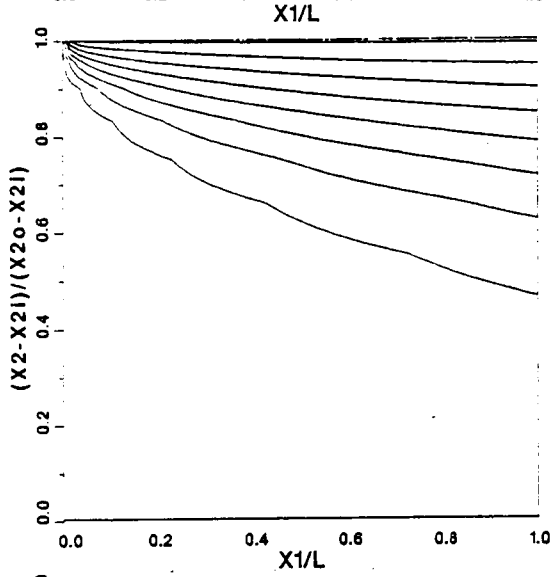

(b) semi-crystalline material

temperature isotherms from left to right:
170°C
150°C
130°C
110°C
90°C
70°C
50°C
30°C

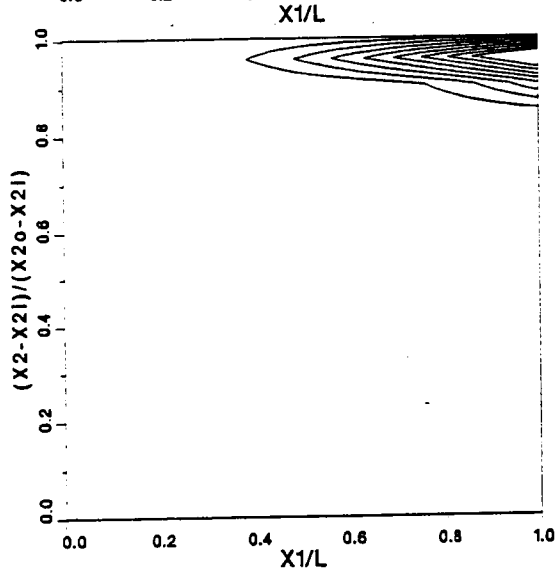

(c) semi-crystalline material

iso-crystallinity curves from left to right (relative values):
0.0270
0.0539
0.0809
0.1079
0.1348
0.1618
0.1887
0.2157

Figure 33. Temperature contours and crystallinity distribution for melt inlet temperature 180°C, Pe_t = 3.97833E+05, Pe_c = 1.95E-11, ξ = 8.0E-03, and ζ = 1.8E-02.

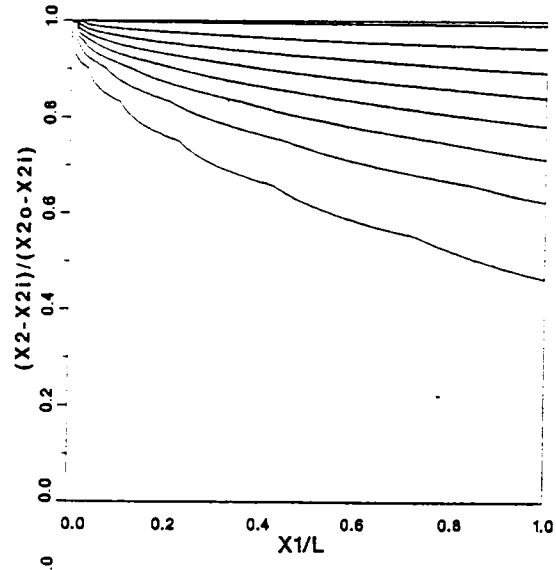

(a) amorphous material

temperature isotherms from left to right:
170°C
150°C
130°C
110°C
90°C
70°C
50°C
30°C

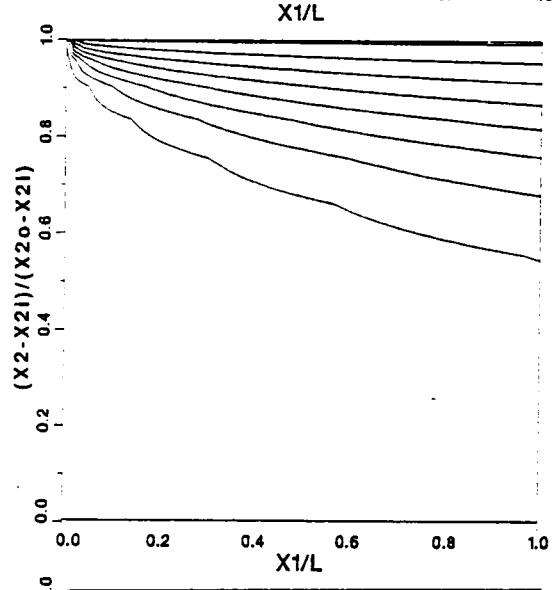

(b) semi-crystalline material

temperature isotherms from left to right:
170°C
150°C
130°C
110°C
90°C
70°C
50°C
30°C

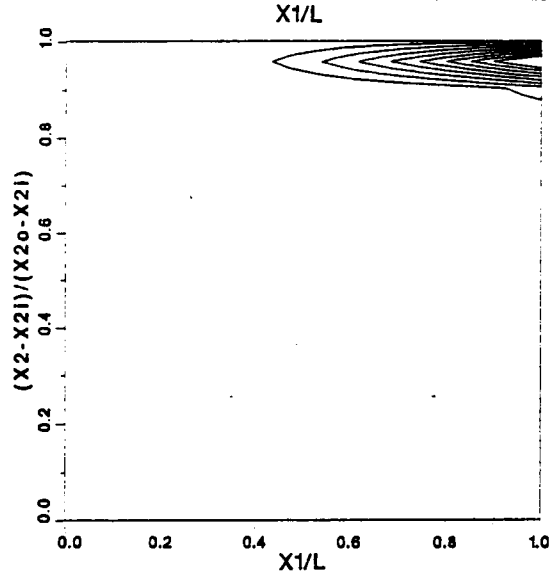

(c) semi-crystalline material

iso-crystallinity curves from left to right (relative values):
0.0158
0.0315
0.0473
0.0631
0.0789
0.0946
0.1104
0.1262

Figure 34. Temperature contours and crystallinity distribution for melt inlet temperature 180°C, Pe_t = 5.3044E+05, Pe_c = 2.60E-11, ξ = 8.0E-03, and ζ = 1.8E-02.

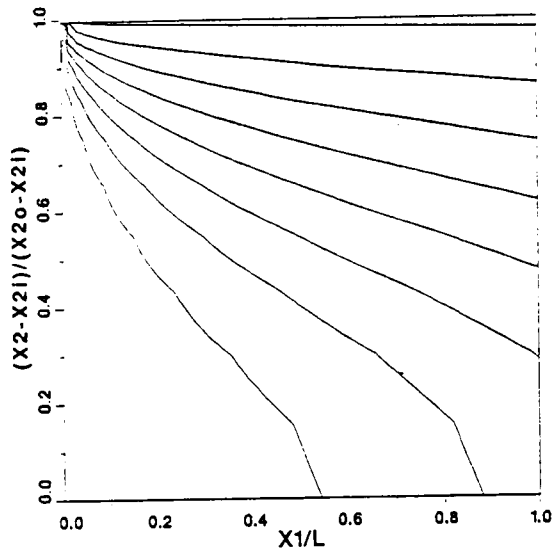

(a) amorphous material

temperature isotherms from left to right:
170°C
150°C
130°C
110°C
90°C
70°C
50°C
30°C

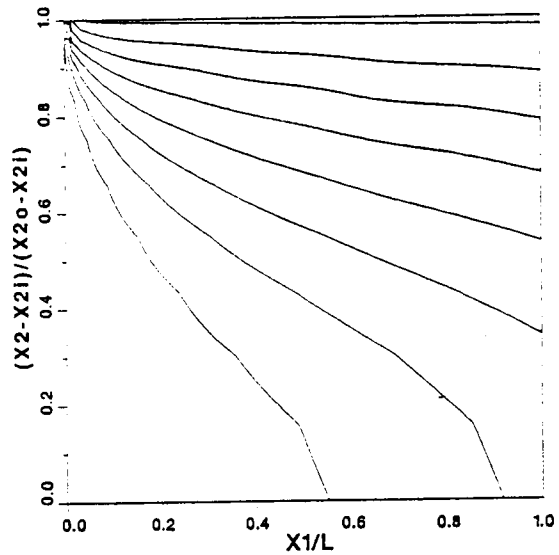

(b) semi-crystalline material

temperature isotherms from left to right:
170°C
150°C
130°C
110°C
90°C
70°C
50°C
30°C

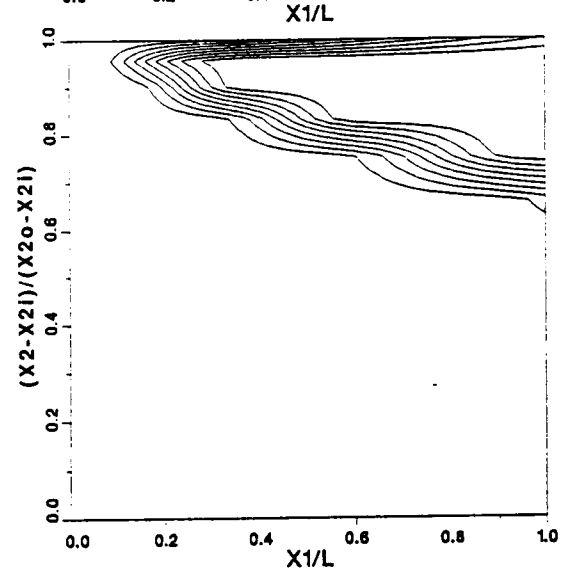

(c) semi-crystalline material

iso-crystallinity curves from left to right (relative values):
0.1111
0.2222
0.3333
0.4444
0.5555
0.6666
0.7777
0.8888

Figure 35. Temperature contours and crystallinity distribution for melt inlet temperature 180°C, Pe_t = 5.3044E+04, Pe_c = 2.60E-12, ξ = 1.0E-02, and ζ = 1.8E-02.

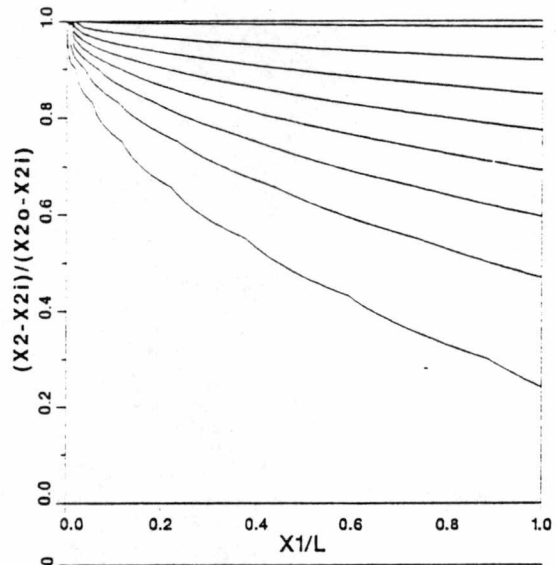

(a) amorphous material

temperature isotherms from left to right:
170°C
150°C
130°C
110°C
90°C
70°C
50°C
30°C

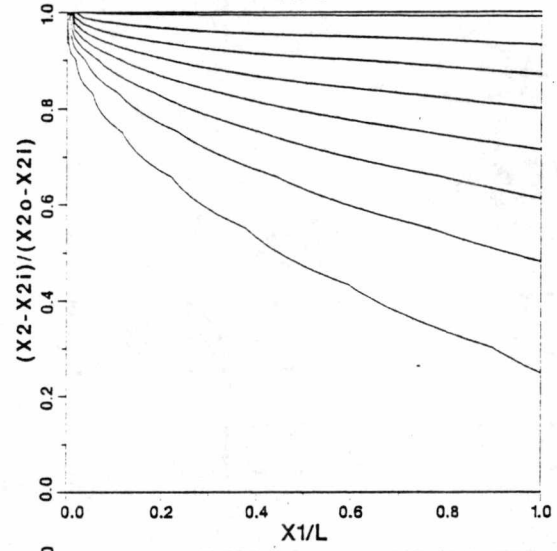

(b) semi-crystalline material

temperature isotherms from left to right:
170°C
150°C
130°C
110°C
90°C
70°C
50°C
30°C

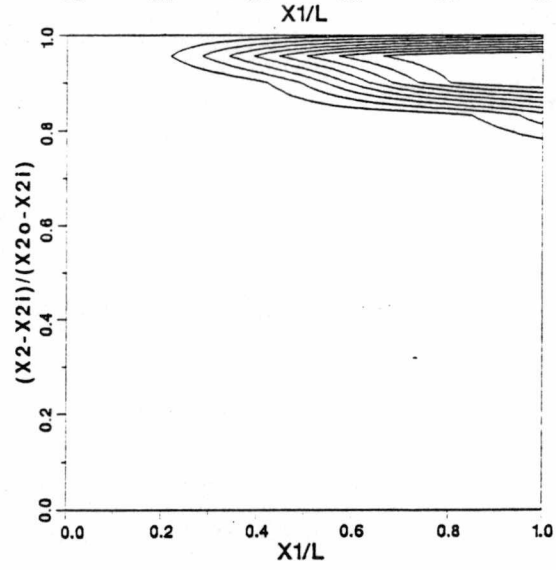

(c) semi-crystalline material

iso-crystallinity curves from left to right (relative values):
0.1072
0.2145
0.3217
0.4289
0.5362
0.6434
0.7507
0.8579

Figure 36. Temperature contours and crystallinity distribution for melt inlet temperature 180°C, Pe_t = 1.32611E+05, Pe_c = 6.50E-12, ξ = 1.0E-02, and ζ = 1.8E-02.

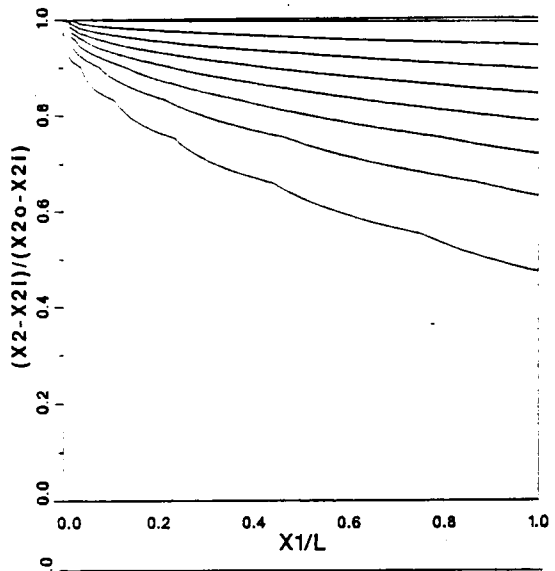

(a) amorphous material

temperature isotherms from left to right:
170°C
150°C
130°C
110°C
90°C
70°C
50°C
30°C

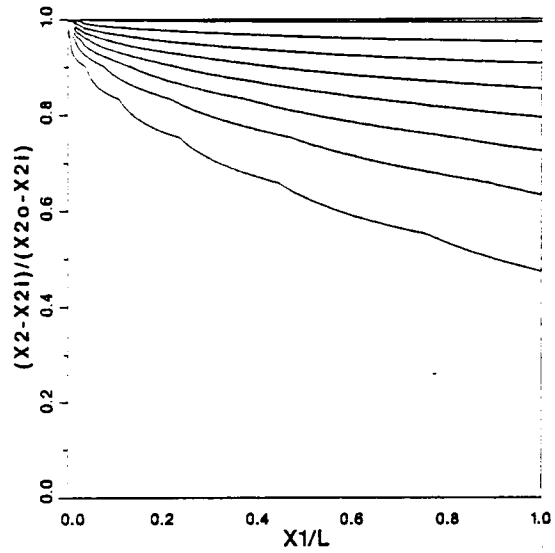

(b) semi-crystalline material

temperature isotherms from left to right:
170°C
150°C
130°C
110°C
90°C
70°C
50°C
30°C

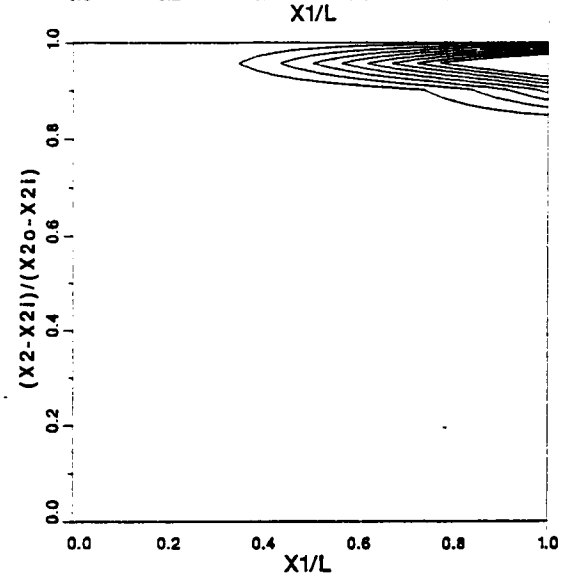

(c) semi-crystalline material

iso-crystallinity curves from left to right (relative values):
0.0519
0.1038
0.1557
0.2076
0.2595
0.3114
0.3633
0.4152

Figure 37. Temperature contours and crystallinity distribution for melt inlet temperature 180°C, Pe_t = 2.65222E+05, Pe_c = 1.30E-11, ξ = 1.0E-02, and ζ = 1.8E-02.

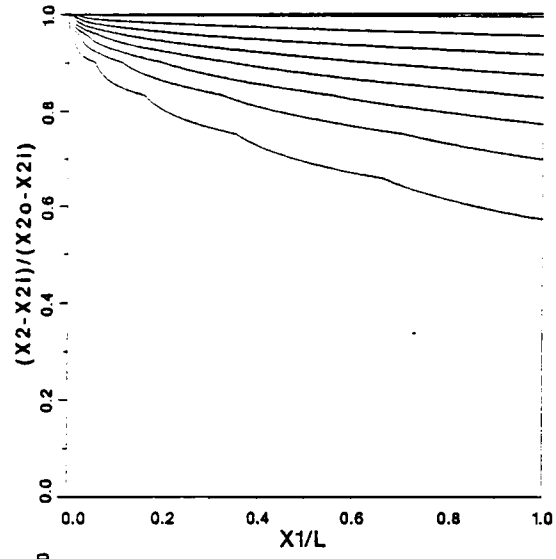

(a) amorphous material

temperature isotherms from left to right:
170°C
150°C
130°C
110°C
90°C
70°C
50°C
30°C

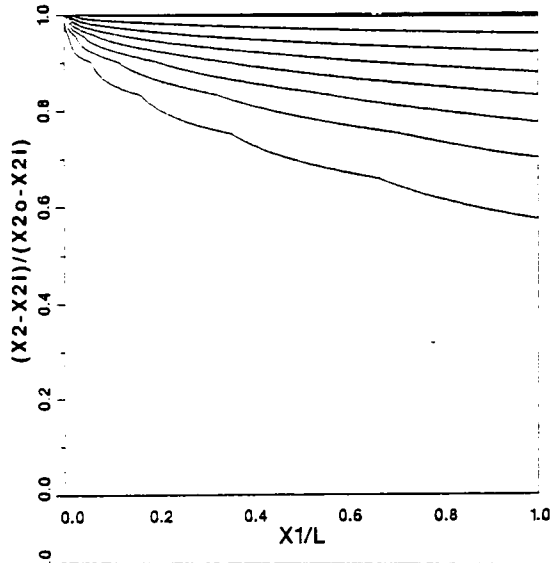

(b) semi-crystalline material

temperature isotherms from left to right:
170°C
150°C
130°C
110°C
90°C
70°C
50°C
30°C

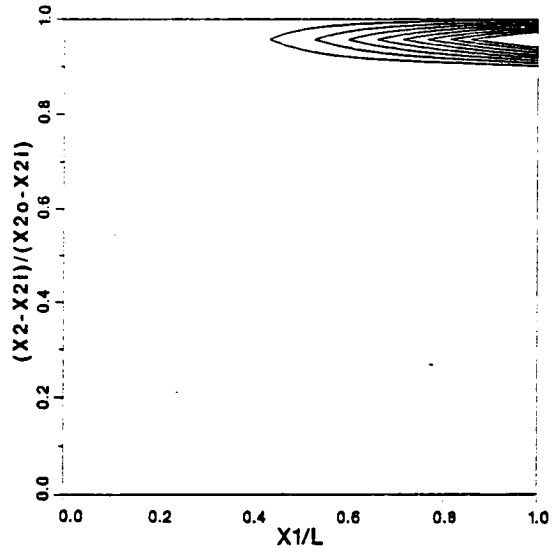

(c) semi-crystalline material

iso-crystallinity curves from left to right (relative values):
0.0270
0.0539
0.0809
0.1079
0.1348
0.1618
0.1887
0.2157

Figure 38. Temperature contours and crystallinity distribution for melt inlet temperature 180°C, Pe_t = 3.97833E+05, Pe_c = 1.95E-11, ξ = 1.0E-02, and ζ = 1.8E-02.

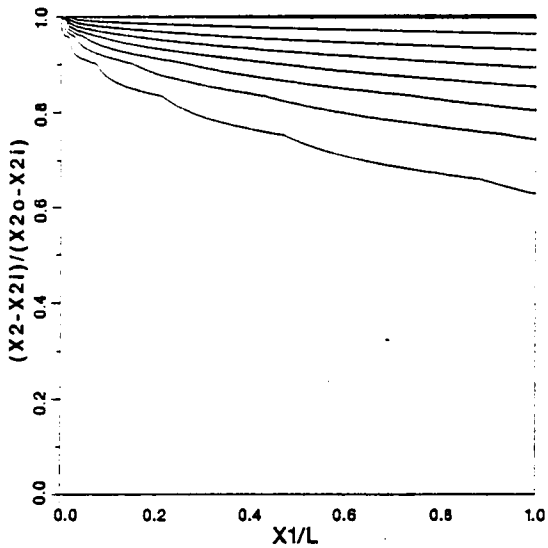

(a) amorphous material

temperature isotherms from left to right:
170°C
150°C
130°C
110°C
90°C
70°C
50°C
30°C

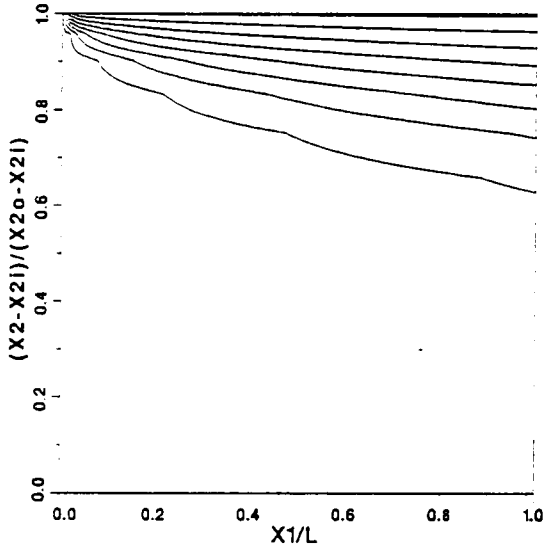

(b) semi-crystalline material

temperature isotherms from left to right:
170°C
150°C
130°C
110°C
90°C
70°C
50°C
30°C

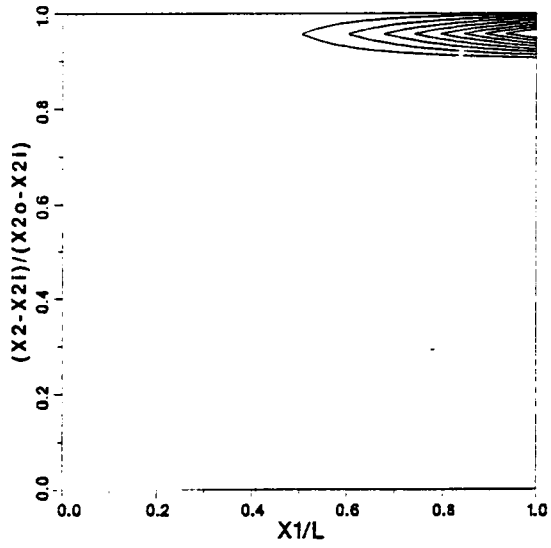

(c) semi-crystalline material

iso-crystallinity curves from left to right (relative values):
0.0158
0.0315
0.0473
0.0631
0.0789
0.0946
0.1104
0.1262

Figure 39. Temperature contours and crystallinity distribution for melt inlet temperature 180°C, Pe_t = 5.3044E+05, Pe_c = 2.60E-11, ξ = 1.0E-02, and ζ = 1.8E-02.

chamber, an increase in thermal Peclet number (i.e. an increase in melt velocity) implies the residence time of polymer melt in the cooling chamber decreases. It is expected that the isotherms will move toward the outer surface of the pipe as shown in figures. Hence, one can easily predict the length of the chamber needed for cooling the pipe to desired room temperature increases corresponding to an increase in pipe haul-off speed.

It is also noted that the maximum degree of crystallinity obtained in the cooling chamber is very sensitive to melt flow velocity. Recall the Peclet number, Pe_c, defined for polymer crystallization. This dimensionless number implies the ratio of crystallization time to element transport time in the cooling chamber. For a given material, an increase in Pe_c means that a material element spends less time in passing through the temperature interval at which crystallization can occur. It is observed that the values of the maximum relative crystallinity can vary from almost 100% for Pe_c = 2.60E-12 to 12.62% for Pe_c = 2.60E-11. In addition, it also has the effects of broadening the crystallization band as well as moving the crystallization band downstream of the pipe line as can be seen in the simulation results.

Due to low thermal conductivity of polymer, elevating melt inlet temperature makes cooling equipments more difficult to cool the hot pipe to desired temperature. Elevating melt inlet temperature only changes a little bit the temperature distribution near the outer pipe surface; however, it has a profound influence in the temperature field near the adiabatic boundary surface. It is observed that the temperature contour near the adiabatic boundary surface is shifted downstream of the pipe line. For temperature dependence of polymer crystallization, the crystallization band is also

affected; however, without shifting it downstream, the band is narrower than that of low melt inlet temperature.

Applying a non-linear regression method, Patel fitted nonisothermal crystallization data on polypropylene obtained by DSC measurement using the differential form of Nakamura's model[31]

$$\frac{d\theta}{dt} = n\cdot\mathcal{K}_c(T)\cdot(1-\theta)[\ \ln(\frac{1}{1-\theta})\ ]^{(n-1)/n} \qquad (1.4\text{-}15)$$

where $\mathcal{K}_c = \{\ln(2)^{1/n}/(t_{0.5})\}$ and again has the following expression

$$\mathcal{K}_c(T) = \mathcal{K}_\infty \exp\{-\frac{U^*}{R(T-T_\infty)}\}\exp\{-\frac{C_3}{T\Delta T}\} \qquad (3.2\text{-}7)$$

As shown in Figure 4, keeping n=2.5, he found that the prediction of non-isothermal crystallization according to equation (1.4-15) agrees with his experimental data very well by taking the averaged value of $\mathcal{K}_{c0}$, 7.696E+07 (1/sec), based on C_3 = 5.0E+05 ($^oK^2$). Equation (3.2-7) thus can be used to predict the crystallization rates at lower temperatures, where experimental determination is impossible. It can be seen in the curve (a) of Figure 8 that the maximum crystallization rate occurs around 60°C. Simulation results shown in figures for ξ ($=\Delta x_2/L$) equal to 2.0E-3 indicate polypropylene crystallizes between 26° and 70°C. Increasing the value of ξ to 0.01 results in a crystallization band between 26° and 90°C. As illustrated in Figure 4, the temperature at which polypropylene begins to crystallize shifts to higher temperature at lower cooling rate. Increasing the value of ξ implies the cooling rates become slower (especially for the polymer melt near the

adiabatic boundary surface); consequently, a broader crystallization interval can be observed.

With the values of $\mathcal{K}_{co}$ = 7.696E+07(1/sec) and C_3 = 5.0E+05($^oK^2$) proposed by Patel, equation (3.2-7) is used to predict the crystallization rates of polypropylene over the crystallization range. For C_3 embedded in the exponent of nucleation term, $\exp\{-C_3/T\Delta T\}$, it is expected that a slight change in the value of C_3 will give a larger deviation from the crystallization rates predicted by Patel than a slight change in the value of the pre-exponential factor, $\mathcal{K}_{co}$. As shown in Figure 8, a 5% decrease (or 5% increase) in C_3 results in a significant increase (or decrease) in crystallization rates and a 5% increase (or 5% decrease) in $\mathcal{K}_{co}$ only causes a slight deviation from Patel's predictions. The sensitivity of crystallization rate to either the change in C_3 or the change in $\mathcal{K}_{co}$ is especially reflected by the comparison of the results of numerical simulation between Figure 15 and Figures 40-43. Depressing crystallization rate implies that crystallization band will be broadened as can be seen in Figures 40 and 42. This fact is obvious in Figure 40 in which a wide-spread crystallization band is observed when the value of C_3 increases from 5.0E+05 to 5.25E+05. The crystallization band is also broadened by decreasing the value of $\mathcal{K}_{co}$ from 7.696E+07 to 7.3112E+07; however, this effect is not so significant by comparing Figure 15 with Figure 42. On the contrary, elevating crystallization rate has the effect of narrowing the crystallization band as illustrated in Figures 41 and 43. Particularly, a quite narrow band is observed in Figure 41 when C_3 is dropped from 5.0E+05 to 4.75E+05. Figure 43 also indicates that increasing the value of $\mathcal{K}_{co}$ from 7.696E+07 to 8.0808E+07 only narrows the band a little bit. The effect of depressing (or elevating)

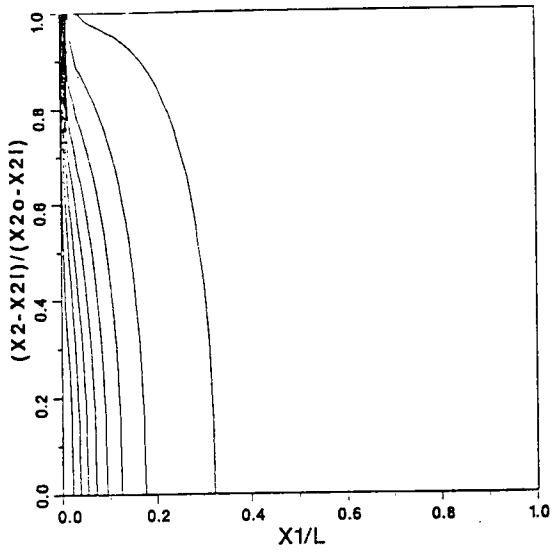

(a) amorphous material

temperature isotherms from left to right:
170°C
150°C
130°C
110°C
90°C
70°C
50°C
30°C

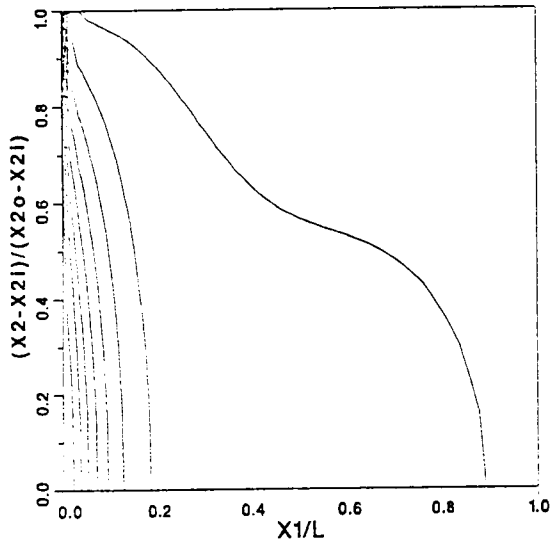

(b) semi-crystalline material

temperature isotherms from left to right:
170°C
150°C
130°C
110°C
90°C
70°C
50°C
30°C

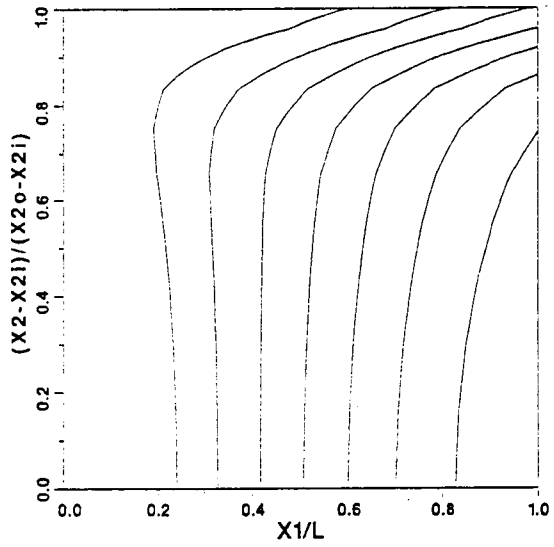

(c) semi-crystalline material

iso-crystallinity curves from left to right (relative values):
0.1111
0.2222
0.3333
0.4444
0.5555
0.6666
0.7777

Figure 40. Temperature contours and crystallinity distribution for C_3 = 5.25E+05($^\circ K^2$) and χ_{co} = 7.696E+07(sec^{-1}) under the same conditions in Figure 15.

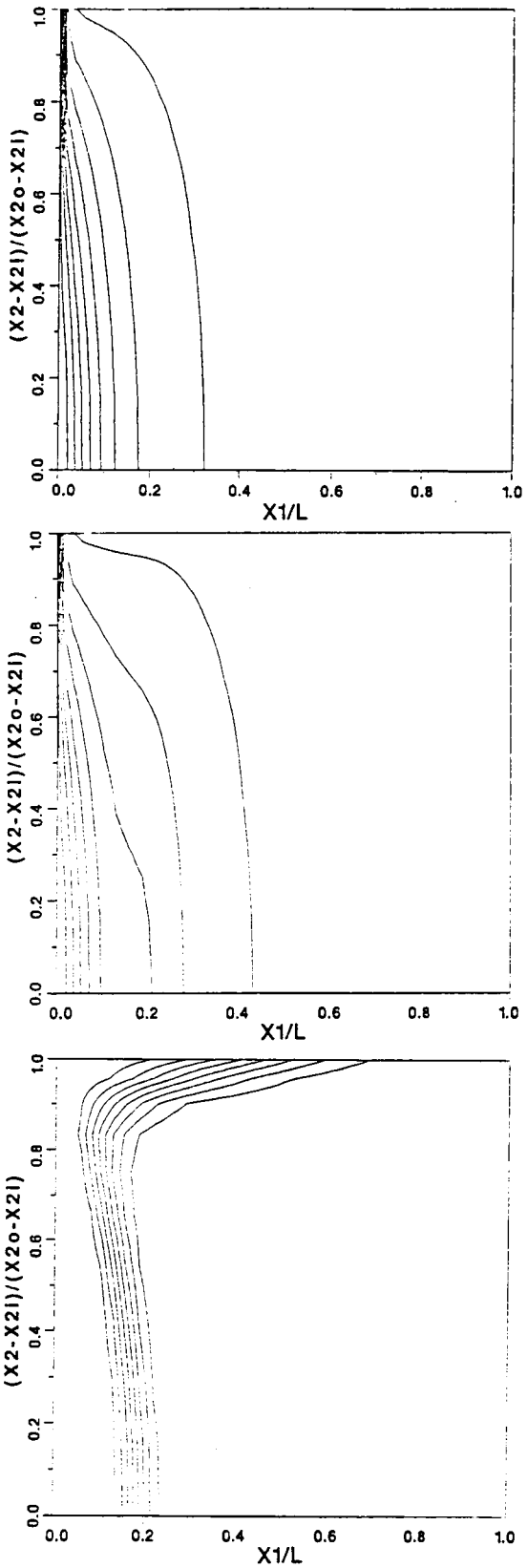

(a) amorphous material

temperature isotherms from left to right:
170°C
150°C
130°C
110°C
90°C
70°C
50°C
30°C

(b) semi-crystalline material

temperature isotherms from left to right:
170°C
150°C
130°C
110°C
90°C
70°C
50°C
30°C

(c) semi-crystalline material

iso-crystallinity curves from left to right (relative values):
0.1111
0.2222
0.3333
0.4444
0.5555
0.6666
0.7777
0.8888

Figure 41. Temperature contours and crystallinity distribution for C_3 = 4.75E+05($^{\circ}K^2$) and χ_{co} = 7.696E+07(sec^{-1}) under the same conditions in Figure 15.

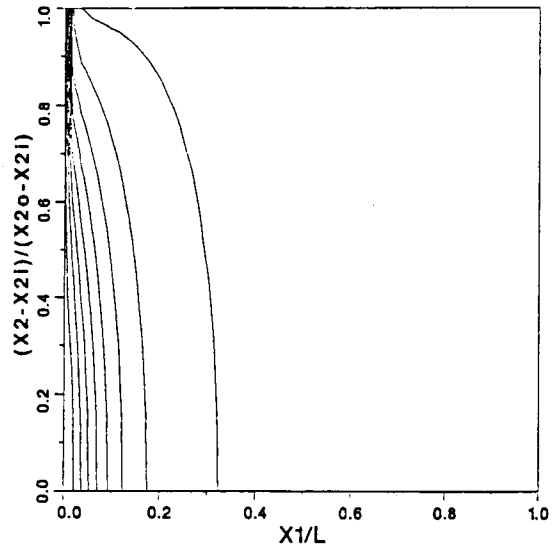

(a) amorphous material

temperature isotherms from left to right:
170°C
150°C
130°C
110°C
90°C
70°C
50°C
30°C

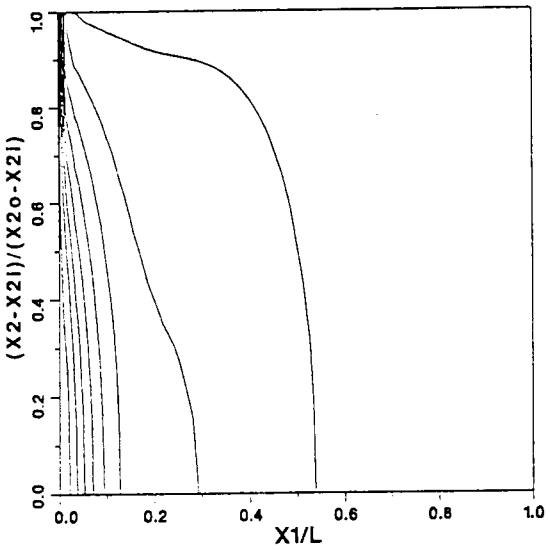

(b) semi-crystalline material

temperature isotherms from left to right:
170°C
150°C
130°C
110°C
90°C
70°C
50°C
30°C

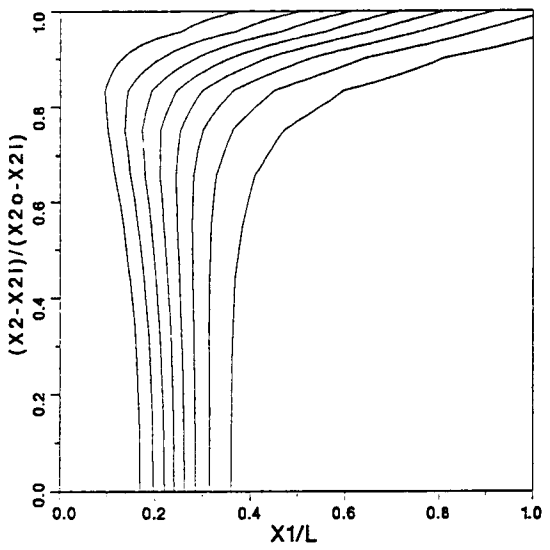

(c) semi-crystalline material

iso-crystallinity curves from left to right (relative values):
0.1111
0.2222
0.3333
0.4444
0.5555
0.6666
0.7777
0.8888

Figure 42. Temperature contours and crystallinity distribution for C_3 = 5.0E+05($^oK^2$) and χ_{co} = 7.3112E+07(sec^{-1}) under the same conditions in Figure 15.

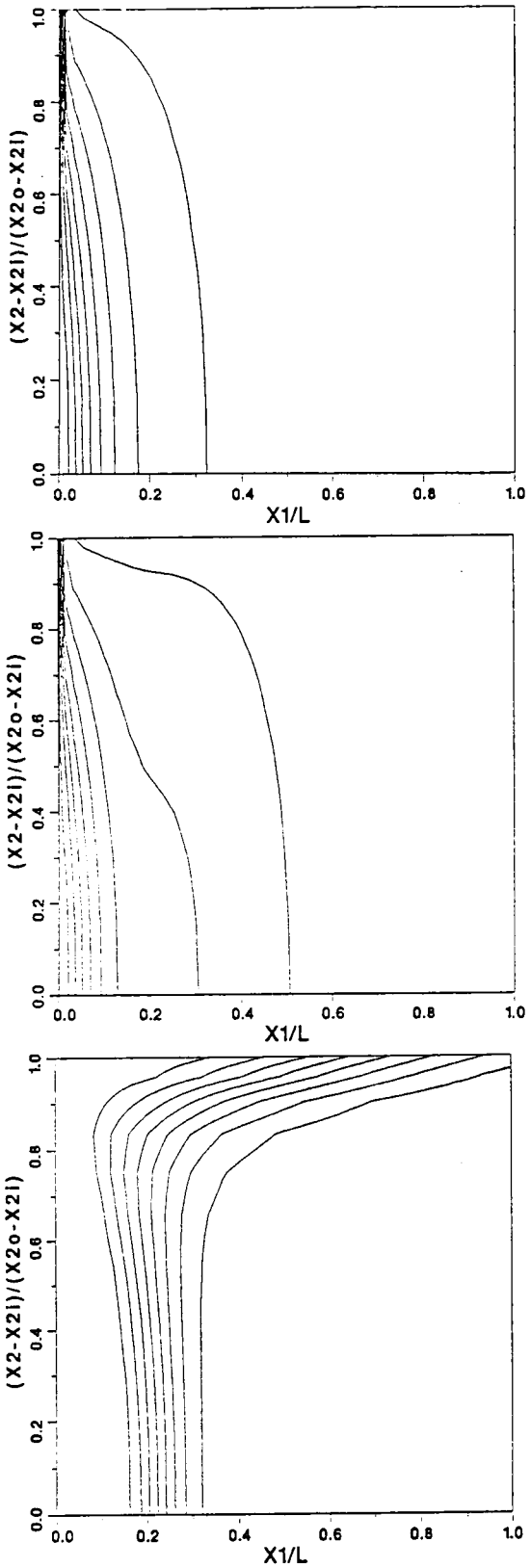

(a) amorphous material

temperature isotherms from left to right:
170°C
150°C
130°C
110°C
90°C
70°C
50°C
30°C

(b) semi-crystalline material

temperature isotherms from left to right:
170°C
150°C
130°C
110°C
90°C
70°C
50°C
30°C

(c) semi-crystalline material

iso-crystallinity curves from left to right (relative values):
0.1111
0.2222
0.3333
0.4444
0.5555
0.6666
0.7777
0.8888

Figure 43. Temperature contours and crystallinity distribution for C_3 = 5.0E+05($^oK^2$) and χ_{co} = 8.0808E+07(sec^{-1}) under the same conditions in Figure 15.

crystallization rate not only broadens (or narrows) the crystallization band but also moves the band downstream (or upstream) of the pipe line.

It is noted that using the same number of elements, as shown in Figure 12, to represent the polymer strip in the cooling chamber will result in unsmoothed iso-crystallinity curves when thicker-walled pipe is analyzed. The presence of these unsmoothed curves is due to insufficient accuracy in interpolating the values between nodes by using fewer elements along the radial direction (i.e. x_2 direction). In order to obtain accurate solution, it is necessary to increase the number of elements along the radial direction corresponding to the increase in pipe thickness. In the case of thicker-walled pipe, it is required to use more and smaller elements in the region of large crystallinity gradients when an accurate solution and interpolation between nodes are demanded. In the system considered, the variation of crystallinity along the radial direction is more larger than that along the axial direction. A study is performed to reduce the number of elements in the x_1 direction and increase the elements in the x_2 direction. As shown from Figure 44 to Figure 48, the iso-crystallinity curves obtained are not smooth enough by decreasing the number of elements in the x_1 direction from 25 to 15 and 10 and increasing the number of elements in the x_2 direction from 10 to 19, 24, and 29. However, keeping 29 elements in the x_2 direction and increasing the number of elements in the x_1 direction to 20, smooth iso-crystallinity curves are obtained as can be seen in Figure 49. Using smaller and more elements to represent the solution domain will, of course, give much more accurate solution; however, using fewer elements is possible corresponding to the direction along which the variation of the variable is small. In the present system, the variation of temperature (and crystallinity)

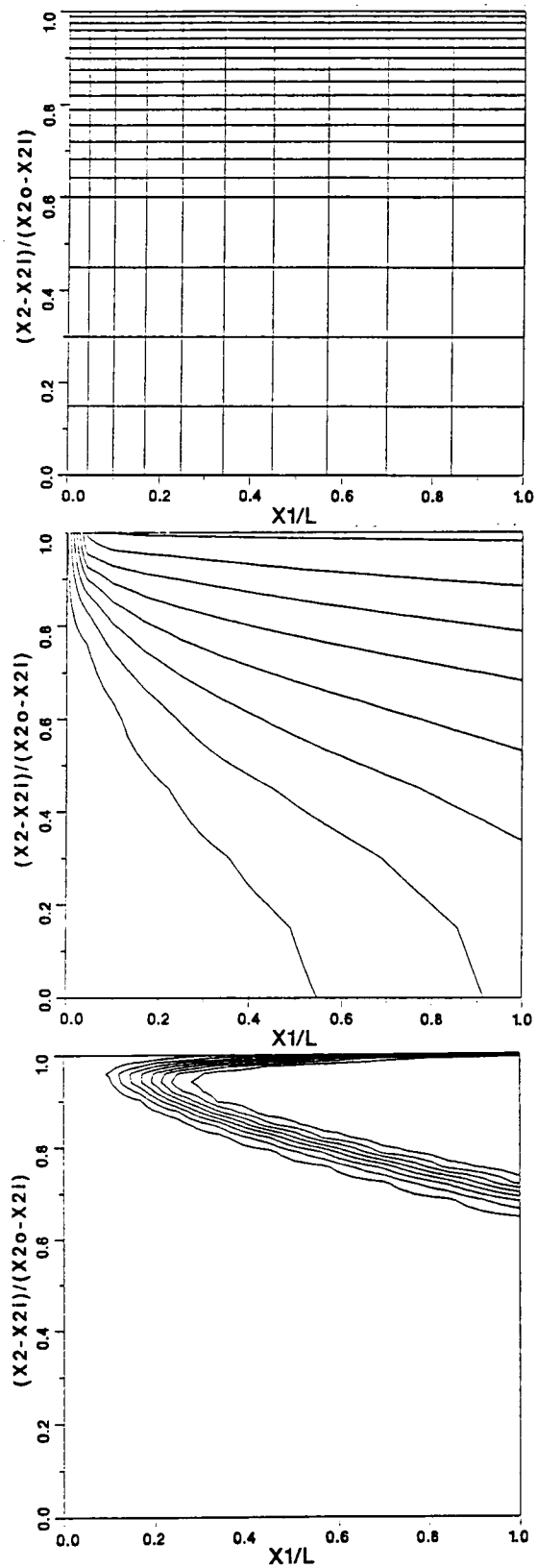

(a) number of elements -- 190
number of nodes -- 819
number of degrees of freedom -- 3496

(b) semi-crystalline material

temperature isotherms from left to right:
170°C
150°C
130°C
110°C
90°C
70°C
50°C
30°C

(c) semi-crystalline material

iso-crystallinity curves from left to right (relative values):
0.1111
0.2222
0.3333
0.4444
0.5555
0.6666
0.7777
0.8888

Figure 44. Simulation results using 10 elements in each row and 19 elements in each column under the same conditions in Figure 35.

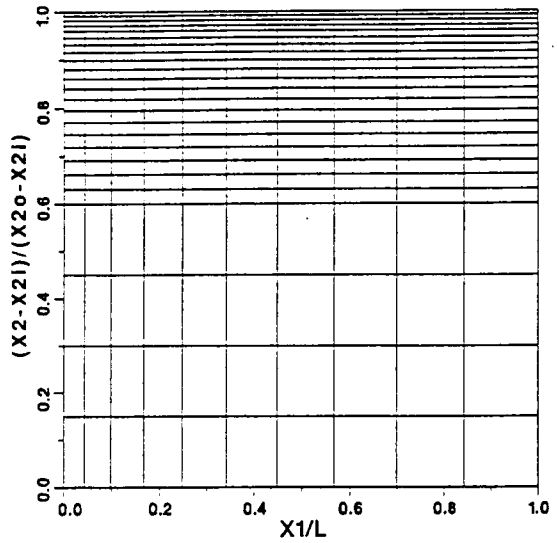

(a) number of elements -- 240
number of nodes -- 1029
number of degrees of freedom -- 4391

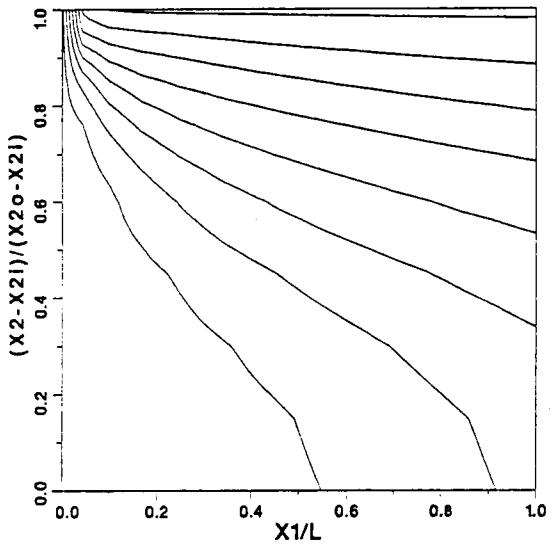

(b) semi-crystalline material

temperature isotherms from left to right:
170°C
150°C
130°C
110°C
90°C
70°C
50°C
30°C

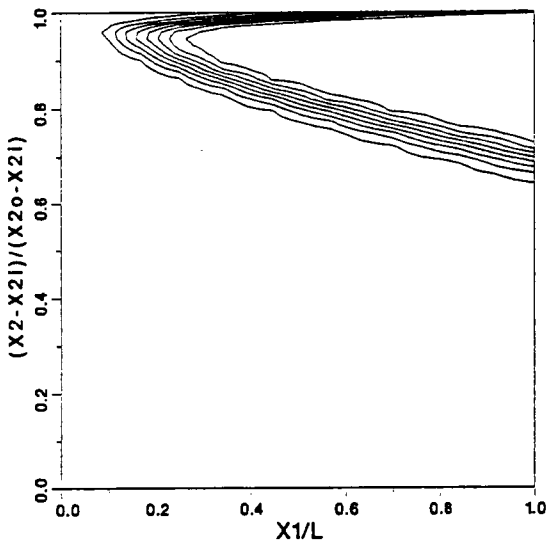

(c) semi-crystalline material

iso-crystallinity curves from left to right (relative values):
0.1111
0.2222
0.3333
0.4444
0.5555
0.6666
0.7777
0.8888

Figure 45. Simulation results using 10 elements in each row and 24 elements in each column under the same conditions in Figure 35.

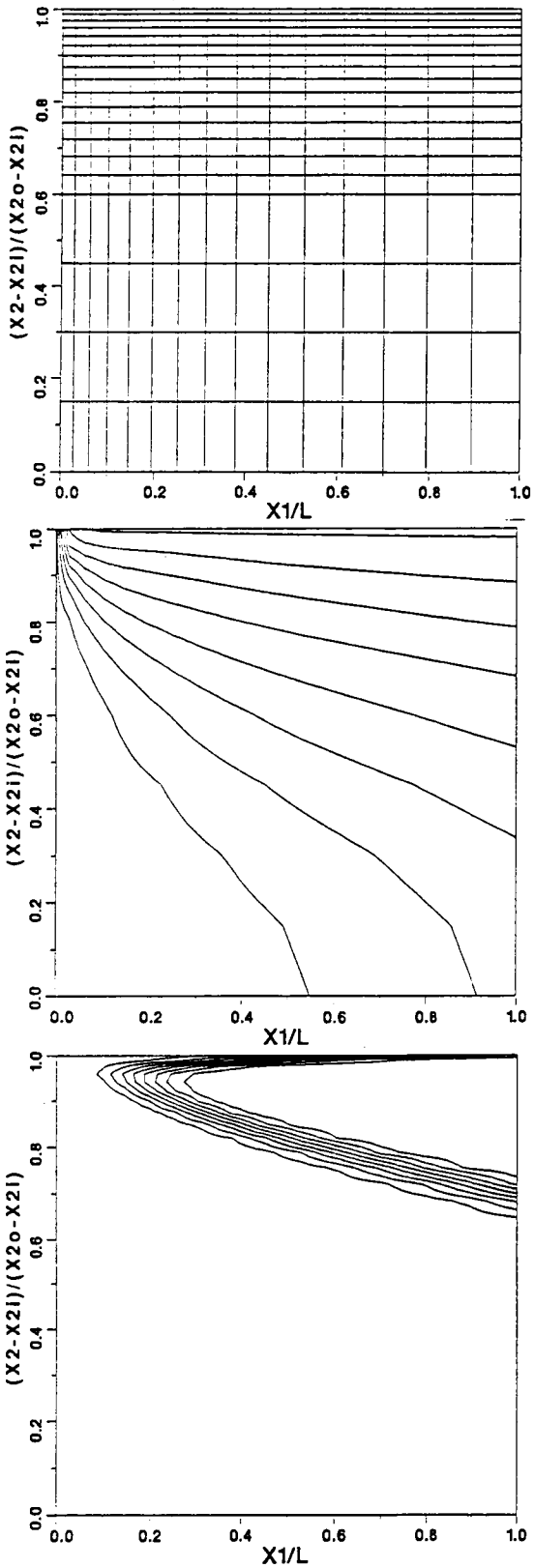

(a) number of elements -- 285
number of nodes -- 1209
number of degrees of freedom -- 5156

(b) semi-crystalline material

temperature isotherms from left to right:
170°C
150°C
130°C
110°C
90°C
70°C
50°C
30°C

(c) semi-crystalline material

iso-crystallinity curves from left to right (relative values):
0.1111
0.2222
0.3333
0.4444
0.5555
0.6666
0.7777
0.8888

Figure 46. Simulation results using 15 elements in each row and 19 elements in each column under the same conditions in Figure 35.

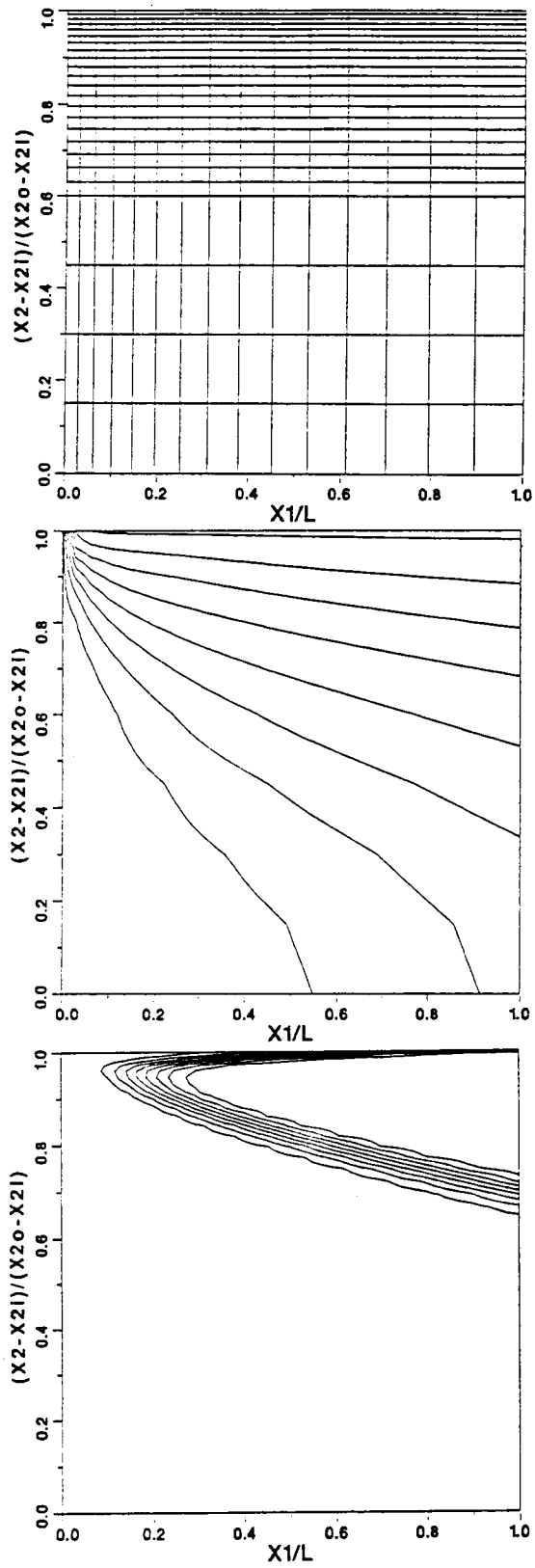

(a) number of elements -- 360
number of nodes -- 1519
number of degrees of freedom -- 6476

(b) semi-crystalline material

temperature isotherms from left to right:
170°C
150°C
130°C
110°C
90°C
70°C
50°C
30°C

(c) semi-crystalline material

iso-crystallinity curves from left to right (relative values):
0.1111
0.2222
0.3333
0.4444
0.5555
0.6666
0.7777
0.8888

Figure 47. Simulation results using 15 elements in each row and 24 elements in each column under the same conditions in Figure 35.

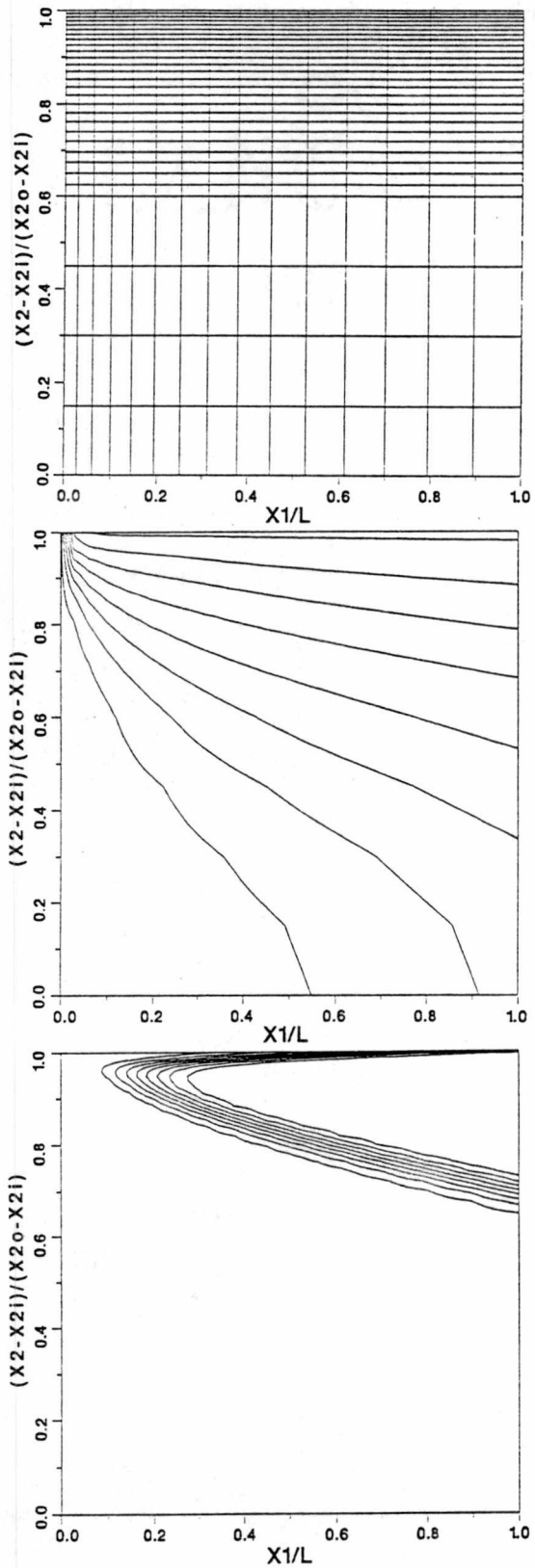

(a) number of elements -- 435
number of nodes -- 1829
number of degrees of freedom -- 7796

(b) semi-crystalline material

temperature isotherms from left to right:
170°C
150°C
130°C
110°C
90°C
70°C
50°C
30°C

(c) semi-crystalline material

iso-crystallinity curves from left to right (relative values):
0.1111
0.2222
0.3333
0.4444
0.5555
0.6666
0.7777
0.8888

Figure 48. Simulation results using 15 elements in each row and 29 elements in each column under the same conditions in Figure 35.

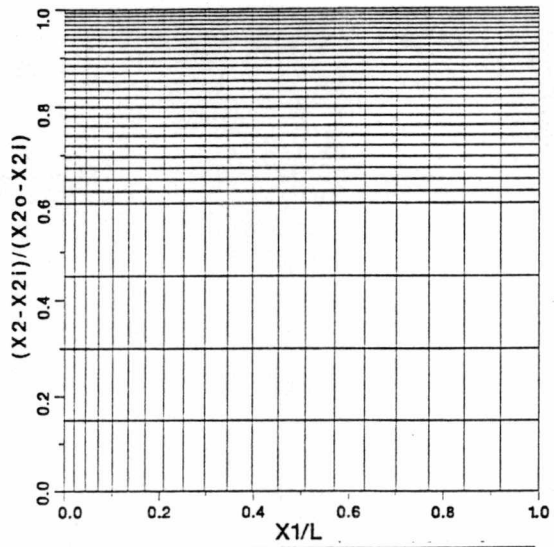

(a) number of elements -- 580
number of nodes -- 2419
number of degrees of freedom -- 10306

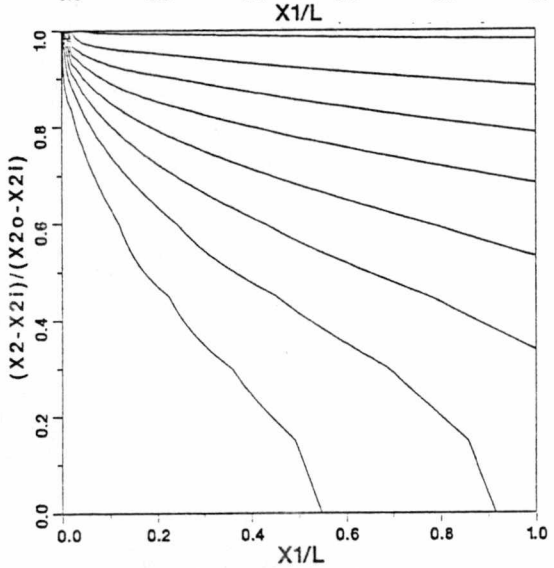

(b) semi-crystalline material

temperature isotherms from left to right:
170°C
150°C
130°C
110°C
90°C
70°C
50°C
30°C

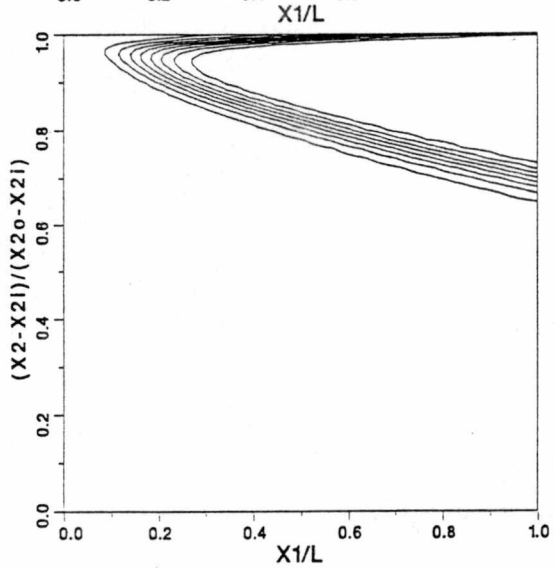

(c) semi-crystalline material

iso-crystallinity curves from left to right (relative values):
0.1111
0.2222
0.3333
0.4444
0.5555
0.6666
0.7777
0.8888

Figure 49. Simulation results using 20 elements in each row and 29 elements in each column under the same conditions in Figure 35.

along the x_1 direction is not so important than that along the x_2 direction. It is evident that the smoothness of the crystallinity curves in Figure 48, where 15 elements are used in the x_1 direction, is very close to that in Figure 49, where 20 elements are used in the x_1 direction.

CHAPTER V

CONCLUSIONS

A numerical simulation has been developed which predicts the steady-state temperature and crystallinity distributions when an extruded polypropylene pipe comes in contact with a cooling medium. The main purpose of this work is to obtain a deeper comprehension of solidification phenomena in the cooling chamber with the intention of improving the conventional "make-and-test" methods used in industry. In the present work the cooling stage in the extrusion of semi-crystalline materials was simulated by a mathematical model consisting of the equations of continuity, momentum, and energy, combined with Nakamura's non-isothermal crystallization rate model.

The computer simulation of the cooling stage is capable of predicting temperature profiles and crystallinity distribution in pipe extrusion of a semi-crystalline material. Although no comparison with data was made, the analysis provides a start toward understanding the complex features of this process.

REFERENCES

REFERENCES

1. Gerhard Schenkel, Plastics Extrusion Technology and Theory: The Design and Operation of Screw Extruders for Plastics, American Elsevier, New York, 1966.

2. P. J. Hendra, J. Vile, H. A. Willis, V. Zichy, and M. E. A. Cudby, "The Effect of Cooling Rate upon the Morphology of Quenched Melts of Isotactic Polypropylenes," Polymer, Vol. 25, June, 785(1984).

3. P. Galli, "Polypropylene: A Quarter of a Century of Increasingly successful development," in Structural Order in Polymer, edited by F. Ciardelli and P. Giusti, Oxford, New York, 1981.

4. Herbert R. Simonds, The Encyclopedia of Plastics Equipment, Reinhold, New York, 1964.

5. Allan L. Griff, Plastics Extrusion Technology, 2nd edition, Reinhold, New York, 1968.

6. E. G. Fisher, Extrusion of Plastics, 3rd edition, Boston: Published for the Plastics and Rubber Institute, 1976.

7. M. Ahmed, Polypropylene Fibers-Science and Technology, Elsevier Scientific Pub., 1982.

8. N. Barakat and A. M. Hindeleh, Textile Res. J., 34, 581(1964).

9. Andrzej Ziabicki, Fundamentals of Fibre Formation, A Wiely-Interscience Publication, New York, 1976.

10. W. L. Sifleet, N. Dinos, and J. R. Collier, "Unsteady-State Heat Transfer in a Crystallizing Polymer," Polym. Eng. Sci., 13, 10(1973).

11. J. D. Muzzy, D. G. Bright, and G. H. Hoyos, J. Polym. Eng. Sci., Vol. 18, No. 6, 437(1978).

12. L. Mandelkern, Crystallization of Polymers, McGraw-Hill, New York, 1964.

13. Ernest C. Bernhardt, Computer Aided Engineering for Injection Molding, Dist. by Macmillan, New York, 1983.

14. K. Nakamura, T. Watanabe, K. Katayama, and T. Amano, J. Appl. Polym. Sci.,vol. 16, 1077(1972).

15. E. Hunter and W. G. Oakes, Trans. Faraday Soc., 41, 49(1945).

16. H. C. Raine, R. B. Richards, and H. Ryder, Trans. Faraday Soc., 41, 56(1945).

17. P. H. Hermans and A. Weidinger, J. Polym. Sci., 4, 135(1949); 5, 565(1950).

18. S. Krimm and A. V. Tobolsky, J. Polym. Sci., 7, 57(1951).

19. B. Ke, J. Polym. Sci., 42, 15(1960).

20. Robert J. Young, Introduction to Polymers, Chapman and Hall, New York, 1981.

21. S. G. Turley and H. Keskkula, J. Appl. Polym. Sci., 9, 2693(1965).

22. M. Avella, E. Martuscelli and M. Pracella, J. Thermal Analysis, Vol. 28, 237(1983).

23. J. H. Magill, Polymer, 3, 43(1962).

24. Andrzej Wlochowicz and Marek Eder, Polymer, Vol. 22, September, 1285(1981).

25. L. Mandelkern, Chem. Rev., 56, 903(1956).

26. P. J. Flory, Science, 124, 53(1956).

27. N. B. Hannay, Treatise on Solid State Chemistry, Vol. 3, Plenum press, New York, 1976.

28. S. Cheng, Advances in Polyolefins, Plenum Press, New York, 1988.

29. I. G. Voigt-Martin and L. Mandelkern, J. Polym. Sci., Polym. Phys. Ed., 22, 1901(1984).

30. K. Ueberreiter, G. Kanig, and A. S. Brenner, J. Polym. Sci., 16, 53(1955).

31. Rajen M. Patel, Ph.D. dissertation research proposal, the University of Tenssessee, Knoxville, October, 1989.

32. J. A. Brydson, Plastics Materials, D. Van Nostrand, Princeton, N. J., 1966.

33. A. A. Duswalt, Soc. Plast. Eng.: Tech. Pap., 17, 223(1971).

34. W. W. Cox and A. A. Duswalt, Polym. Eng. and Sci., 7, 1(1967).

35. R. D. Deanin, Polymer Structure, Properties, and Applications, Boston, Cahners books, 1972.

36. G. Natta, J. Polym. Sci., 34, 531(1959).

37. R. L. Miller, J. Polym. Sci., 57, 975(1962).

38. G. Farrow, Polymer, 4, 191(1963).

39. J. P. Fogerty, and E. Poindexter, "Effect of Processing Conditions Upon Specific Gravity of High Density Polyethylene," SPE J., April, 41(1958).

40. N. Bekkedahl, J. Research Natl. Bur. Standards, 13, 411(1934).

41. L. Marker, P. M. Hay, G. P. Tilby, R. M. Early, and O. J. Sweeting, J. Poly. Sci., 38, 33(1959).

42. A. N. Kolmogoroff, Isvest. Akad, Nauk SSSR Ser. Math., 1, 335(1937).

43. W. A. Johnson and R. F. Mehl, Trans. Am. Inst. Mining Met. Engrs., 135, 416(1939).

44. M. Avrami, J. Chem. Physics, 7, 1103(1939).

45. M. Avrami, J. Chem. Physics, 8, 212(1940).

46. U. R. Evans, Trans. Faraday Soc., 41, 365(1945).

47. L. A. Wood and N. Bekkedahl, J. Appl. Phys., 17, 362(1946).

48. P. J. Flory, J. Chem. Phys., 17, 223(1949).

49. L. Mandelkern, Growth and Perfection of Crystals, R. H. Doremus, B. W. Roberts, and D. Turnbull, eds., Wiley, New York, 1958.

50. J. M. McKelvey, Polymer Processing, Wiley, New York, 1962.

51. J. H. Griffith and B. G. Ranby, J. Polym. Sci., 38, 107(1959).

52. W. H. Cobbs, Jr., and R. L. Burton, J. Polym. Sci., 10, 275(1953).

53. F. P. Reding and A. Brown, J. Appl. Phys., 25, 848(1954).

54. J. H. Magill, Polymer, Vol. 3, 35(1962).

55. J. R. Collier and E. Baer, J. Appl. Polym. Sci., 10, 1409(1966).

56. J. H. Magill, Polymer, 2, 221(1961).

57. Jerold Schultz, Polymer Materials Science, Prentice-Hall, N. J., 1974.

58. L. B. Morgan, J. Appl. Chem., 4, 160(1964).

59. W. Banks, M. Gordon, R. J. Roe, and A. Sharples, Polymer (London), 4, 61(1963).

60. Yu. K. Godovsky and G. L. Slonimsky, J. Polym. Sci., Polym. Phys. Ed., 12, 1053(1974).

61. J. N. Hay, Brit. Polym. J., 3, 74(1971).

62. J. N. Hay, J. Polym. Sci., Polym. Lett. Ed., 14, 543(1976).

63. A. Sharples, Polymer (London), 3, 250(1962).

64. I. H. Hillier, J. Polym. Sci., A3, 3069(1965).

65. Musa R. Kamal and Edward Chu, Polym. Eng. Sci., January, Vol. 23, No. 1, 27(1983).

66 C. Velisaris and J. Seferis, Polym. Eng. Sci., 26, 1574(1986).

67. A. Ziabicki, Appl. Polym. Symposia, 6, 1(1967).

68. A. Ziabicki, Polimery, 12, 405(1967).

69. J. W. Cahn, Acta Metallurgica, 4, 572(1956).

70. T. Ozawa, Polymer, 12, 150(1971).

71. K. Nakamura, K. Katayama and T. Amano, J. Appl. Polym. Sci., 17, 1031(1973).

72. K. Nakamura, T. Watanabe, T. Amano,K. Katayama, J. Appl. Polym. Sci., 18, 615(1974).

73. A. Ziabicki, Colloid and Polymer Sci., 252, 433(1974).

74. W. J. Kozlowski, J. Polym. Sci., C, 38, 47(1972).

75. Marek Eder and Andrzej Wlochowicz, Polymer, 24, 1593(1983).

76. W. Dietz, Colloid and Polymer Sci., 259, 413(1981).

77. K. Katayama, J. Soc. Rheol., Japan, 4, 96(1976).

78. G. S. Y. Yeh and K. Z. Hong, Polym. Eng. Sci., 19, 395(1979).

79. G. S. Y. Yeh, K. Z. Hong, and D. L Krueger, Polym. Eng. Sci., 19, 401(1979).

80. R. L. Miller, Flow-Induced Crystallization in Polymer Systems, Gordon and Breach, New York, 1977.

81. The Society of Fiber Science and Technology, Japan, Ed., Formation of Fibers and Development of Their Structure, Kagaku Dojin, Kyoto, Vol. 1, (1969), Vol. 2, (1970), Vol. 3, (1971).

82. F. S. Smith and R. D. Steward, Polymer, 15, 283(1974).

83. L. B. Morgan, Phil. Trans. Royal Soc. (London), A247, 13(1954).

84. Lawrence E. Nielsen, Mechanical Properties of Polymers, Reinhold, New York, 1962.

85. A. S. Kenyon, R. C. Gross, and A. L. Wurstner, J. Polymer Sci., 40, 159(1959).

86. R. Becker, Ann. Phys., 32, 128(1938).

87. L. Mandelkern, F. A. Quinn, Jr., and P. J. Flory, J. Appl. Phys., 25, 830(1954).

88. A. H. Gent, J. Polym. Sci., 18, 321(1955).

89. F. P. Price, J. Am. Chem. Soc., 74, 311(1952).

90. P. J. Flory and A. D. McIntyre, J. Polym. Sci., 18, 592(1955).

91. A. Ziabicki, J. Chem. Phys., 48, 4368(1968).

92. A. Ziabicki, J. Chem. Phys., 48, 4374(1968).

93. J. Frenkel, Kinetic Theory of Liquids, Oxford University Press, London, 1946; D. Turnbull and J. C. Fisher, J. Chem. Phys., 17, 71(1949).

94. T. Suzuki and A. J. Kovacs, Polymer, 1, 82(1970).

95. J. D. Hoffman, SPE trans., 4, 315(1964).

96. H. L Williams, R. F. Landel and J. D. Ferry, J. Am. Chem. Soc., 77, 3701(1955).

97. J. D. Hoffman and J. I. Lauritzen, J. Res. Natl. Bur. Stand., A. 65, 297(1961).

98. J. D. Hoffman and J. J. Weeks, J. Chem. Phys., 37, 1723(1962).

99. J. Boon, G. Challa and D. W. Van Krevelen, J. Polym. Sci., Part A-2, 6, 1791(1968).

100. J. H. Magill, J. Polym. Sci., Part A, 3, 1195(1965).

101. J. H. Magill and D. J. Plazek, J. Chem. Phys., 46, 3757(1967).

102. J. D. Ferry, Viscoelastic properties of polymers, 2nd ed., Wiley, New York, 1970.

103. J. I. Lauritzen and J. D. Hoffman, J. Res. Natl. Bur. Stand., A. 64, 73(1960).

104. K. F. Zieminsky, Ph. D. dissertation, the University of Tennessee, Knoxville, June, 1986.

105. W. S. Lambert, MS Thesis, the University of Tennessee, 1988.

106. M. Takayanagi and T. Kusumoto, Kogyo Kagaku Zasshi, 62, 587(1959).

107. B. Wunderlich, Macromolecular Physics, 2nd ed., Academic Press, New York,1976.

108. P. Meares, Polymers structure and Bulk Properties, Van Nostrand, New York, 1965.

109. W. M. Rohsenow and J. P. Hartnett, Handbook of Heat Transfer, McGraw-Hill, New York, 1973.

110. D. R. Anderson, Chem. Rev., 66, 677(1966).

111. D. W. Van Krevelen, and P. J. Hoftyzer, Properties of Polymers, Elsevier, Amsterdam, 1972.

112. K. Eiermann, Kolloid-Z, 201, 3(1965).

113. M. Luba, T. Pelt, R. G. Griskey, J. Appl. Polym. Sci., 23, 55(1979).

114. J. R. A. Pearson and S. M. Richardson, Computational Analysis of Polymer Processing, Elsevier Science Publishing Co., New York, 1983.

115 D. R. Atthey, "A Finite Difference Scheme for Melting Problems," J. Inst. Maths. Applics., 13, 353(1974).

116. C. Bonacina and G. Comini, A. Fasano and M. Primicerio, " Numerical Solution of Phase-Change Problem," Int. J. Heat Mass Transfer, Vol. 16, 1825(1973).

117. J. F. T. Pittman,"Computer-Aided Analysis of Some Thermoplastics Processing Operations," in Developments in Plastics Technology, ed. by A. Whelan and J. Craft, Applied Science Publishers, New York, 1982.

118. C. Bonacina and G. Comini, A Fasano and M. Primicerio, Int. Heat Mass Transfer, 16, 1825(1973).

119. C. Gutfinger, E. Broyer, and Z. Tadmor, Polym. Eng. Sci., 15, 515(1975).

120. M. R. Kamal and D. Kalyon, Polym. Eng. Sci., 23, 503(1983).

121. M. E. Ryan and A. Dutta, Polym. Eng. Sci., 22, 1075(1982).

122. W. Dietz, Polym. Eng. Sci., 18, 1030(1978).

123. K-H Tacke, "Discretization of the Explicit Enthalpy Method for Planar Phase Change," Int. J. for Num. Meth. in Engng., 21, 543(1985).

124. G. Comini, S. Del Guidice, R. W. Lewis and O. C. Zienkiewicz, "Finite Element Solution of Non-Linear Heat Conduction Problems with Special Reference to Phase Change," Int. J. Num. Meth. Engng., 8, 613(1974).

125. K. Morgan, R. W. Lewis and O. C. Zienkiewicz, Int. J. Num. Meth. Eng., 12, 1191(1978).

126. M. R. Kamal and E. Chu., "Isothermal and Nonisothermal Crystallization of Polyethylene," Polym. Eng. Sci., 23, 27(1983).

127. M. R. Kamal and P. G. Lafleur, "A Model for the Prediction of Microstructure Distribution in Thermoplastics Injection Molding," Polym. Eng. Sci., 24, 692(1984).

128. J. T. Oden, "A Finite Element Analogue of the Navier-Stokes Equations," J. Eng. Mech. Div., Proc. Am. Soc. Civ. Eng., 96, 529(1970).

129. M. J. Crochet, A. R. Davies, and K. Walters, Numerical Simulation of Non-Newtonian Flow, Elsevier, New York, 1984.

130. Avraam I. Isayev, Injection and Compression Molding Fundamentals, Marcel Dekker, Inc., New York, 1987.

131. D. K. Gartling, NACHOS II - A Finite Element Computer Program for Incompressible Flow Problems, Part I - Theoretical Background, SAND 86-1816, Sandia National Laboratories, Albuquerque, N.M.(1987).

132. D. K. Gartling, NACHOS II - A Finite Element Computer Program for Incompressible Flow Problems, Part II - User's Manual, SAND 86-1817, Sandia National Laboratories, Albuquerque, N.M.(1987).

133. H. A. Watts and L. F. Shampine, Sandia Laboratories Report, SAND 75-0182, Albuquerque, New Mexico or SIAM Review, 18, 376(1976).

APPENDICES

APPENDIX A: DIMENSIONLESS ANALYSIS OF ENERGY EQUATION.

Recall the melt flow considered in Figure 9 and its corresponding energy equation given in equation (3.2-3). It is noted that the polymer melt is considered to be an incompressible annular plug flow with u_1 velocity along the x_1 direction. The energy equation for constant material properties is again given by

$$\rho C_p u_1 \frac{\partial T}{\partial x_1} = k\left(\frac{\partial^2 T}{\partial {x_1}^2} + \frac{1}{x_2}\frac{\partial}{\partial x_2}\left(x_2\frac{\partial T}{\partial x_2}\right)\right) + Q \qquad (1)$$

By introducing the definition of thermal diffusivity $\alpha \equiv k/\rho C_p$, equation (1) can be rewritten into

$$\left(\frac{u_1}{\alpha}\right)\frac{\partial T}{\partial x_1} = \frac{\partial^2 T}{\partial {x_1}^2} + \frac{1}{x_2}\frac{\partial}{\partial x_2}\left(x_2\frac{\partial T}{\partial x_2}\right) + \frac{Q}{k} \qquad (2)$$

The dimensionless variables are defined as follows,

$$\Gamma \equiv \frac{T-T_{water}}{T_m-T_{water}} \equiv \frac{T-T_{water}}{\Delta T_{mw}} \qquad (3)$$

$$\eta_1 \equiv \frac{x_1}{L} \qquad (4)$$

$$\eta_2 \equiv \frac{x_2-x_{2i}}{x_{2o}-x_{2i}} \equiv \frac{x_2-x_{2i}}{\Delta x_2} \qquad (5)$$

in which T_{water} is the bulk water temperature in the cooling chamber, T_m is the melting point of the polymer, L is the length of the pipe inside the cooling chamber, and the thickness of the pipe is $\Delta x_2 = x_{2o} - x_{2i}$, where $x_{2i} \le x_2$

$\leq x_{2o}$. The ratios of the thickness and the inner radius to the length of the pipe can be defined by,

$$\xi \equiv \frac{\Delta x_2}{L} \tag{6}$$

$$\zeta \equiv \frac{x_{2i}}{L} \tag{7}$$

When equations (3)-(7) are substituted into equation (2), a dimensionless form of energy equation leads to

$$\left(\frac{u_1 L}{\alpha}\right)\frac{\partial \Gamma}{\partial \eta_1} = \frac{\partial^2 \Gamma}{\partial \eta_1^2} + \frac{1}{(\xi\eta_2+\zeta)\xi}\frac{\partial \Gamma}{\partial \eta_2} + \frac{1}{\xi^2}\frac{\partial^2 \Gamma}{\partial \eta_2^2} + \frac{L^2 Q}{k\Delta T_{mw}} \tag{8}$$

with the values of normalized coordinates η_1 and η_2 between zero and one. The dimensionless variable $u_1 L/\alpha$ is specifically defined as the thermal Peclet number, Pe_t, and can be physically interpreted as the ratio of characteristic time for diffusion of thermal energy to the residence time for a material element to be transported through the cooling chamber.

The volumetric heat source for phase transformation of a semi-crystalline polymer can be expressed in terms of relative degree of crystallinity by

$$Q = \rho \cdot \Delta H \cdot u_1 \cdot \chi_c(\infty) \cdot \frac{\partial \theta}{\partial x_1} \tag{9}$$

Using the normalized expression for coordinate x_1 in equation (4), equation (9) becomes

$$Q = \rho \cdot \Delta H \cdot u_1 \cdot \chi_c(\infty) \cdot \frac{1}{L} \frac{\partial \theta}{\partial \eta_1} \qquad (10)$$

Thus with equation (10), the last term on the right side of equation (8) becomes

$$\begin{aligned} \frac{L^2 Q}{k \Delta T_{mw}} &= \frac{L^2}{k \Delta T_{mw}} \cdot \rho \cdot \Delta H \cdot u_1 \cdot \chi_c(\infty) \cdot \frac{1}{L} \frac{\partial \theta}{\partial \eta_1} \\ &= \left(u_1 L\right)\left(\frac{\rho}{k}\right)\frac{\Delta H \chi_c(\infty)}{\Delta T_{mw}} \frac{\partial \theta}{\partial \eta_1} \\ &= \left(u_1 L\right)\left(\frac{1}{\alpha C_p}\right)\frac{\Delta H \chi_c(\infty)}{\Delta T_{mw}} \frac{\partial \theta}{\partial \eta_1} \\ &= \left(\frac{u_1 L}{\alpha}\right)\left(\frac{\Delta H \chi_c(\infty)}{C_p \Delta T_{mw}}\right)\frac{\partial \theta}{\partial \eta_1} \\ &= Pe_t\left(\frac{\Delta H \chi_c(\infty)}{C_p \Delta T_{mw}}\right)\frac{\partial \theta}{\partial \eta_1} \end{aligned} \qquad (11)$$

From the differential form of Nakamura's model for the kinetics of crystallization

$$u_1 \frac{\partial \theta}{\partial x_1} = n \cdot \mathcal{K}_c(T) \cdot (1-\theta) \cdot \{ \ln(\frac{1}{1-\theta}) \}^{(n-1)/n} \qquad (12)$$

which becomes, applying equation (4),

$$\frac{\partial \theta}{\partial \eta_1} = n \cdot \left(\frac{L \mathcal{K}_c(T)}{u_1}\right)(1-\theta) \cdot \{ \ln(\frac{1}{1-\theta}) \}^{(n-1)/n} \qquad (13)$$

where

$$\mathcal{K}_c(T) = \mathcal{K}_\infty \exp\{- \frac{U^*}{R(T-T_\infty)} \} \exp\{- \frac{C_3}{T \Delta T} \} \qquad (14)$$

For convenience let

$$g(\theta) = (1-\theta)\cdot\{\ \ln(\frac{1}{1-\theta})\}^{(n-1)/n} \tag{15}$$

then equation (13) can be expressed by

$$\frac{\partial\theta}{\partial\eta_1} = n\cdot\left(\frac{L\mathcal{K}_c(T)}{u_1}\right)g(\theta) \tag{16}$$

According to equation (14), let

$$f(T) \equiv \frac{\mathcal{K}_c(T)}{\mathcal{K}_\infty} = \exp\{-\frac{U^*}{R(T-T_\infty)}\}\exp\{-\frac{C_3}{T\Delta T}\} \tag{17}$$

Thus,

$$\frac{\partial\theta}{\partial\eta_1} = n\cdot\left(\frac{L\mathcal{K}_{co}}{u_1}\right)f(T)\cdot g(\theta) \tag{18}$$

It is noted that L/u_1 implies a material element residence time for crystallization in the cooling chamber and that $1/\mathcal{K}_{co}$ implies a characteristic time of crystallization unique to a given material. Then it follows that $u_1/(L\mathcal{K}_{co})$ implies the ratio of crystallization time to material transport time. Thus, a Peclet number for crystallization, Pe_c, similar to Pe_t can be defined as follows,

$$Pe_c = \frac{u_1}{L\mathcal{K}_\infty} \tag{19}$$

Then equation (18) becomes,

$$\frac{\partial\theta}{\partial\eta_1} = \frac{n}{Pe_c} f(T)\cdot g(\theta) \qquad (20)$$

The dependent variable in equation (8) is the normalized temperature $\Gamma=\Gamma(\eta_1,\eta_2)$ and hence it follows that $Q=Q(\Gamma)$. Furthermore, from equation (11) we concluded that θ, the relative crystallization function, has Γ as its independent variable. We then further concluded from equations (17) and (20) that the indcpendent variable of the crystallization function, f(T), needs to be changed from T to Γ. We now proceed with the change of variable task by considering separately the exponents of equation (17).

$$\begin{aligned} T - T_\infty &= T - T_\infty + T_w - T_w \\ &= (T - T_w) - (T_\infty - T_w) \\ &= (T - T_w) - T_{\infty w} \end{aligned} \qquad (21)$$

where $T_{\infty w} \equiv (T_\infty - T_w) < 0$. Furthermore,

$$\begin{aligned} T - T_\infty &= [(T - T_w) - T_{\infty w}] \frac{(T_m - T_w)}{(T_m - T_w)} \\ &= \frac{(T - T_w)}{(T_m - T_w)} (T_m - T_w) - T_{\infty w} \\ &= \Gamma\Delta T_{mw} - T_{\infty w} \\ &= \Delta T_{mw} [\Gamma - \frac{T_{\infty w}}{\Delta T_{mw}}] \end{aligned} \qquad (22)$$

Thus, the exponent of the "diffusion function" in f(T) becomes,

$$-\frac{U^*}{R(T-T_\infty)} = -\frac{U^*}{R\Delta T_{mw}\left[\Gamma - \frac{T_{\infty w}}{\Delta T_{mw}}\right]} \tag{23}$$

Considering the other exponent,

$$\begin{aligned} T\Delta T &= T(T_m^{\,o} - T) \\ &= T(T_m^{\,o} - T + T_w - T_w) \\ &= T[(T_m^{\,o} - T_w) - (T - T_w)] \\ &= T[T_{mw}^{\,o} - (T - T_w)] \end{aligned} \tag{24}$$

where $T_{mw}^{\,o} \equiv (T_m^{\,o} - T_w) > 0$.

$$\begin{aligned} T\Delta T &= T[T_{mw}^{\,o} - (T - T_w)]\,\frac{(T_m - T_w)}{(T_m - T_w)} \\ &= T[T_{mw}^{\,o} - \Gamma\Delta T_{mw}] \\ &= T\,\Delta T_{mw}\left[\frac{T_{mw}^{\,o}}{\Delta T_{mw}} - \Gamma\right] \\ &= T\beta \end{aligned} \tag{25}$$

where for convenience $\beta \equiv \Delta T_{mw}\left[\frac{T_{mw}^{\,o}}{\Delta T_{mw}} - \Gamma\right]$. Thus,

$$\begin{aligned} T\Delta T &= T\beta + T_w\beta - T_w\beta \\ &= (T - T_w)\beta + T_w\beta \\ &= (T - T_w)\beta\frac{(T_m - T_w)}{(T_m - T_w)} + T_w\beta \\ &= \Gamma\Delta T_{mw}\beta + T_w\beta \\ &= \Gamma(\Delta T_{mw})^2\left[\frac{T_{mw}^{\,o}}{\Delta T_{mw}} - \Gamma\right] + T_w\Delta T_{mw}\left[\frac{T_{mw}^{\,o}}{\Delta T_{mw}} - \Gamma\right] \\ &= (\Delta T_{mw})^2\left[\frac{T_w}{\Delta T_{mw}} + \Gamma\right]\left[\frac{T_{mw}^{\,o}}{\Delta T_{mw}} - \Gamma\right] \end{aligned} \tag{26}$$

Thus, the exponent of the "nucleation function" in f(T) becomes,

$$-\frac{C_3}{T\Delta T} = -\frac{C_3}{(\Delta T_{mw})^2\left[\frac{T_w}{\Delta T_{mw}} + \Gamma\right]\left[\frac{T_{mw}^{o}}{\Delta T_{mw}} - \Gamma\right]} \qquad (27)$$

Hence, equations (23) and (27) along with equation (17) define $f(\Gamma(\eta_1,\eta_2))$ resulting in a fully normalized equation for crystallization kinetics, equation (20) becomes,

$$\frac{\partial\theta}{\partial\eta_1} = \frac{n}{Pe_c} f(\Gamma).g(\theta) \qquad (28)$$

Realizing that equation (28) is a function of Γ, then equation (11) is substituted into equation (8),

$$\left(\frac{u_1 L}{\alpha}\right)\frac{\partial\Gamma}{\partial\eta_1} = \frac{\partial^2\Gamma}{\partial\eta_1^2} + \frac{1}{(\xi\eta_2+\zeta)\xi}\frac{\partial\Gamma}{\partial\eta_2} + \frac{1}{\xi^2}\frac{\partial^2\Gamma}{\partial\eta_2^2} + \left(\frac{u_1 L}{\alpha}\right)\left(\frac{\Delta H \chi_c(\infty)}{C_p\Delta T_{mw}}\right)\frac{\partial\theta}{\partial\eta_1} \qquad (29)$$

After rearrangement and use of the definition of thermal Peclet number, the final dimensionless form of the energy equation is

$$Pe_t\left[\frac{\partial\Gamma}{\partial\eta_1} - (JH)\frac{\partial\theta}{\partial\eta_1}\right] = \frac{\partial^2\Gamma}{\partial\eta_1^2} + \frac{1}{(\xi\eta_2+\zeta)\xi}\frac{\partial\Gamma}{\partial\eta_2} + \frac{1}{\xi^2}\frac{\partial^2\Gamma}{\partial\eta_2^2} \qquad (30)$$

where JH is a dimensionless number defined as $JH = (\Delta H \chi_c(\infty))/(C_p\Delta T_{mw})$. This dimensionless number has the meaning of the ratio of the energy of crystallization relative to the total transportable thermal energy of the system. For the amorphous polymer this dimensionless is equal to zero.

APPENDIX B:

```
**********************************************************************
*                                                                    *
*            USER SUBROUTINE TO EVALUATE VOLUMETRIC HEAT SOURCE      *
*                                                                    *
**********************************************************************
**********************************************************************
*  THE MAIN PROGRAM-NACHOS FORTRAN CODE-PROVIDES USER SUBROUTINE     *
*  "USRVHS" TO EVALUATE VOLUMETRIC HEAT SOURCE TERM IN ENERGY        *
*  EQUATION. THE INTERNAL HEAT GENERATION RATE DUE TO CRYSTALLIZATION OF *
*  POLYMER IS COMPUTED BY CALLING THIS SUBROUTINE WHICH IN TURN CALLS *
*  SUBROUTINE "CRYSTAL" TO CALCULATE THE CRYSTALLINITY GRADIENT ALONG *
*  THE X1 DIRECTION. HOWEVER, THE CALCULATION FOR THE VALUES OF      *
*  CRYSTALLINITY AND ITS DERIVATIVE IS CARRIED OUT BY CALLING ANOTHER *
*  SUBROUTINE "RKF45" WHICH IS DESIGNED BY WATTS ET AL. TO SOLVE A SET OF *
*  FIRST ORDER DIFFERENTIAL EQUATIONS WHEN DERIVATIVE EVALUATIONS ARE *
*  NOT EXPENSIVE.                                                    *
**********************************************************************
C
**********************************************************************
* A LIST OF VARIABLES USED IN THESE SUBROUTINES:                     *
*                                                                    *
* DEN      : THE DENSITY OF THE MATERIAL, MG/CM^3.                   *
* DH       : THE LATENT HEAT OF CRYSTALLIZATION, ERG/MG.             *
* DTMW     : THE TEMPERATURE DIFFERENCE BETWEEN MELTING POINT AND    *
*              REFERENCE TEMPERATURE.                                *
* DXC      : AN ARRAY CONTAINING THE DERIVATIVE VALUES OF THE RELATIVE *
*              CRYSTALLINITY WITH RESPECT TO X1 AT LOCAL NODES IN AN ELEMENT. *
* ICON     : AN ARRAY(INPUT).                                        *
* ICYCLE   : AN INTEGER SPECIFYING THE NUMBER OF THE CURRENT ITERATION *
*              CYCLE(INPUT).                                         *
* INODE    : AN INTEGER SPECIFYING THE GLOBAL NUMBER OF THE NODAL POINT. *
* LISTEL   : AN ARRAY(INPUT).                                        *
* MAT      : AN INTEGER SPECIFYING THE MATERIAL NUMBER AS SET ON THE *
*              MATERIAL DATA CARD(INPUT).                            *
* NELEM    : AN INTEGER SPECIFYING THE NUMBER OF THE CURRENT ELEMENT(INPUT). *
* NN       : AN INTEGER SPECIFYING THE NUMBER OF THE NODES IN AN ELEMENT *
*              (INPUT).                                              *
* NNODES   : AN INTEGER SPECIFYING THE NUMBER OF THE CORNER NODES IN AN *
*              ELEMENT(INPUT).                                       *
* QVALUE : AN ARRAY CONTAINING THE VALUES OF THE VOLUMETRIC HEAT SOURCE *
*              (OUTPUT).                                             *
* T        : AN ARRAY CONTAINING NODAL POINT VALUES OF THE TEMPERATURE *
*              (INPUT).                                              *
* TIME     : THE VALUE OF THE CURRENT TIME(INPUT).                   *
* U1, U2   : ARRAYS CONTAINING NODAL POINT VALUES OF THE VELOCITY    *
*              COMPONENTS AT THE X1, AND X2 DIRECTIONS, RESPECTIVELY. *
* UN       : AN ARRAY CONTAINING GLOBAL NODAL POINT VALUES OF THE FIELD *
*              SOLUTIONS.                                            *
*                UN(NUMNOD,1)=VELOCITY COMPONENT AT X2 DIRECTION.    *
```

```
*               UN(NUMNOD,2)=VELOCITY COMPONENT AT X1 DIRECTION.          *
*               UN(NUMNOD,3)=PRESSURE.                                    *
*               UN(NUMNOD,4)=TEMPERATURE.                                 *
*               UN(NUMNOD,5)=RELATIVE DEGREE OF CRYSTALLINITY.            *
*               UN(NUMNOD,6)=SECOND AUXILIARY VARIABLE.                   *
* VAR2    : AN ARRAY CONTAINING NODAL POINT VALUES OF THE SECOND          *
*             AUXILIARY VARIABLE(INPUT).                                  *
* X1, X2  : ARRAYS CONTAINING NODAL POINT VALUES OF THE X1 AND X2         *
*             COORDINATES(INPUT).                                         *
* XMAXCR : THE MAXIMUM ABSOLUTE DEGREE OF CRYSTALLINITY THAT POLYMER      *
*             CAN ACHIEVE.                                                *
* XN      : AVRAMI EXPONENT.                                              *
* Y(1)    : THE NODAL POINT VALUE OF THE RELATIVE CRYSTALLINITY.          *
* Y(2)    : THE NODAL POINT VALUE OF THE TEMPERATURE.                     *
* YP(1)   : THE NODAL POINT VALUE OF THE DERIVATIVE OF RELATIVE           *
*             CRYSTALLINITY WITH RESPECT TO X1.                           *
* YP(2)   : THE NODAL POINT VALUE OF THE DERIVATIVE OF TEMPERATURE WITH   *
*             RESPECT TO X1.                                              *
*                                                                         *
* SUBROUTINE "RKF45" WHICH IS CALLED IN SUBROUTINE "CRYSTAL" INTEGRATES   *
* A SYSTEM OF NEQN FIRST ORDER ORDINARY DIFFERENTIAL EQUATIONS OF THE     *
* FORM                                                                    *
*            DY(I)/DX1 = F(X1,Y(1),Y(2),....,Y(NEQN))                     *
* WHERE THE Y(I) ARE GIVEN AT X1.                                         *
* TYPICALLY THE SUBROUTINE RKF45 IS USED TO INTEGRATE FROM X1IN TO X1OUT  *
* BUT IT CAN BE USED AS A ONE-STEP INTEGRATOR TO ADVANCE THE SOLUTION A   *
* SINGLE STEP IN THE DIRECTION OF X1OUT. ON RETURN THE PARAMETERS IN THE  *
* CALL LIST ARE SET FOR CONTINUING THE INTEGRATION. THE USER HAS ONLY TO  *
* CALL RKF45 AGAIN. ACTUALLY, RKF45 IS AN INTERFACING ROUTINE WHICH CALLS *
* SUBROUTINE RKFS FOR THE SOLUTION. RKFS IN TURN CALLS SUBROUTINE FEHL    *
* WHICH COMPUTES AN APPROXIMATE SOLUTION OVER ONE STEP.                   *
*                                                                         *
* THE VARIABLES IN THE SUBROUTINE PARAMETER LIST REPRENSENT:              *
*                                                                         *
* F       : SUBROUTINE F(X1,Y,YP) TO EVALUATE DERIVATIVES YP(I)=DY(I)/DX1.*
*             SUBROUTINE NAME MUST APPEAR IN AN EXTERNAL STATEMENT IN     *
*             CALLING PROGRAM.                                            *
* NEQN    : NUMBER OF EQUATIONS TO BE INTEGRATED(INPUT).                  *
* Y       : AN ARRAY CONTAINING THE SOLUTION VECTORS AT X1.               *
* X1      : INDEPENDENT VARIABLE(INPUT).                                  *
* X1IN    : STARTING POINT OF INTEGRATION(INPUT).                         *
* X1OUT   : OUTPUT POINT AT WHICH SOLUTION IS DESIRED(INPUT).             *
* RELERR  : RELATIVE ERROR TOLERANCES FOR LOCAL ERROR TEST(INPUT).        *
* ABSERR  : ABSOLUTE ERROR TOLERANCES FOR LOCAL ERROR TEST(INPUT).        *
* IFLAG   : INDICATOR FOR STATUS OF INTEGRATION. IFLAG=1 IS TO INITIALIZE *
*             THE CODE FOR EACH NEW PROBLEM(INPUT).                       *
* WORK    : ARRAYS CONTAINING THE FIRST DERIVATIVES OF THE SOLUTION VECTOR*
*             Y AT X1OUT(OUTPUT).                                         *
* IWORK   : ARRAYS USED TO HOLD INFORMATION INTERNAL TO RKF45 WHICH IS    *
*           NECESSARY FOR SUBSEQUENT CALLS.                               *
*************************************************************************
```

```
C
C
      SUBROUTINE USRVHS (QVALUE,T,VAR2,X2,X1,NNODES,MAT,NELEM,TIME,
     1  ICYCLE,NN,ICON,LISTEL,UN)
C
C
      IMPLICIT DOUBLE PRECISION (A-H,O-Z)
      COMMON /SZDAT/ NUMEL,NUMNOD,NUMVAR,NUMDOF,NODSOL
      COMMON /MATDAT/ NMAT,NPROP,PROP(15,10),NXMAT,NXPROP,XPROP(15,10)
      COMMON /PRBDAT/ IAXSYM,ITMDEP,IFORCE,IFREE,IVAR1,IVAR2,IIVAR2,
     1                IPFUNC,IPNLTY,PNLTY
      DIMENSION QVALUE(*), T(*), X1(*), X2(*), VAR2(*)
      DIMENSION ICON(NUMEL,*), LISTEL(*)
      DIMENSION UN(NUMNOD,*)
      DIMENSION DXC(9), U1(9), U2(9)
C
C     ************************************************************
C
C     THE LATENT HEAT OF CRYSTALLIZATION OF PP IS 2370 CAL/G-MOLE.
C     THE MOLECULAR WEIGHT OF PP IS 42 GM/G-MOLE AND 1 CAL = 4.2D7 ERGS.
C
      DTMW=XPROP(4,MAT)
      XMAXCR=XPROP(5,MAT)
      DH=2370.0*4.2D7/42.0
      DEN=PROP(1,MAT)
      DO 1 J=1,NN
      INODE=ABS(ICON(NELEM,J))
      U2(J)=UN(INODE,1)
      U1(J)=UN(INODE,2)
    1 CONTINUE
C
C     CALL SUBROUTINE "CRYSTAL" TO CALCULATE THE DERIVATIVE OF
C     CRYSTALLINITY WITH RESPECT TO X1 AT EACH NODE IN AN ELEMENT.
C
      ALL CRYSTAL(DXC,T,X1,X2,U1,U2,NN,UN,ICON,NELEM)
C
C     CALCULATE THE VALUES OF THE VOLUMETRIC HEAT SOURCE.
C
      DO 2 I=1,NNODES
      QVALUE(I)=DEN*DH*XMAXCR*U1(I)*DXC(I)/DTMW
    2 CONTINUE
      RETURN
      END
C
C
      SUBROUTINE CRYSTAL(DXC,T,X1,X2,U1,U2,NN,UN,ICON,NELEM)
C
C     ************************************************************
C
C     SUBROUTINE TO EVALUATE CRYSTALLINITY AND ITS DERIVATIVE WITH
C     RESPECT TO X1 AT EACH NODE IN AN ELEMENT
C
```

```
C     ************************************************************
C
      IMPLICIT DOUBLE PRECISION (A-H,O-Z)
      COMMON /SZDAT/ NUMEL,NUMNOD,NUMVAR,NUMDOF,NODSOL
      COMMON /MATDAT/ NMAT,NPROP,PROP(15,10),NXMAT,NXPROP,XPROP(15,10)
      COMMON /PRBDAT/ IAXSYM,ITMDEP,IFORCE,IFREE,IVAR1,IVAR2,IIVAR2,
     1                IPFUNC,IPNLTY,PNLTY
      COMMON /TANDV/ VV, A, B
      DIMENSION T(*), X1(*), X2(*)
      DIMENSION U1(*), U2(*)
      DIMENSION ICON(NUMEL,*)
      DIMENSION UN(NUMNOD,*)
      DIMENSION DXC(9), Z(9), Y(2), YP(2), WORK(15)
      INTEGER NEQN, IFLAG, IWORK(5)
C
C     ************************************************************
C
      EXTERNAL F
      NEQN=2
      RELERR=1.0D-8
      ABSERR=1.0D-4
C
C     INITIALIZATION OF DERIVATIVE OF THE CRYSTALLINITY WITH RESPECT TO X1.
C
      DO 1 I=1,NN
      DXC(I)=0.0
      Z(I)=1.0D-10
    1 CONTINUE
C
C     USE OF RUNGE-KUTTA-FEHLBERG METHOD TO CALCULATE THE CRYSTALLINITY
C     AND ITS DERIVATIVE AT EACH NODE WHEN NINE-POINT ELEMENT IS USED.
C
      DO 2 J=1,NN
      VV=U1(J)
      IFLAG=1
      INODE=ABS(ICON(NELEM,J))
      GO TO (10,20,30,40,50,60,70,80,90), J
C
C     CALCULATION OF THE CRYSTALLINITIES AND THEIR DERIVATIVES WITH
C     RESPECT TO X1 AT THE FIRST AND THE EIGHTH NODES.
C
   10 Y(1)=UN(INODE,5)
      Y(2)=T(1)*150.0+26.0
      X1IN=X1(1)
      X1OUT=X1(8)
      CALL DTX1(T(1),T(8),T(4),X1(1),X1(8),X1(4),A,B)
      CALL F(X1IN,Y,YP)
      DXC(1)=YP(1)
      CALL RKF45(F,NEQN,Y,X1IN,X1OUT,RELERR,ABSERR,IFLAG,WORK,IWORK)
      Z(8)=Y(1)
      DXC(8)=WORK(1)
```

```
      GO TO 2
C
C     CALCULATION OF THE CRYSTALLINITIES AND THEIR DERIVATIVES WITH
C     RESPECT TO X1 AT THE SECOND AND THE SIXTH NODES.
C
   20 Y(1)=UN(INODE,5)
      Y(2)=T(2)*150.0+26.0
      X1IN=X1(2)
      X1OUT=X1(6)
      CALL  DTX1(T(2),T(6),T(3),X1(2),X1(6),X1(3),A,B)
      CALL F(X1IN,Y,YP)
      DXC(2)=YP(1)
      CALL RKF45(F,NEQN,Y,X1IN,X1OUT,RELERR,ABSERR,IFLAG,WORK,IWORK)
      Z(6)=Y(1)
      DXC(6)=WORK(1)
      GO TO 2
   30 INODE3=INODE
      GO TO 2
   40 INODE4=INODE
      GO TO 2
C
C     CALCULATION OF THE CRYSTALLINITIES AND THEIR DERIVATIVES WITH
C     RESPECT  TO X1 AT THE FIFTH AND THE NINTH NODES.
C
   50 Y(1)=UN(INODE,5)
      Y(2)=T(5)*150.0+26.0
      X1IN=X1(5)
      X1OUT=X1(9)
      CALL  DTX1(T(5),T(9),T(7),X1(5),X1(9),X1(7),A,B)
      CALL F(X1IN,Y,YP)
      DXC(5)=YP(1)
      CALL RKF45(F,NEQN,Y,X1IN,X1OUT,RELERR,ABSERR,IFLAG,WORK,IWORK)
      Z(9)=Y(1)
      DXC(9)=WORK(1)
      GO TO 2
C
C     CALCULATION OF THE CRYSTALLINITY AND ITS DERIVATIVE WITH RESPECT TO
C     X1 AT THE THIRD NODE.
C
   60 UN(INODE,5)=Z(6)
      Y(1)=Z(6)
      Y(2)=T(6)*150.0+26.0
      X1IN=X1(6)
      X1OUT=X1(3)
      CALL  DTX1(T(2),T(6),T(3),X1(2),X1(6),X1(3),A,B)
      CALL RKF45(F,NEQN,Y,X1IN,X1OUT,RELERR,ABSERR,IFLAG,WORK,IWORK)
      UN(INODE3,5)=Y(1)
      DXC(3)=WORK(1)
      GO TO 2
   70 INODE7=INODE
      GO TO 2
C
C     CALCULATION OF THE CRYSTALLINITY AND ITS DERIVATIVE WITH RESPECT TO
```

```
C       X1 AT THE FOURTH NODE.
C
   80 UN(INODE,5)=Z(8)
      Y(1)=Z(8)
      Y(2)=T(8)*150.0+26.0
      X1IN=X1(8)
      X1OUT=X1(4)
      CALL  DTX1(T(1),T(8),T(4),X1(1),X1(8),X1(4),A,B)
      CALL RKF45(F,NEQN,Y,X1IN,X1OUT,RELERR,ABSERR,IFLAG,WORK,IWORK)
      UN(INODE4,5)=Y(1)
      DXC(4)=WORK(1)
      GO TO 2
C
C       CALCULATION OF THE CRYSTALLINITY AND ITS DERIVATIVE WITH RESPECT TO
C       X1 AT THE SEVENTH NODE.
C
   90 UN(INODE,5)=Z(9)
      Y(1)=Z(9)
      Y(2)=T(9)*150.0+26.0
      X1IN=X1(9)
      X1OUT=X1(7)
      CALL  DTX1(T(5),T(9),T(7),X1(5),X1(9),X1(7),A,B)
      CALL RKF45(F,NEQN,Y,X1IN,X1OUT,RELERR,ABSERR,IFLAG,WORK,IWORK)
      UN(INODE7,5)=Y(1)
      DXC(7)=WORK(1)
    2 CONTINUE
      RETURN
      END
C
C
      SUBROUTINE F(X1,Y,YP)
      IMPLICIT DOUBLE PRECISION (A-H,O-Z)
      COMMON /TANDV/ VV, A, B
      DIMENSION Y(2), YP(2)
C
C       THE TEMPERATURE AT WHICH CRYSTALLIZATION OCCURS IS CONSTRAINED
C       BETWEEN -50C AND 187.5C.
C
      IF (VV .EQ. 0.0) VV=1.0D-6
      IF  (Y(1).EQ.1.0)  Y(1)=0.999999999
      IF (Y(2).GE.187.5) GO TO 1
      IF (Y(2).LE.-50.0) GO TO 1
C
C       UU, SS REPRESENT THE DIFFUSION AND NUCLEATION TERMS IN THE EXPRESSION
C       WHICH PREDICTS THE VARIATION OF HALF-TIMES WITH CRYSTALLIZATION
C       TEMPERATURE.
C
      XN=2.5
      XM=(XN-1.0)/XN
      UU=EXP(-754.9/ABS(Y(2)+50.0))
      SS=EXP(-5.0D5/ABS(Y(2)+273.0)/ABS(187.5-Y(2)))
      XK=7.696D7*UU*SS
      QQ=(1.0-Y(1))*(ABS(LOG(1.0/ABS(1.0-Y(1)))))**XM
```

```
C
C       YP(1)=DY(1)/DX1 IS THE DERIVATIVE OF CRYSTALLINITY WITH RESPECT TO X1.
C       YP(2)=DY(2)/DX1 IS THE DERIVATIVE OF TEMPERATURE WITH RESPECT TO X1.
C
C
        YP(1)=XN*XK*QQ/VV
        YP(2)=2.0*A*X1+B
        GO TO 2
    1   CONTINUE
        YP(1)=1.0D-10
        YP(2)=2.0*A*X1+B
    2   CONTINUE
        RETURN
        END
C
C       SUBROUTINE DTX1 IS USED TO CALCULATE THE CONSTANTS, A AND B, IN
C       THE POLYNOMIAL EQUATION: T = AX^2 + BX + C
C
        SUBROUTINE DTX1(T1,T2,T3,X1,X2,X3,A,B)
        IMPLICIT DOUBLE PRECISION (A-H,O-Z)
        AA=(T1-T2)*(X1-X3)*150.0-(T1-T3)*(X1-X2)*150.0
        XX=(X1**2-X2**2)*(X1-X3)-(X1**2-X3**2)*(X1-X2)
        A=AA/XX
        BB=(T1-T2)*150.0-A*(X1**2-X2**2)
        B=BB/(X1-X2)
        RETURN
        END
C
C
        SUBROUTINE RKF45(F,NEQN,Y,T,TOUT,RELERR,ABSERR,IFLAG,WORK,
    1   IWORK)
        IMPLICIT DOUBLE PRECISION (A-H,O-Z)
        INTEGER NEQN,IFLAG,IWORK(5)
        DIMENSION Y(NEQN),WORK(1)
        EXTERNAL F
        INTEGER  K1,K2,K3,K4,K5,K6,K1M
        K1M=NEQN+1
        K1=K1M+1
        K2=K1+NEQN
        K3=K2+NEQN
        K4=K3+NEQN
        K5=K4+NEQN
        K6=K5+NEQN
        CALL RKFS(F,NEQN,Y,T,TOUT,RELERR,ABSERR,IFLAG,WORK(1),WORK(
    1   K1M),WORK(K1),WORK(K2),WORK(K3),WORK(K4),WORK(K5),WORK(K6),
    2      WORK(K6+1),IWORK(1),IWORK(2),IWORK(3),IWORK(4),IWORK(5))
        RETURN
        END
C
C
        SUBROUTINE RKFS(F,NEQN,Y,T,TOUT,RELERR,ABSERR,IFLAG,YP,H,F1,
    1           F2,F3,F4,F5,SAVRE,SAVAE,NFE,KOP,INIT,JFLAG,KFLAG)
        IMPLICIT DOUBLE PRECISION (A-H,O-Z)
```

```
      LOGICAL HFAILD,OUTPUT
      INTEGER  NEQN,IFLAG,NFE,KOP,INIT,JFLAG,KFLAG
      DIMENSION Y(NEQN),YP(NEQN)
     1         ,F1(NEQN),F2(NEQN),F3(NEQN),F4(NEQN),F5(NEQN)
      EXTERNAL F
      INTEGER  K,MAXNFE,MFLAG
      DATA  REMIN/1.D-12/
      DATA  MAXNFE/3000/
      IF (NEQN .LT. 1) GO TO 10
      IF ((RELERR .LT. 0.0D0)  .OR.  (ABSERR .LT. 0.0D0)) GO TO 10
      MFLAG=IABS(IFLAG)
      IF ((MFLAG .EQ. 0) .OR. (MFLAG .GT. 8)) GO TO 10
      IF (MFLAG .NE. 1) GO TO 20
      EPS = 1.0D0
    5 EPS = EPS/2.0D0
      EPSP1 = EPS + 1.0D0
      IF (EPSP1 .GT. 1.0D0) GO TO 5
      U26 = 26.0D0*EPS
      GO TO 50
   10 IFLAG=8
      RETURN
   20 IF ((T .EQ. TOUT) .AND. (KFLAG .NE. 3)) GO TO 10
      IF (MFLAG .NE. 2) GO TO 25
      IF ((KFLAG .EQ. 3) .OR. (INIT .EQ. 0)) GO TO 45
      IF (KFLAG .EQ. 4) GO TO 40
      IF ((KFLAG .EQ. 5)  .AND.  (ABSERR .EQ. 0.0D0)) GO TO 30
      IF ((KFLAG .EQ. 6)  .AND.  (RELERR .LE. SAVRE)  .AND.
     1         (ABSERR .LE. SAVAE)) G O TO 30
      GO TO 50
   25 IF (IFLAG .EQ. 3) GO TO 45
      IF (IFLAG .EQ. 4) GO TO 40
      IF ((IFLAG .EQ. 5) .AND. (ABSERR .GT. 0.0D0)) GO TO 45
   30 STOP
   40 NFE=0
      IF (MFLAG .EQ. 2) GO TO 50
   45 IFLAG=JFLAG
      IF (KFLAG .EQ. 3) MFLAG=IABS(IFLAG)
   50 JFLAG=IFLAG
      KFLAG=0
      SAVRE=RELERR
      SAVAE=ABSERR
      RER=2.0D0*EPS+REMIN
      IF (RELERR .GE. RER) GO TO 55
      RELERR=RER
      IFLAG=3
      KFLAG=3
      RETURN
   55 DT=TOUT-T
      IF (MFLAG .EQ. 1) GO TO 60
      IF (INIT .EQ. 0) GO TO 65
      GO TO 80
   60 INIT=0
      KOP=0
```

```
      A=T
      CALL F(A,Y,YP)
      NFE=1
      IF (T .NE. TOUT) GO TO 65
      IFLAG=2
      RETURN
   65 INIT=1
      H=DABS(DT)
      TOLN=0.
      DO 70 K=1,NEQN
      TOL=RELERR*DABS(Y(K))+ABSERR
      IF (TOL .LE. 0.) GO TO 70
      TOLN=TOL
      YPK=DABS(YP(K))
      IF (YPK*H**5 .GT. TOL) H=(TOL/YPK)**0.2D0
   70 CONTINUE
      IF (TOLN .LE. 0.0D0) H=0.0D0
      H=DMAX1(H,U26*DMAX1(DABS(T),DABS(DT)))
      JFLAG=ISIGN(2,IFLAG)
   80 H=DSIGN(H,DT)
      IF (DABS(H) .GE. 2.0D0*DABS(DT)) KOP=KOP+1
      IF (KOP .NE. 100) GO TO 85
      KOP=0
      IFLAG=7
      RETURN
   85 IF (DABS(DT) .GT. U26*DABS(T)) GO TO 95
      DO 90 K=1,NEQN
   90 Y(K)=Y(K)+DT*YP(K)
      A=TOUT
      CALL F(A,Y,YP)
      NFE=NFE+1
      GO TO 300
   95 OUTPUT= .FALSE.
      SCALE=2.0D0/RELERR
      AE=SCALE*ABSERR
  100 HFAILD= .FALSE.
      HMIN=U26*DABS(T)
      DT=TOUT-T
      IF (DABS(DT) .GE. 2.0D0*DABS(H)) GO TO 200
      IF (DABS(DT) .GT. DABS(H)) GO TO 150
      OUTPUT= .TRUE.
      H=DT
      GO TO 200
  150 H=0.5D0*DT
  200 IF (NFE .LE. MAXNFE) GO TO 220
      IFLAG=4
      KFLAG=4
      RETURN
  220 CALL  FEHL(F,NEQN,Y,T,H,YP,F1,F2,F3,F4,F5,F1)
      NFE=NFE+5
      EEOET=0.0D0
      DO 250 K=1,NEQN
      ET=DABS(Y(K))+DABS(F1(K))+AE
```

```
      IF (ET .GT. 0.0D0) GO TO 240
C     INAPPROPRIATE ERROR TOLERANCE
      IFLAG=5
      RETURN
  240 EE=DABS((-2090.0D0*YP(K)+(21970.0D0*F3(K)-15048.0D0*F4(K)))
     1                    +(22528.0D0*F2(K)-27360.0D0*F5(K)))
  250 EEOET=DMAX1(EEOET,EE/ET)
      ESTTOL=DABS(H)*EEOET*SCALE/752400.0D0
      IF (ESTTOL .LE. 1.0D0) GO TO 260
      HFAILD= .TRUE.
      OUTPUT= .FALSE.
      S=0.1D0
      IF (ESTTOL .LT. 59049.0D0) S=0.9D0/ESTTOL**0.2D0
      H=S*H
      IF (DABS(H) .GT. HMIN) GO TO 200
      IFLAG=6
      KFLAG=6
      RETURN
  260 T=T+H
      DO 270 K=1,NEQN
  270 Y(K)=F1(K)
      A=T
      CALL F(A,Y,YP)
      NFE=NFE+1
      S=5.0D0
      IF (ESTTOL .GT. 1.889568D-4) S=0.9D0/ESTTOL**0.2D0
      IF (HFAILD) S=DMIN1(S,1.0D0)
      H=DSIGN(DMAX1(S*DABS(H),HMIN),H)
      IF (OUTPUT) GO TO 300
      IF (IFLAG .GT. 0) GO TO 100
      IFLAG=-2
      RETURN
  300 T=TOUT
      IFLAG=2
      RETURN
      SUBROUTINE FEHL(F,NEQN,Y,T,H,YP,F1,F2,F3,F4,F5,S)
      IMPLICIT DOUBLE PRECISION (A-H,O-Z)
      INTEGER NEQN
      DIMENSION Y(NEQN),YP(NEQN),F1(NEQN),F2(NEQN),
     1  F3(NEQN),F4(NEQN),F5(NEQN),S(NEQN)
      INTEGER K
      CH=H/4.0D0
      DO 221 K=1,NEQN
  221 F5(K)=Y(K)+CH*YP(K)
      CALL F(T+CH,F5,F1)
      CH=3.0D0*H/32.0D0
      DO 222 K=1,NEQN
  222 F5(K)=Y(K)+CH*(YP(K)+3.0D0*F1(K))
      CALL  F(T+3.0D0*H/8.0D0,F5,F2)
      CH=H/2197.0D0
      DO 223 K=1,NEQN
  223 F5(K)=Y(K)+CH*(1932.0D0*YP(K)+(7296.0D0*F2(K)-7200.0D0*
     1  F1(K)))
```

```
      CALL  F(T+12.0D0*H/13.0D0,F5,F3)
      CH=H/4104.0D0
      DO 224 K=1,NEQN
  224 F5(K)=Y(K)+CH*((8341.0D0*YP(K)-845.0D0*F3(K))+
     1                    (29440.0D0*F2(K)-32832.0D0*F1(K)))
      CALL  F(T+H,F5,F4)
      CH=H/20520.0D0
      DO 225 K=1,NEQN
  225 F1(K)=Y(K)+CH*((-6080.0D0*YP(K)+(9295.0D0*F3(K)-
     1          5643.0D0*F4(K)))+(41040.0D0*F1(K)-28352.0D0*F2(K)))
      CALL  F(T+H/2.0D0,F1,F5)
      CH=H/7618050.0D0
      DO 230 K=1,NEQN
  230 S(K)=Y(K)+CH*((902880.0D0*YP(K)+(3855735.0D0*F3(K)-
     1         1371249.0D0*F4(K)))+(3953664.0D0*F2(K)+
     2       277020.0D0*F5(K)))
      RETURN
      END
```

VITA

Jung-He Wu was born in Taipei, Taiwan, R. O. C. on April 11, 1962. He attended elementary, junior high ,and high schools in Taipei, Taiwan and graduated from Taipei Kien-Kow Senior High School in June 1981. The following September he passed the entrance examination and entered the National Cheng-Kung University (NCKU) in Tainan, Taiwan.

In 1985 he received a B. S. degree in Chemical Engineering and in the same year he was recruited by the Army for two-year military service. In the Fall of 1988, he began graduate studies in the Department of Chemical Engineering at the University of Tennessee, Knoxville. He received the Master of Science degree in August 1990.